NOVEL MICROFLUIDIC APPROACHES FOR RAPID POINT-OF-CARE QUANTITATION OF *ESCHERICHIA COLI* USING IMMUNOASSAYS

By

Isabel Patricia Azevedo Alves

A Doctoral Thesis

Submitted in partial fulfilment of the requirements

for the award of the degree

Doctor of Philosophy from Loughborough University

March 2019

Abstract

There is a major clinical demand for rapid diagnostic tests capable of detecting pathogens in human samples. This is driven by an unprecedented clinical need in prescribing antibiotics more objectively and fighting antimicrobial resistance. Despite the remarkable breakthroughs, miniaturisation of such bioassays is challenging and expensive.

Urinary Tract Infections are the most common bacterial infection, with *Escherichia coli (E. coli)* being responsible for >80% of cases, presenting concerning resistance levels to the last generation of antibiotics. Currently, diagnostics industry struggle to deliver miniaturised biosensors capable of detection and identifying bacteria at format compatible with point-of-care.

This thesis presents novel experimental insights for sensitive and rapid detection of *E. coli* using polyclonal antibodies immobilized on the inner surface of an inexpensive 10-bore FEP-Teflon® MicroCapillary Film. Overall the results achieved allowed identification of three major challenges for miniaturisation of bacteria detection: the interrogation volume, gravity and shear stress. Coated capillaries acted as a very high affinity system, capturing up to 100% of *E. coli* cells, with clear evidence of immunospecificity. In addition, an opportunity to explore the 'open' fluidics aspect of microcapillary systems to concentrate bacteria from a large sample volume was identified and therefore speed up the detection of bacteria in clinical samples without the need for microbiological incubation. Therefore, this enabled the development of a fluorescence sandwich immunoassay capable of quantifying *E. coli* in buffer and synthetic urine in less than 25 minutes, yielding a limit of detection (LoD) up to 240 CFU/ml, commensurate with the cut-off value required for UTIs (10^3-10^5 CFUs/ml). This proof-of-concept was achieved exploiting low cost readout systems such as a smartphone and demonstrated reproducible and robust performance in synthetic urine. Ultimately, two new gravity-driven microfluidic devices, denominated MCF-funnel and MCF-siphon, were designed and manufactured to address autonomy, power-free and portability requirements.

Key words: Bacterial detection, *E. coli* quantitation, fluorescent immunoassay, FEP-Teflon® microcapillaries, point-of-care.

Acknowledgements

I would like to thankful to my supervisors for their guidance and support through all this PhD. As Newton said once: ‘’If I have seen further, it is by standing upon the shoulders of giants’’. Many thanks to Dr Nuno Reis for believed in me giving me this opportunity. I am thankful for his continuous scientific insight in all experimental work, data analysis and production of manuscripts. Even in the distance he remained feeding this PhD with his great ideas and enthusiasm. I am also ver thankful to Dr Karen Coopman who step up as my main supervisor by the end of my first year and since then showed care, respect and support unconditional by me as student and by my research. She ensured all conditions to conduct this work till the end, yet and mainly her motivation was fundamental to face all challenges along last years.

Secondly I would like to thankful to Loughborough University and Chemical Engineering Staff for providing all funding, equipmant and training to proceed with my work. Special big thanks to Tony by his kindness and 3D model design of the gravity driven devices presented in chapter 5 and 6, also to Monika and Tim for their availability and support to help with Bio work related problems.

I am also thankful to Lamina Dielectrics Ltd for providing the microcapillary platform.

This PhD would not be the same without an uncountable list of amazing peeople that filled my life with joy and smiles, which I gratefully thanks: Ana Barbosa and Ni for their friendship,continuous motivation, help in my first project steps and for being great teammates; Andrea, Francesco and Salvo for being the best mini-CDT and lab teamates; To Abdul for his wise insights in descomplicating problems and assistance with LSCM experiments; To all my office colleagues with who I shared many moments, laughts and frustrations (Keith, Monalie, Gurinder, Barbara, Serena, Federika, Rafaela, Alejandra, Sharleigh, Rodrigo and Maria Sotenko); to other important friends, that despiste distance they constantly supported me ; For the streght, kindness and restless support of my core friends of this journey (Ana Rebelo, Luis and Maria) and for the unconditional motivation and encouragemnt from my sunny person Bernd in the last phase of this PhD.

In last, I am therefore grateful to my family, for their unconditional love and support in this journey and specially to my mum and my brother - my role models of resilience and courage.

List of Publications

1. **Alves, I. P**. & Reis, N. M. Immunocapture of *Escherichia coli* in a fluoropolymer microcapillary array. Journal of Chromatography A, 1585 (2019), 46–55, doi:10.1016/j.chroma.2018.11.067 (chapter 3)

2. **Alves, I. P**. & Reis, N. M. Microfluidic smartphone quantitation of *E. coli* in synthetic urine. 2019 - To be submitted at Biosensors and Bioelectronics Journal. (chapter 4)

3. **Alves, I. P**. & Reis, N.M Hydrodynamic characterization of two new power free microfluidic devices. 2019 – To be submitted (chapter 5)

4. A. Edwards, J. Pivetal, A. Loo-Zazueta, J. Barros, **I. Alves** and N. Reis, Conference proceeding, 20th International Conference on Miniaturized Systems for Chemistry and Life Sciences, The development of a Lab-on-a-Stick for one-step multi-analyte cellular microfluidic dipstick assays'' Dublin, October of 2016.

Table of Contents

List of Figures

List of Tables

List of Abreviations

AMR	Antimicrobial resistance
E. coli	*Escherichia coli*
UTI	Urinary Tract Infection
POC	Point-of-care
ASSURED	Affordable, Sensitive, Specific, User friendly, Rapid & Robust, Equipment-free and Deliverable to end-users
MCF	Microcapillary film
PBS	Phosphate Buffer Saline
TBS	Tris-Buffer Saline
HSS-HRP	High Sensitive Streptavidin- Horseradish Peroxidase
PVOH	Polyvinyl alcohol
SVR	Surface-area-to-volume ratio
SEM	Scanning electron microscopy
LSCM	Laser scanning confocal microscopy
PCR	Polymerase chain reaction
AMPs	Antimicrobial peptides
ELISA	Enzyme-Linked Immunosorbent Assay
PNA	Peptide nucleic acids
SPR	Surface plasmon resonance
capAb	Capture antibody
detAb	Detection antibody
4 PL	4 Parameter logistic
CV	Coefficient of variation
BSA	Bovine serum albumin
PDMS	Polydimethylsiloxane
AP	Alkaline phosphatase
Fc	Constant fragment of antibody
Fab	Variable fragment of antibody
CDRs	Complementary-determining regions
FEP	Fluorinated ethylene propylene
hCG	Human chorionic gonadotropin
LoD	Limit of detection
LoQ	Limit of quantitation
MTP	Microtiter plate

MSA	Multi syringe aspirator
MS	Manual syringe
OPD	o- Phenylenediamine dihydrochloride
IS	Impedance spectrometry
LOC	Lab on a chip
IMS	Immunomagnetic separation
PMMA	Poly-(methylmethacrylate)
PC	Polycarbonate
PS	Polystyrene
RTD	Residence time distribution

CHAPTER 1 | Introduction

1.1 Background and Research gap

Organisms such as bacteria, fungi and viruses are responsible for a wide range of infectious diseases. They can be highly adaptable to extreme conditions, catalysing their ability to spread and overcome the susceptibility to antimicrobial drugs.[1,2,3] The treatment of human infectious diseases in England, including costs to the health service, labour market and the individual expenses, are estimated at £30 million per year.[1,2,3] Moreover, around 25% of the population is affected by gastrointestinal infections each year, leading to approximately 1 million GP visits and nearly 29 million days lost from school or work.[1] Although treatable, most of these major infectious diseases represent the second cause of mortality with rates over 50 % in developing countries.[2,4,5] According to O'Neill [2,6], drug-resistant strains of tuberculosis (TB), malaria, HIV and certain bacterial infections (the most common caused by *E. coli, Klebsiella sp. and Staphyloccocus sp.*) are taking 700 thousand anually lives worldwide, estimated to increase to 10 million per year by 2050.

Bacterial infections are the predominant infectious diseases.[2,7] Currently healthcare systems are experiencing a huge demand for effective and portable miniaturized diagnostics tests for bacterial detection and quantification at the point-of-care, in order to help with the fight against AMR. Yet the diagnostics industry has failed so far to deliver miniaturised biosensors capable of detection and identifying bacteria at the point-of-care. Thus, effective and reliable diagnosis still depends on centralized laboratories fully equiped with sophisticated technologies not accesible or affordable worldwide. In low resource settings, medical or laboratory facilities are still limited and inaccessible to most patients, resulting in high mortality rates caused by comunicative and non comunicative diseases. The reality for the majority of population on limited and impoverished income remains very basic health care due to scarce resources such as lack of acess to eletricity, pipped water, no transport network, low economic yield or specialised health care professionals.

It is known the massive impact of point-of-care diagnostics in improving life expectancy, where increasingly healthcare decisions are based.[8,9] Nevertheless, rural areas still struggle to match the reality of developed countries lacking fully automated and cutting edge facilities to afford sensitive (able to quantify lower concentration of

analyte), rapid (in less than 1 h), and reproducible (assay procedure and results do not change with environment) diagnostics.

Effective pathogen detection is mandatory for the prevention and treatment of human infectious diseases and to tackle the spread of resistant strains worldwide.[4,5] The development of suitable diagnostic platforms is crucial for screening of asymptomatic individuals[4], which needs to follow the ASSURED criteria stablished by the World Health Organization (WHO): **a**ffordable to everyone, **s**ensitive in any ranges of analyte, **s**pecific for each target to avoid false positives, **u**ser friendly to be used by each patient in a non invasive and simple way, **r**apid and **r**obust (no fluctuations with environment and very reproducible), **e**quipment-free and **d**eliverable to end-users who need it.[10]

Microfluidic platforms are emerging as mighty tools to develop decentralized diagnostics that meet the majority of ASSURED criteria.[8] Miniaturized or microfluidic analysis systems, also denominated ‘’micro total analysis systems” (μTAS) or “lab-on-a-chip” (LOC) have grown in popularity due to enhanced analytical performance, less reagents consumption and reducing the time span between sampling and monitorization.[5,11] Microfluidic devices provide a higher surface to volume ratio, a faster rate of mass and heat transfer and the ability to precisely handle very small volumes of bodily fluid, including blood, saliva and urine, ranging from nanoliter to picoliter in microchannel support.[5,8] Moreover, miniaturized versions of high throughput laboratory equipment offer portability, low cost, reliability, power free function (it is not dependent of electricity to be used, for example pregnancy tests present a simple optical results by color change without need of power supply) as well as simple designs for independent patients.[11]

Nowadays, pathogen diagnosis in modern clinical setting is still dependent on culture rich plates which total procedure can take between 48 to 72 h.[12,13] Despite its sensitivity, cross contamination is still the major issue of this method. Other techniques rely on polymerase chain reaction (PCR)[14,15,16], ELISA[14,16–18], aptamers[14,16], antimicrobial peptides (AMPs)[16], peptide nucleic acids (PNA)[5,16], surface plasmon resonance (SPR)[5], impedance[19] or magnetic beads[5,19]. However, the majority of those methods present characteristics which are not suitable for point-of-care applications. Currently, immunological methods are well understood and widely accepted for pathogen detection. Although polyclonal or monoclonal antibodies are easily produced and sold in commercial companies, a major limitation of antibodies includes quality-assured preparation, which poor binding-site and cross reactivity recognition results in decreased sensitivity.[5,16,19]

In addition, sample preparation is a major stubling block in point-of-care testing. Bodily fluids as blood, urine or saliva present complex matrix components interfering in

diagnostic performance. For instance, it is estimated the yearly occurrence of 150 million of urinary tract infections (UTIs) worldwide, where so far there is no commercial available device able to quantify *E. coli* directly from human urine.[13,20] In turn, diagnosis of UTIs is still very challenging, relying on multiple biomarkers detection which do not gather consensus by the medical community. Symptomatic signs are very often unclear and demanding further clinical tests. Furthermore, some symptoms can be masked by other clinical conditions which for example an immunosuppressed patients (eg. patients with HIV and cancer) may not develop fever being the source of infection sometimes impossible to identify. In UTI, the culture plate remain the gold standard of clinical assesment however it is not rapid for enabling early treatment.[9,11,21,22]

1.2 Thesis aim

The overall aim of this thesis is therefore to bring novel insights and engineering strategies to enhance the performance of rapid and sensitive quantitation of *E. coli* using immunoassays in a miniaturized microfluidic platform denominated Microcapillary film (MCF). The affordable MCF is mass produced from a melt extrusion process from Fluorinated ethylene propylene (FEP). This flat plastic film consists in 10-paralel microarray with i.d≈200 µm and successful validated previously in non-communicable immunoassay quantitation.[23,24,25]

The main objectives of this work were:

- To understand the miniaturization challenges onto FEP-Teflon microcapillary film for a bacterial bioassay and its direct effects in bacteria-probe interaction to enhance performance of quantitative bacterial immunoassays;
- To study the effect of several parameters on the performance of *E. coli* quantification immunoassay including the performance of the immunoassay using *E. coli* sample in synthetic urine;
- To validate a proof of concept fluorescent quantitative immunoassay for *E. coli* detection integrating, a smartphone as readout system.
- To design, manufacturing and characterization of new gravity-driven microfluidic approaches, towards the development of automated and power free POC diagnosis and enhancement of fluidic handling system.
- To develop and test a power-free high throughput microfluidic approaches for bacteria quantitation.

1.3 Thesis Outline

Chapter 1 introduces the problem statement around AMR and the need to develop rapid and effective bacterial detection POC diagnostics. It describes briefly the current situation worldwide, the research gap and main objectives of this thesis, presenting the outline of each chapter.

Chapter 2 explains the fundamentals of immunoassays and informs about current methodologies and terms used along this thesis, fundamental to understand the research work performed. It presents the state of the art of microfluidic platforms for bacterial detection with special emphasis for *E. coli* and details some of the research challenges on the field. An overview about miniaturization and FEP-Teflon platforms in comparison to other materials and microfluidic platforms are provided in parallel with a description of properties and previous applications successfully validated into FEP-Teflon MCF for point-of-care.

Chapter 3 identifies quantitatively for the first time some core engineering challenges that limit bacteria identification at small scale, by showing bacteria detection is intrinsically linked to the level of miniaturization. It explores the immunocapture of *E. coli* as first step for rapid detection in FEP platform. In addition, an opportunity is identified to explore the 'open' fluidics aspect of microcapillary systems to concentrate bacteria from a large sample volume and therefore speed up the detection and recognition of pathogen bacteria in clinical samples without the need for microbiological incubation, something the clinical microbiology community would argue as impossible. This work was published in Journal of Chromatography A (Alves & Reis, 2019, 1585, 25, 46-55, https://doi.org/10.1016/j.chroma.2018.11.067)

Chapter 4 presents the quantitation of *E. coli* under clinical range in synthetic urine using a fluorescent immunoassay integrated with smartphone technology as readout system. The development and optimization study exploit some of miniaturization challenges indentified in chapter 3, such as how to achieve sensitivity and integrate several components including MCF microarray to provide a portable, effective and sensitive *E. coli* assay in less than 25 minutes. The proof of concept and results were presented at Biosensors Conference 2018 in Miami and submission to Biosensors and Bioelectronics Journal is planned.

Chapter 5 presents a hydrodynamic acessment of two new portable and automated microfluidic devices for POC diagnosis. Funnel and Siphon were two novel designs driven by gravity and manufactured in house. They were designed and

characterized to enhance fluid handling system not adressed in chapter 4 and minimize miniaturization challenges pointed out in chapter 3.

Chapter 6 discusses the implications and the effect of hydrophilic coating into FEP-teflon platform for development of automated *E. coli* detection assay into the siphon microfluidic device from chapter 5. It introduces challenges of developing immunoassays which result from surface modification with PVOH. It is attempted of integration of proof of concept shown in chapter 4 with new gravity driven microfluidic device.

Chapter 7 sums up the work performed in this PhD thesis, highlighting the main conclusions and discussing future developments that could be undertaken to further improve automation and sensitive quantitation of bacteria in the MCF platform at point-of-care settings.

Chapter 8 provides a cumulative references list of all citations in this thesis.

CHAPTER 2 | Literature Review

'' Before using an antibiotic, healthcare systems need to leapfrog to using rapid diagnostics wherever possible over the next five years... ''

James O'Neill, October 2015

2.1 Antimicrobial Resistance as a global burden

Empirical antibiotic prescription and overuse of antibiotics are are leading to an alarming increase rate of antimicrobial resistance (AMR), demanding more rapid and effective point-of-care (POC) diagnostics for pathogen detection, avoiding the broad range antibiotic prescription without need.[2,3]

''Getting the right drug, to the right patient at the right time'' is the basis of the problem and not easy to solve.[2] For instance, in the USA, of the forty thousand patients who receive antibiotics to treat respiratory issues annually, twenty seven thousand receive them unnecessarily.[6] Ultimately, technology plays a fundamental role in the development of new rapid diagnostic tools, enabling the decision-making process around antimicrobial drugs to become more accurate.[1,6,9]

Bacterial infectious diseases are the most prevalent and common, with effective treatment based on antibiotics, in contrast to infections caused by viruses or fungi. Nevertheless, the use of antibiotics are promoting animal growth, preventing disease in livestock and other food animals, which contributes to the increase rates of antibiotic consumption daily.[1,6] Additionally they have been used as additives in agriculture and food industrial processes. As a consequence, multidrug resistant bacteria (bacteria with resistant genes) are developing and being transferred to humans through consumption of food or environmental spread (ex. human sewage and runoff water).[3]

Nowadays, diagnosis of a disease and prescription of antimicrobial drugs is still based on expertise of the doctor, or in some cases patients are self-medicating or being recommended antibiotics by pharmacists.[2] In centralised laboratories, bacteria are cultured to confirm the presence of infection and acess the correct antibiotic to treat it, a

process taking more than 36 hours considering the following steps: sample collection, sample transport to centralized labs, culturing samples overnight on agar plates followed by a microscopic examination). In acute illness, patients cannot wait such a long period to receive a treatment, therefore ending up with a broad spectrum antibiotic prescription.[2,6] Regarding low income countries, the scarcity of resources and life conditions are the main causes for the increasing rates of infectious diseases as the majority of population do not have access to treatment. Unfortunately, huge quantities of antimicrobials, in particular antibiotics, are wasted globally on patients who do not need them while others who need them cannot afford them.

The development of rapid and accurate point-of-care diagnostics can create a step change into current situation, enabling any healthcare setting in high or low income areas to use a more informed prescription of antimicrobial drugs, slowing down the development of superbugs (resistant bacterial strains).[9,11]

2.2 *Escherichia coli* - the antibiotic resistant superbug

Escherichia coli (E. coli) is one of the gram-negative prokaryotic bacteria that belongs to the Enterobacteriaceae family.[26] Their cell wall consists of a peptidoglycan layer with a cylindrical structure and multiple flagella rearranged around the cell.[26] Extensively studied due to their rapid growth (has a doubling time of approximately 20 minutes) as facultative anaerobes and they are usually non-pathogenic of the human colonic flora.

E. coli is commonly associated with four clinical syndromes: sepsis, neonatal meningitis, urinary tract infections (UTI) and enteric intestinal diseases/diarrhoea.[26] Furthermore it is used as a biological indicator for water quality and depending on the type of disease, it is divided into different 'pathotypes' responsible for intestinal diseases: enterotoxigenic, enteropathogenic, enteroinvasive, enterohaemorrhagic; enteroaggregative and diffusely adherent.[27]

Serological analyses (serotyping) at various levels of complexity are common as a bacterial identification test. The serotyping of *E. coli* is based on their characteristic antigens, which interact with specific antibodies. A bacterial cell surface carries one or more of the following antigens: somatic (O-antigenic polysaccharide or O-antigen) present into lipopolysaccharides (LPS) of the cell outer membrane of Gram-negatives and positives, being generally less defined in the former ones, flagella (H) which are flagellar proteins providing mobility to the bacteria and capsular polysaccharide antigens (K) which are made of carbohydrates of cell capsule.[28] The different antigens or epitopes are polysaccharides (O & K) or proteins (H). Figure 2.1 presents the cell surface and

epitopes, which may be unique for a serogroup or shared, resulting in cross reactions with other serogroups (or serovars) of *E. coli* or even with other Enterobacteriaceae strains.

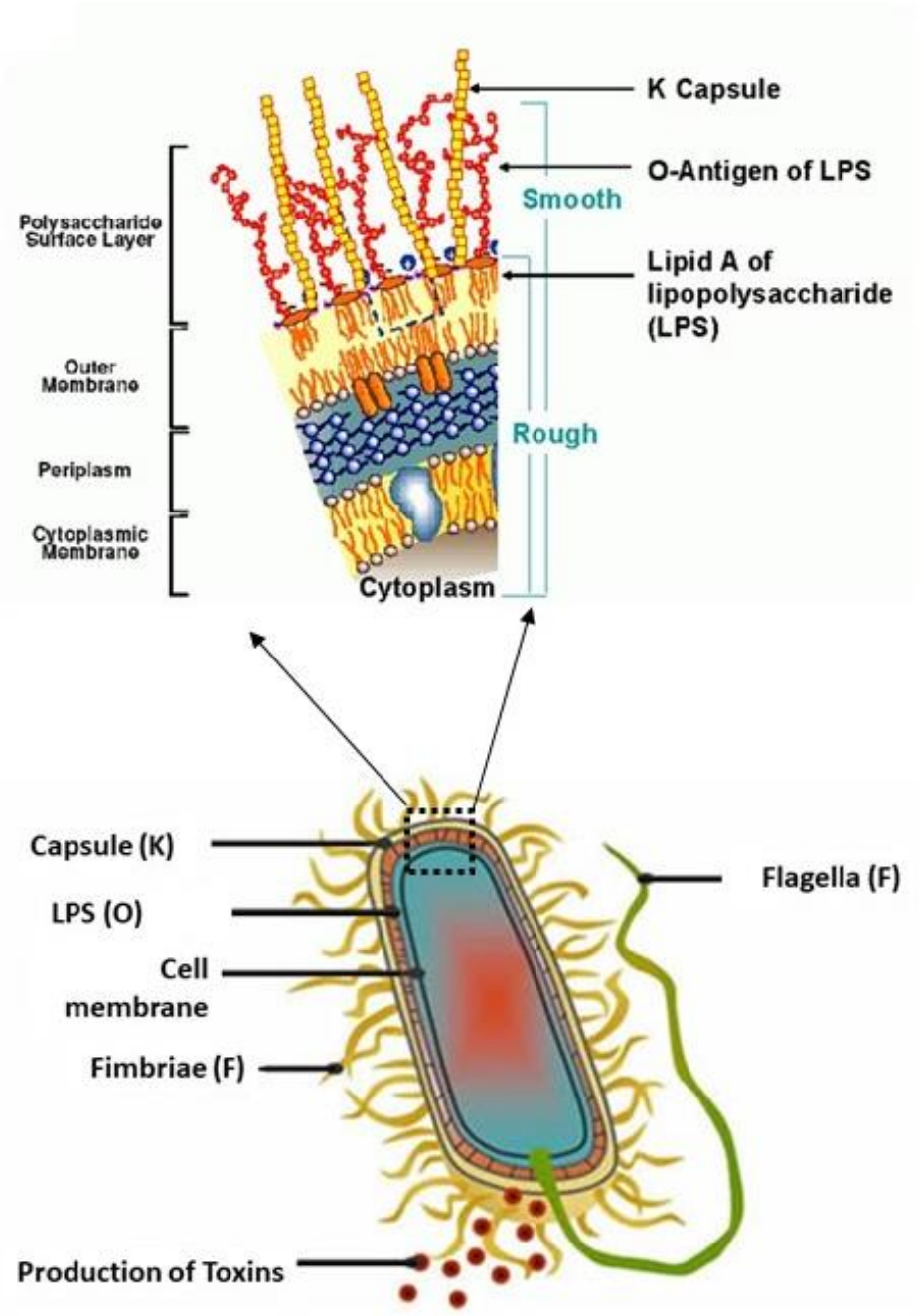

Figure 2.1 Morphology of *E. coli* and outer surface composition: antigens are represented and demonstrated being respectively: somatic antigenic polysaccharide or O-antigen, present into lipopolysaccharides (LPS) of the cell outer membrane of Gram-negatives and positives, flagella (H) antigen consisting in a protein providing mobility to the bacteria and capsular polysaccharide antigens (K) which are made of carbohydrates of cell capsule (adapted from Alexander et al.[29] and online source[30] with permission of Sage Publishing).

Species with well defined antigens are relatively easy to identify based on serology. There are currently known 332 antigens of *E. coli*: 173 O-antigens, 56 H-antigens, and 103 K-antigens. These are valuable in serotyping members of this species.[14,28]

Specific diagnosis of *E. coli* serotypes is totally dependent on the clinical sample being cultured in a centralized clinical laboratory or sophisticated lab based technology such as polymerase chain reaction (PCR).[18,22] Furthermore these methods are long (on average more than 36 h), laborious or expensive.

For instance, PCR technique can be used to make copies of a segment of target DNA, generating a large amount of copies of the initial small sample and for example detect *E. coli*. Firstly *E. coli* sample would be lysed and the purified genetic material (eluate) containing the target DNA sequence (ex. a gene only present in K-12) would be placed in a eppendorf containing specific primers to correct pair the bacterial sequence, nucleotides dNTPs and Tac polymerase resistant to high temperatures. The thermal cycles would be carried out in the PCR device, being characterized by 3 phases: Denaturation at 95ºC for 20-30 sec to split the double chain of DNA, the annealing between 55-65ºC allowing of hybridization the specific primers with complementary extremities in 5'-to-3' direction to each of the single-stranded DNA template and the Extension phase at 72ºC during 10-15 min, where Tac polymerase polymerise the nucleotides in the target sequence elongating the sequence and producing the DNA double chain. Those cycles will be repeated during the time wished and the number of DNA target copies (equivalent to 1 *E. coli* cell) formed after a given number of cycles is given by 2^n, where *n* is the number of cycles[31,32].

UTIs are a major cause of illness affecting mainly women of any age, children and older men.[33] According with The European Urinalysis Guidelines, the limits for symptomatic UTI caused by *Escherichia coli* is 10^3 CFU/ml.[21,22,34,35] There is currently no commercially available test for directly quantify *E. coli* or other UTI-causing bacteria from human urine.[13]

The differentiation of asymptomatic bacteriuria (presence of bacteria in urine) from UTI is subjective and urinary infection symptoms are nonspecific and overlap with numerous other symptoms.[22,34] Generally, the diagnosis of UTIs begins with empirical diagnosis based on typical symptoms (such as pain in back, sometimes blood in urine and so on). Then a quick urine test is performed with colorimetric strip or standard dipstick tests that gives a quick response about the presence of a possible marker of inflamation (presence of nitrite, protein, leukocyte esterase, blood), lacking specificity regarding the correct bacterial strains.[22] This leads to a prescription of a broad range antibiotic. Very often and after a period between 15 days to 6 months, about 50% of

patients will suffer a persistence reoccurrence of the syndromes that can present serious levels as urethritis (urethra infection) and pyelonephritis (severe kidney infection). Very often complicated UTIs are associated to catheter use in hospital, leading to serious pyelonephritis with sepsis, renal damage in young children and further high-level of antibiotic resistance.[20–22]

A reduction of unecessary use of antimicrobials is intrinsically correlated to rapid and accurate diagnostics, which could slow down the pace of multi-drug resistant pathogen. Globally, extended-spectrum beta-lactamase (ESBL) Enterobacteriaceae, fluoroquinolone-resistant *Pseudomonas* and methicillin-resistant *staphylococcus aureus* (MRSA) are among the most challenging public health issues.[7,13] Figure 2.2 shows the distribution of ESBL geographically according level of resistance to the last generation of antibiotics (cephalosporins).

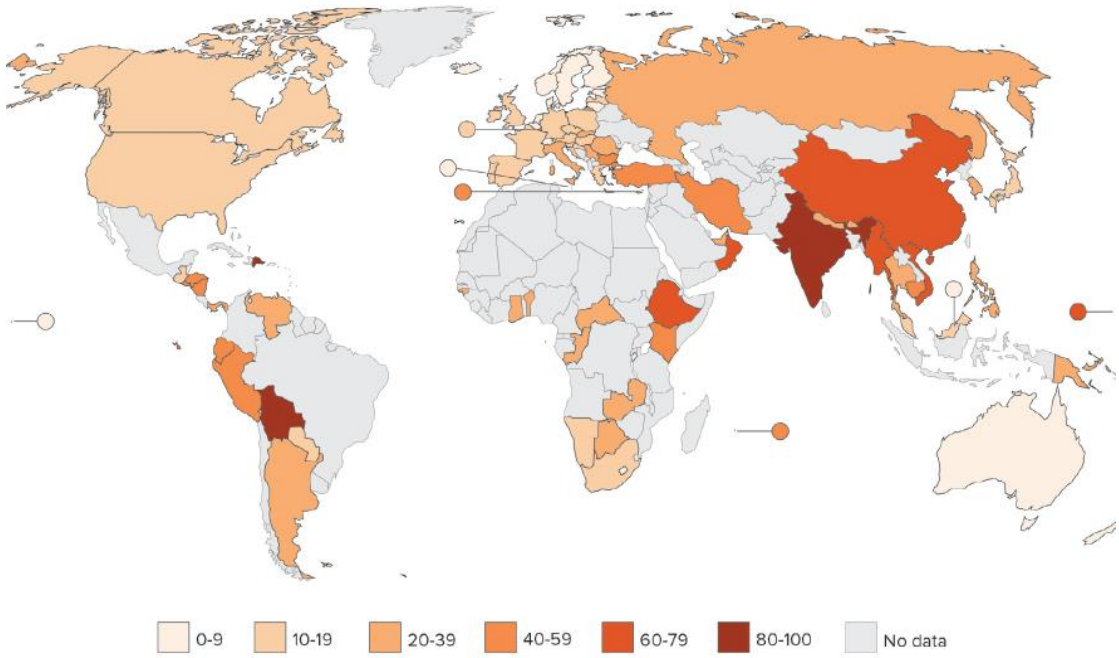

Figure 2.2 Percentage of extended-spectrum beta-lactamase resistant to the third-generation of cephalosporin, by country from 2011 to 2014, adapted from O'neill[2] (with source permission from CDDEP 2015 and WHO 2014).

2.3 Bacterial detection methods

Culture and colony counting-based microbiological method has been used as the gold standard for bacteria identification and quantitation owing to its high sensitivity, ideal specificity, and good reliability.[18] Although powerful, this approach is not suitable for POC testing and rapid screening due to labour-intensive manipulation, time-consuming culture, requiring highly trained people and laboratory facilities.[14,36] Polymerase chain reaction (PCR) is a culture-free technique allowing rapid and multiplexed assay of pathogenic bacteria.[18] However, it is only applicable to DNA and RNA and usually requires cell disruption and nucleic acid extracting, thus limiting its usage in POC testing. In the last few years, molecular recognition, such as antibody, aptamers, polypeptide, bacteriophage and proteins, has become more suitable for direct assaying whole cells of pathogenic bacteria.[18] Some of those methods present requirements as high assay speed, simple manipulation and easy development of portable POC devices, which become an attractive potential to be applied in microfluidic platforms.[14,37–39]

Regarding *E. coli* infections, namely UTIs induce the symptomatic disease and cause serious health effects to the patient. Lately, lateral flow assays, colorimetric strips to detect presence of nitrite and μPADs (microfluidic paper analytical devices) are the approach applied in the available commercial kits to detect an UTI in urine sample, in parallel to the laborious task of urine culture. Urine is a complicated bio-fluid that usually requires sample pretreatment, such as purification and/or enrichment steps prior to analytical steps to determine specific components in the urine.[13,40,41] Nevertheless benchtop-based protocols increase the prevalence of cross contamination cultures, demanding in average large sample volume. Thus, there is a need for automated, miniaturized, inexpensive and easy-to use microdevices for urinalisis.

Lately, microfluidic biosensors for pathogen detection rely dominantly in methods based in antibody recognition.[42] Immunoassays offering a high degree of selectivity in many applications, they demand signal amplification mainly in lower concentration of bacterial sample, achieved by use of enzymes.[43] In addition, multi-step assays are preferable due high sensitivity and specificity offered and suitable for miniaturization format compatible with POC.[44]

2.4 Immunoassay Fundamentals

Immunoassays are a powerful bioanalytical tool developed to measure the presence of an analyte through antigen-antibody interaction. The sensitivity and specificity of the immunoassays is highly dependent on the choice of antibodies and their

affinity to the target molecule. ELISA (enzyme-linked immunosorbent assay) and enzyme immunoassay (EIA) are immunological techniques to describe the same technology. ELISA is a plate-based assay technique where the target antigen must be immobilized on a solid surface and then complexed with an antibody that is linked to an enzyme. The signal detected from this techniques can be radioactive, colorimetric or fluorescent.[14,45]

Antibody (Ab), also known as immunoglobulin or glycoprotein, is produced mainly by plasma cells (also called B cells or B-lymphocytes) that are used by the immune systems to identify and neutralize pathogens such as bacteria and viruses. Furthermore, it has high ability for biorecognition and to bind molecules and complexes, denominated antigens. Therefore are indispensable molecules for broad application including diagnosis and disease prevention.[14,46]

Animals are routinely used as host organisms to produce polyclonal and monoclonal antibodies. An Ab molecule presents a "Y" shape molecule, as shown in Figure 2.3, consisting of two pairs of identical polypeptide chains, named light and heavy chains linked by disulphide (-SS-) bonds, responsible for stabilizing the molecular structure. The two variable domains on the light (VL) and heavy (VH) chains make up the antigen (Ag) recognition and binding site.

The amino acid sequence of antigen binding site is highly variable and this contributes to the broad recognition of the antibody to a wide range of target molecules. The antigen fragment (Fab) contains the variable domains of light and heavy chains, plus the first constant domains, while the constant fragment (Fc) is composed by constant domains (C) and disulphide bonds (-SS-), which binds to the Fc receptors located on many mammalian cells.

Immunoglobulin exist as 5 different classes: IgA, IgG, IgM, IgE, and IgD (rare) and subclasses which slightly vary between humans and other species.[14,45] For immunoassay applications, IgG class is highly desirable due to their stability, binding affinity, high retention time on cell surface receptors and low cross reactivity.[47]

The antibody's ability to recognize and bind with high affinity to specific antigenic sites (denominated epitopes or complementarity determining regions (CDR's)) is exploited for qualitative and quantitative measurement of the antigens, even in a complex mixture. To obtain a successful immunoassay, the production and selection of a suitable antibody is imperative, which depends on the assay parameters.[14,48] Conventional immunoassay methods such as lateral flow and enzyme-linked immunoassays (ELISA) are the most applied in commercially available immunoassays and therefore widely used.[49]

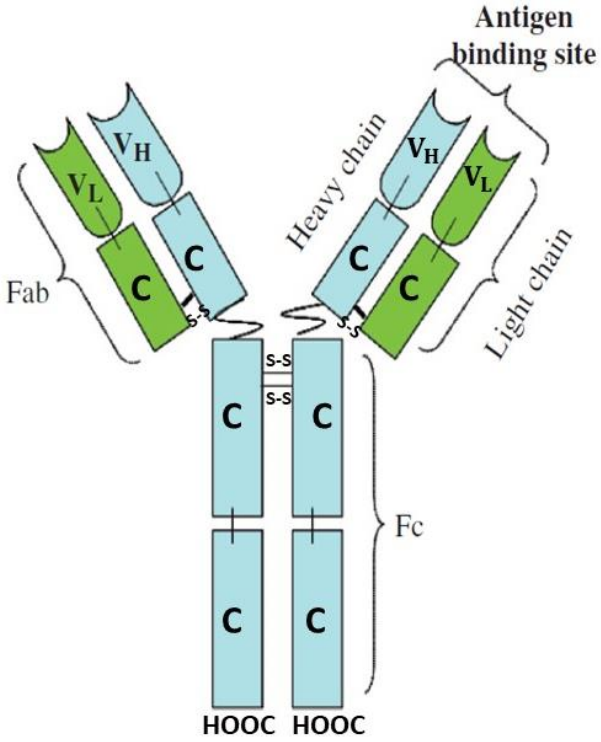

Figure 2.3 Scheme representative of Immunoglobulin (IgG) structure molecule, adapted from Zourob[14]. On the whole antibody (IgG) molecule, the heavy chain is blue and the light chain is green. Antigen binding receptor is located in Fab domain while Fc is composed bye constant domains C and disuphide bonds (-SS) which confers stability of IgG and bonds light to the heavy chains.

A polyclonal antibody (PAb) is a heterogeneous mixture of antibody molecules arising from a variety of constantly evolving B-lymphocytes, so that even successive bleeds from one animal are unique. PAbs recognize multiple antigens or multiple epitopes located on the same antigen, in contrast, a monoclonal antibody recognizes only a specific epitope on an antigen.[14,49] For bacterial detection, PAbs were widely used by early immunologists and microbiologists for their ability to react with a variety of epitopes of bacteria. PAbs are also more stable over a broad pH and salt concentration, whereas MAbs can be highly susceptible to small changes in both.[49]

Commercial assays use polyclonal antibodies due to the high cost involved in the production of monoclonal antibodies and because they also found to be superior in capturing and concentrating target molecules.[46] The type of antibodies (PAb vs. MAb) to be used depends on the specific application. Whenever possible, monoclonal antibodies are preferred due their high specificity, however the production of a target-specific and

high performance antibody depends on the proper strategy in selecting and delivering the antigenic molecules.[14,46,49]

2.4.1. Antibody-antigen interaction

The strength of interaction between a single epitope and antigen binding site is called its affinity and it is determined by the sum of multiple non-covalent bonds. Each antibody-antigen interaction has a distinct affinity, which affects the reaction kinetics and therefore the speed and sensitivity of the immunoassay. Whereas the affinity of an antibody reflects its binding energy to a single epitope, avidity reflects the overall binding intensity between antibodies and a multivalent antigen presenting multiple epitopes. Avidity is determined by the affinity of the antibody for the epitope, the number of antibody binding sites, and the geometry of the resulting antibody-antigen complexes.[47,49–51]

Equilibrium binding equation (Equation 2.1) is represented for the law of mass reaction, where $[\mathrm{Ag}]$ is the concentration of antigen, $[\mathrm{Ab}]$ the concentration of antibody, $[\mathrm{Ag}-\mathrm{Ab}]$ the concentration of antigen-antibody complex and K_{eq} is the equilibrium or affinity constant, which represents the ratio of bound and unbound analyte – antibody.[47,51]

$$[Ag] + [Ab] \overset{K_{eq}}{\longleftrightarrow} [Ag - Ab] \tag{2.1}$$

The equilibrium binding is a fundamental key to understand and maximize antibody performance in immunoassays. According to the Scatchard model, the Ab-Ag equilibrium is given by Equation 2.2:

$$\frac{B}{F} = K_{eq}(N - B) \tag{2.2}$$

where B and F represent the concentration of bound and free antibody, K_{eq} is the affinity constant, and $(N - B)$ is the concentration of unoccupied sites. If binding is weak the equilibrium will be shifted to the left. If binding is strong, equilibrium will be shifted to the right.[47]

2.4.2. Possible immunoassay configurations

Homogeneous methods have been developed for large and small analytes using both competitive and non-competitive protocols. They are characterized by adding all

sample and reagents in a single step where rate of binding reaction is not limited by slow diffusion, decreasing incubation time and reducing automation requirements.[43] For instance, direct ELISA is implemented in one step when analyte contacts the sensor's receptor layer. Direct ELISA is typically used in analysis of an antigen immune response, in contrast to heterogeneous assays where immunoassay are developed in multi steps, allowing to constituents be removed easily by a wash step, minimizing variations in signal caused by nonspecific effects of the sample matrix.[43]

Immunological methods combine a specific antibody-antigen interaction and an efficient catalysis between enzyme-substrate resulting a chromogenic, radioactive or fluorescent signal.[48] The specific association of antigens and antibodies is dependent on the lock and key complex (for ex. enzyme - substrate, antigen - antibody) and affinity between the two molecules on the solid surface. There are three different heterogeneous ELISA assays formats[48]: competitive, indirect and sandwich ELISA (described by Figure 2.4).

In competitive ELISA (Figure 2.4A), the primary antibody is mixed in a separate tube with various dilutions of bacteria (or antigen) and added to the wells containing immobilized antigen. Only the free, unbound antibody will bind the immobilized antigen. A secondary antibody-enzyme conjugate and substrate system is added for colorimetric detection. The signal reaction measured is inversely proportional to the concentration of bacteria. Despite cross reactivity be a challenge typical in ELISA, this format is more susceptible to signal interference, where non target analytes in a sample compete for binding sites on antibody, resulting in inaccurate analyte concentration being determined. It is commonly used for detecting small antigens that cannot be bound by two different antibodies or when only one antibody is available for the antigen of interest.[14,47,48]

In indirect ELISA (Figure 2.4B), the antigen from the sample is previously immobilized in the wells of a microtiter plate and then added to the antibody solution. A secondary antibody conjugated with substrate modifying enzyme, e.g., horseradish peroxidase (HRP) or alkaline phosphatase (AP), is added to bind to the primary antibody, and the reaction is developed with a suitable substrate to produce a colour reaction. If a fluorescent molecule (e.g., FITC, Atthophos®) is used, the reaction is quantified by the amount of fluorescence emitted proportional to concentration of antigen[14,48]. Indirect ELISA is suitable for quantification of total antibody concentration present in samples. Sandwich assays (Figure 2.4C) tend to be more sensitive and robust and therefore tend to be the most commonly used. It works similarly to indirect ELISA, except that capture antibody (capAb) is firstly immobilized in microtiter plates, followed by antigen incubation.

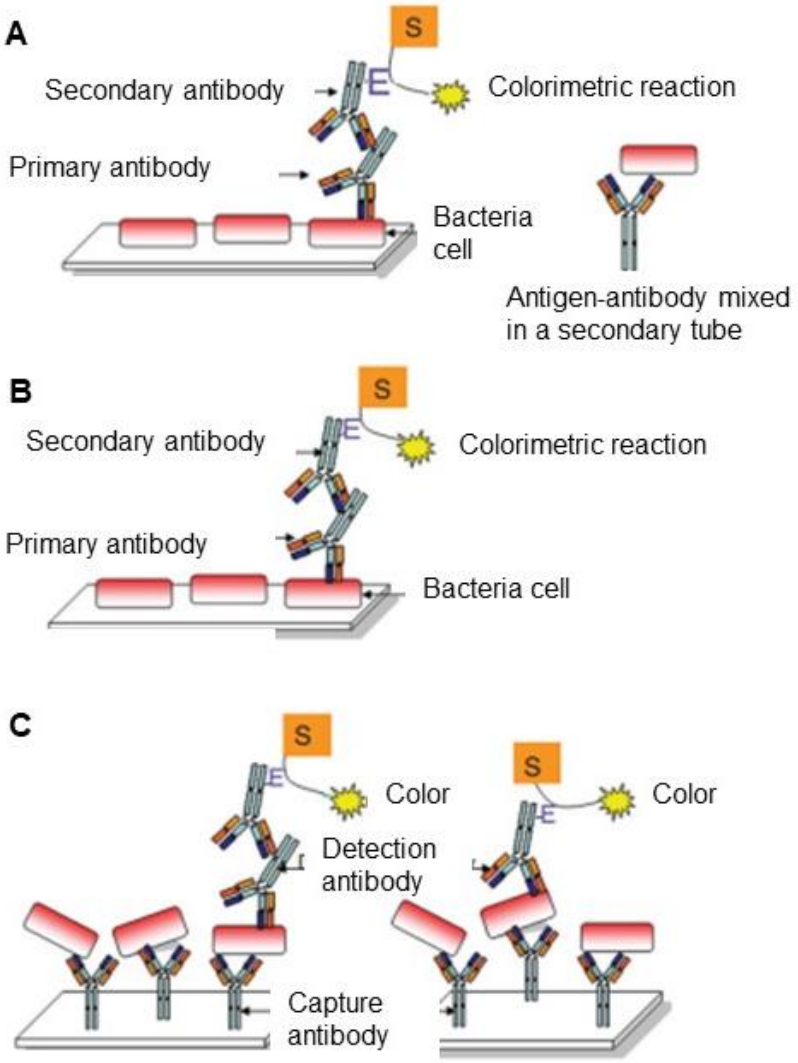

Figure 2.4 Heterogeneous ELISA formats for bacteria colorimetric detection (E =enzyme; S = substrate). **A** Competitive ELISA. **B** Indirect ELISA. **C** Sandwich ELISA, adapted from Zourob[14] (with permission of Springer).

The reaction is developed adding a detection antibody (detAb) forming a complex sandwich with capAb-antigen-detAb.

Afterwards enzyme is added and respective enzymatic subtract (FITC, Atthophos®) for fluorescence signal quantitation. This format is preferable when it is aimed to quantify lower concentrations of analyte and reduce the non-specific binding. This method is highly suitable for complex matrix samples analysis and normally does not need pre-treatment sample prior to measurement.[47,48]

For better understanding of each ELISA format Table 2.1 summarizes the main advantages and disadvantages.

Table 2.1 Summary of advantages and disadvantages of possible immunoassay configurations.[52–56]

Types of ELISA	Advantages	Disadvantages
Direct	➢ Faster ➢ Less prone to error due require no steps	❖ Immunoreactivity with enzymes ❖ High background ❖ No flexibility in pair of antibodies. ❖ Minimal signal amplification-reducing signal sensitivity
Indirect	➢ Wide commercial availability of detAb ➢ Versatile ➢ High sensitivity Allows signal amplification	❖ Cross-reactivity from detAb ❖ Background ❖ Extra incubation step is required in the procedure
Competitive	➢ Less variability ➢ More consistent assay ➢ No sample pre treatment	❖ Complex procedure steps ❖ Limited to small antigens that cannot bind to capAb and detAb as in sandwich assay
Sandwich	➢ High sensitivity ➢ High specificity ➢ High throughput in complex matrix samples	❖ Cross-reactivity might occur

2.4.3. Immunoassay Performance

The success of assay development is intrinsically related to key parameters to evaluate performance. Specificity, sensitivity, precision or reproducibility, calibration model and limit of quantification are some core characteristics to be accessed early on development.[52,55,57]

Precision, also known as reproducibility or variability of the assay, gives the level of confidence of the assay performance. It expresses the coefficient of variation (CV) for each specific analyte concentration point. When precision is evaluated in the same assay experiment is named intra-assay, if it is accessed in different assay runs is denominated inter-assay variability. The limit of acceptance recommended for intra-assay precision is ≤ 10% and inter-assay precision between 20 - 25 %.[15,43,55,58]

Assay specificity is highly dependent of the specificity of antibody directed against the bacteria/analyte. This parameter evaluates the capability of assay to detect or quantify unequivocally the target, even in presence of other components in the sample analysed. Biological samples present complex matrices that can highly increase non specificity. For instance urine is composed by around 95% water and 5% of solids that are generally urea, uric acid, chloride, sodium potassium, creatinine and other dissolved ions, inorganic and organic compounds (proteins, hormones and metabolites). Therefore, sample preparation is often an extra step considered in attempt to reduce any interference by pH, viscosity sample, and presence of urine constituents or even the presence of other bacterial strains common in UTI as *Pseudomonas sp, Klebsiella sp*. and *Enterobacteriaceae sp.*[15,45,57]

Calibration models enables determine the response-error relationship denominated ‘’curve fitting’’ or just ‘’response curve’’ between experimental data and parameters estimated. Four parameter logistic model (4PL) is the reference model for many immunoassays providing an accurate representation of the fitting between experimental measured response and theoretical response expected by the equation[15]:

$$y = d + \frac{a-d}{1+\left(\frac{x}{c}\right)^{b}} \tag{2.3}$$

where x is the concentration of analyte known, y is the cromogenic or fluorescence signal quantified, a the minimum value that can be obtained by the assay, d is the maximum colorimetric or fluorescent value obtained from the assay, c the point of inflection of

sigmoidal curve, (halfway between a and d), b the slope of the curve related to the steepness at inflection point.[59]

The limit of quantitation is provided by the highest and lowest concentration of analyte in a sample denominated validated range or dynamic range. They are determined from the lower limit of detection (LLoD) to the upper limit of detection (ULoD) which requirements for each dynamic range vary according assay and analyte target. Accuracy and precision of detection dynamic range is determined from the lower limit of detection quantified, from Equation 2.4, which means the lowest concentration of an analyte detected in a sample, but not necessarily quantified. [15,48]

$$LLoD = Blank + (3 * \sigma) \quad (2.4)$$

where $blank$ represent the signal quantified by the negative control or diluent sample without antigen, σ is the standard deviation of measurement and lower limit of quantitation is given by Equation 2.5 and represent the lowest concentration of analyte determined in a sample with acceptable precision and accuracy according protocol conditions.[60]

$$LLoQ = Blank + (10 * \sigma) \quad (2.5)$$

Providing those values gives insight into positional biases and the precision profile. Nevertheless sensitivity evaluates the capacity of the assay to detect the lowest analyte concentration which is different of value of cut off or blank (sample without analyte). This parameter is assessed by comparing several replicates being the limit of sensitivity determined by lower limit of detection according Equation 2.4.

2.4.4. Immunoassay standard platform and general considerations

Microtiter plate (MTP) is the standard platform for ELISA worldwide used (see Figure 2.5A). It is produced from polystyrene and characterized by 96-well format, arranged in 8 rows by 12 columns. It presents a maximum volume capacity of 300 µl with 80% of volume surface effectively usable (Figure 2.5B).

Dependent on a non-portable and expensive microtiter reader, MTP also does not provide flow, is time consuming (each immunoassay needing long time incubations, normally more than 1 hour due transport limitations) and demands high reagent volumes.[43,52]

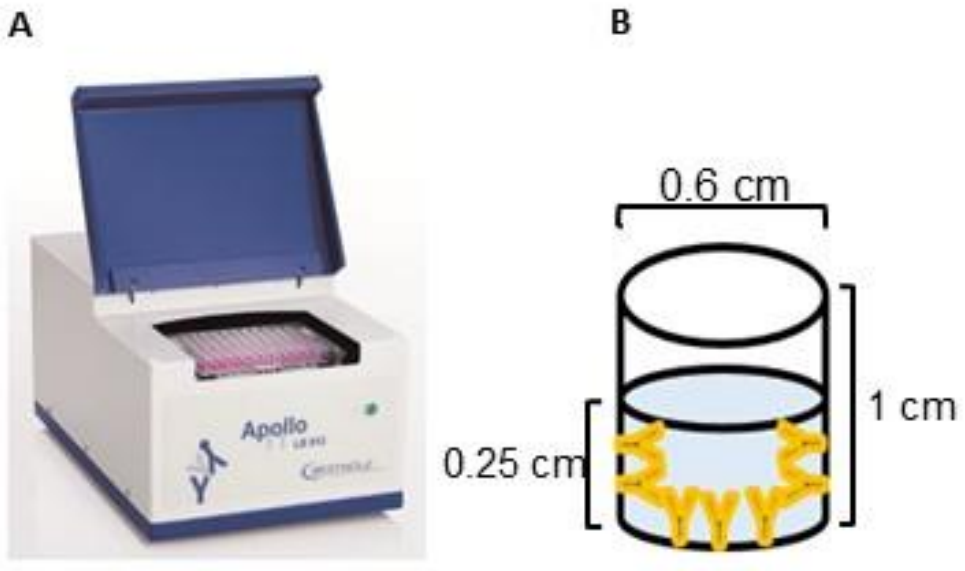

Figure 2.5 Standard platform of immunoassay. **A** Microplate reader and microtiter plate (MTP) adopted from Berthold Technologies[61]. **B** Structure and dimensions of a single well of a 96-well plate filled with 100 µl of reagent.

Enzymes are considered biocatalysts accelerating bioconversions and transformations of subtracts in specific products being the most widely used in antibody conjugation. In immunoassays, the most versatile and common enzymes are horseradish peroxidase (HRP) and alkaline phosphatase (AP). Those enzymes are bound to detection antibody via biotin. The substrate conversion is respectively H_2O_2 and Atthophos to produce a colorimetric and fluorescent signal. Like the antibodies, enzymes are susceptible to pH, and temperature variation which can affect immunoassay performance.[43,62] Therefore, understanding optimal reaction conditions regarding enzyme concentration, buffer diluent and time incubation are fundamental to achieve maximum rate and perform immunoassay in less time with high throughput and sensitivity. The kinetics of enzymatic reaction is described by a linear rate with substrate concentration conversion until reaches saturation at maximum. This means all active sites of enzyme are occupied which intrinsic enzymatic rate per second is described by Kinetics of Michaelis–Menten model[62]:

$$v_0 = \frac{v_{max}.[S]}{K_M + [S]} \tag{2.6}$$

$$v_{max} = K_s.C_E \tag{2.7}$$

where v_0 the initial reaction velocity, $[S]$ the substrate concentration, C_E the enzyme concentration, v_{max} the maximum reaction velocity, K_M correspond to the substrate concentration where $v = \frac{1}{2} v_{max}$, and K_s the enzyme turnover number or dissociation enzyme-substrate constant.

2.5 Microfluidic platforms for bacterial detection and quantification

Sensitive, specific and rapid pathogen detection methods are crucial in POC diagnostics[19,42,63], bioterrorism defence[14], food safety[18] and drug production.[36,37] The current 'ASSURED' POC microfluidic devices struggle to achieve lower limits of detection of bacteria with high sensitivity and specificity unable to early detection of such infections. The clinical threshold for symptomatic UTI caused by *E. coli* is 10^3 CFU/ml[21,22,34], which is intrinsically difficult to achieve in a conventional 'dip stick' test or a microfluidic test, the last related to the very small sample volumes used. Currently, diagnosis industry has failed to find any microfluidic platform that suits those ASSURED requirements in a format compatible to point-of-care. Therefore healthcare systems face a technological gap by the absence of any commercially available test capable to detect directly from human urine *E. coli* or other UTI-causing bacteria.[12,13]

Recently, novel sensors and assays for rapid pathogen detection have been proposed, including the capture of whole pathogen cells or molecular fragments for further amplification and identification, with detection methods using a variety of transducing technologies (optical, electrochemical, surface plasmon resonance and piezoelectric)[17,64,65,66–71,72,73,74] Sensitive detection methods such as immunoassays are broadly applied for biomolecules.[68]

Microfluidic platforms are suitable for this purpose, as they allow fluid volumes manipulation in pico- and nanoliter range with easy accurate transport and cells positioning.[68] Pathogen sensing demands disposable systems to eliminate the risk of cross-contamination, so there is a need to minimize the cost of materials involved in microfabrication of technological devices.

Controversially, many drugs companies producing affordable generic antibiotics present challenges to improving diagnostics, having no commercial interest in the advent of rapid microfluidic diagnostics.[2] Improving diagnosis has the impact of improving life quality and average life expectancy but would act to limit the antibiotic prescription.

Mass device fabrication in a cost-effective way and technological challenges as sample pre-treament, compatibility with fluorescence detection and chemical resistance explain why use of microfluidic diagnostics in clinicians' offices and patient's homes is

not yet widespread.[2] Prize initiatives in the UK, USA and EU have been important catalysts in raising attention for the need for rapid POC diagnostics. Longitude prize is one example to promote an accurate, rapid, affordable and easy to use anywhere in the world.[75] But to sustain innovation in the medium and long term, and to encourage uptake of the resultant technology, further and more sustained interventions are needed.[2,6]

Therefore, finding new, cost effective, and simple approaches for simple signal detection and readout systems, fluid actuation and storing reagents on chip are essential for broad POC diagnostics commercialisation.[76] Miniaturization of immunoassays increases the challenges regarding surface tension, reduced volume of sample in lower concentration samples and influence the antibody-antigen kinetics.

Biological fluids (blood, urine, saliva) present increased levels of viscosity that bring additional surface tension into microfluidic platforms, affecting sample distribution and accuracy of results. In addition, handling lower sample volumes means less bacterial cells per sample which is challenging for achieving lower LoD and high sensitivity, although analyte concentration is the same. Shear stress from reagents and sample flow might represent a drawback in quantitation systems using antibodies immobilized in surface wall, being fundamental understanding the binding between bacteria-capture antibody.[22,74,77]

On the other hand, miniaturization of immunoassays exploits the potential of reduced diffusion distance between capture antibody and antigen, enabling scientists to reduce time of immunoassay and therefore reduce equilibrium time. Therefore increasing the reactivity of the system with incremented surface-area-to-volume ratio (SVR), making immunoassays more sensitive and faster. Development of quantitative heterogeneous immunoassays at microscale has promoted the reduction of environmental space and need for sophistated facilities, making them affordable and pratical anywhere.[9,74]

The current ASSURED POC microfluidic devices struggle to quantify low detection limits with high sensitivity and specificity in a short time window to enable early detection of such infections without extra steps.[10,66,78] Despite the limitations highlighted above, several microfluidic devices were developed with the capability of performing sensitive *E. coli* detection and quantitation from biological or synthetic samples.[5,13,19] Majority of those devices use immunoassays or other detection techniques mentioned previously.

Table 2.2 summarises a few microfluidic assays reported in the literature for pathogen detection. The review foccused in target bacteria, method of detection in sensing platform, limit of detection (LoD), pretreatment steps, assay time and the type of sample. The most commonly targeted pathogens in those biosensing platforms are: *E.*

coli, Salmonella sp., *Staphylococcus aureus*, *Pseudomonas sp*. and *Klebsiella pneumonia*. All these bacteria are commonly recognized as superbugs of antibiotics resistance and responsible for a wide range of symptomatic infections as UTIs and sepsis.[79] For instance, Chang et al.[41] have presented a microfluidic chip embedded with antimicrobial peptides (AMPs) able to detect 10 cells/ml in 20 min. Wang et al.[80] have shown a microfluidics fluorescence assay able to quantify 50 CFU/ml of *E. coli* in 30 min testing blood and buffer but with extra filtering step. Golberg et al.[67] and Yoo et al.[16] have reported microfluidic fluorescence assay approaches with LoD below 10^3 CFU/ml, however those approaches require sample pretretament or long assay times. Cho et al.[13] and Olanrewaju et al.[12] shown fastest microfluidic platforms to quantify *E. coli* with LoD matching the clinical threshold for an UTI in less than 10 min of total assay. It is important to highlight that *E. coli* O157:H7 is often presented as bacteria case study, reported in those microfluidic platforms due the huge commercial availability of antibodies, however they are not cause–related to symptomatic UTIs.

Table 2.3 Summary of microfluidic assay previously reported for pathogen detection in literature. Reported techniques are compared regarding target bacteria, method of detection, sensing platform, limit of detection (LoD), pretreatment, assay time and the type of sample.

Reference	Pathogen	Detection method	LoD - *E. coli*	Pretreatment	Assay time	Sample
Liao et al. 2006[81]	*E. coli, P. mirabilis, K.pneumoniae, E.aerogenes, Pseudomonas sp., Enterococcus sp.*	Micro-fabricated electrode array	2.6×10^8 CFU/ml	Lysis	45 min	Urine
Boehm et al. 2007[82]	*E. coli* (BL21(DE3))	Impedance-based microfluidic biosensor	10^4 CFU/ml	-	-	synthetic
Lackza et al. 2011[83]	*E. coli and Salmonella sp.*	EIS microelectrode Capacitive Immunosensor	10^4-10^5 cells/ml	-	1 h	PBS
Bercovici et al. 2011[84]	*E. coli*	Microfluidic isotachophoresis with FRET	10^6 CFU/ml	Centrifugation, lysis and dilution	15 min	Urine
Yang et al. 2011[81]	*E. coli*	Microfluidic cell impedance assay	3.4×10^4 CFU/ml	-	100 min	synthetic urine
Sanvicens N. 2011[85]	*E. coli* O157:H7	fluorescent quantum dot-based antibody array	10 CFU/ml	-	2 h	PBS
Safavieh et al. 2012[17]	*E. coli*	Microfluidic LAMP with electrochemical detection	48 CFU/ml	Filtration	60 min	filtered urine
Zhu et al. 2012[39]	*E. coli* O157:H7	Quantum dot immunoassay	5-10 CFU/ml	-	> 1.5 h	2% gelatine–PBS, food matrix
Wang et al. 2012[80]	*E. coli*	Microfluidic fluorescence assay	50 CFU/ml	Filtering	30 min	PBS, blood and food

Table 2.3 Summary of microfluidic assay previously reported for pathogen detection in literature. Reported techniques are compared regarding target bacteria, method of detection, sensing platform, limit of detection (LoD), pretreatment, assay time and the type of sample (continuation).

Reference	Pathogen	Detection method	LoD - *E. coli*	Pretreatment	Assay time	Sample
David et al. 2013[36]	*E. coli* O157:H7	Ac electrical impedance lab on a chip	10^2 cells/ml	-	-	HBS buffer
Yoo et al. 2014[16]	*E. coli*	Microfluidic fluorescence assay	10^3 CFU/ml	-	30 min + 45 min staining	PBS
Golberg et al. 2014[67]	*E. coli*	Microfluidic fluorescence assay	150 CFU/ml	Filtering, incubation on-chip enrichment	8 h	water with feces
Stratz et al. 2014 [68]	*E. coli* O157:H7	Immunoassay- based analysis on-Chip Enzyme Quantification	Single *E. coli* / β-glucosidase	-	3 h	culture medium
Safavieh M. 2014[64]	*E. coli*	Ribbon cassette LAMP with colorimetry	30 CFU/ml	-	<1 h	water
Rajendran V. 2014[86]	*Salmonella spp.* and *E. coli* O157	Smartphone based bacterial detection using biofunctionalized fluorescent nanoparticles	< 10^5 CFU/mL	-	> 10 min	PBS
Cho et al. 2015[13]	*E. coli and N. gonorrhoeae*	Smartphone using microfluidic paper analytical device (μPAD) was	10 CFU/ml	1% Tween 80	> 5 min	urine
Shih et al. 2015[40]	*E. coli* DH-5α	Paper based ELISA	10^4-10^5 cells/ml	-	5 h	culture medium
Chang et al. 2015[41]	*E. coli* O157:H7	Microfluidic chip embedded with AMPs	10 cells/ml	-	20 min	PBS

Table 2.3 Summary of microfluidic assay previously reported for pathogen detection in literature. Reported techniques are compared regarding target bacteria, method of detection, sensing platform, limit of detection (LoD), pretreatment, assay time and the type of sample (continuation).

Reference	**Pathogen**	**Detection method**	**LoD - *E. coli***	**Pretreatment**	Assay time	**Sample**
Angus et al. 2015[87]	*E. coli* K12	surface-heated droplet PCR	10^3 genome copies per sample	-	19 min	buffer
Chang et al. 2015	*E. coli, S. aureous, P. syringae, Enterococcus sp., Staphylococci sp.*	Colorimetric/ PCR on a chip	10^2 CFU/ml	Automated washing	30 min + 40 min PCR	Human fluid
Kokkinis et al. 2016 [4]	*E. coli* K12	Bitinylated antibodies funcionalized with magnetic microparticles	Positive/negative signal	Centrifugal separation	≥ 90 min	PBS-Tween 20 (0.01% v/v)
Olanrewaju A. et al. 2017[12]	*E. coli* O157:H7	microfluidic capillaric circuit (CC) with antibody-functionalized microbeads	1.2×10^2 CFU/ml	-	< 7 min	synthetic urine

2.6 Microfluidic platform materials

First microfluidic platforms were fabricated by silicon and glass, although lately microfluidic pathogen sensing devices are based on polymeric materials, such as poly-(methylmethacrylate) (PMMA), polycarbonate (PC) and poly(dimethylsiloxane) (PDMS). Polymers like PDMS are known as rubber –like elastomers offering optical transparency, potential for down-scaling, disposability, they are a cheaper material compared to silicon or glass.[42,88,89] Besides polymers offer the potential of easy manufacturing, reconfiguration, microfabrication and injection molding. PDMS was firstly introduced by George Whiteside's group[76] in optical microfluidic devices fabrication, being widely applied in several microfluidic fields.[90] On the other hand PDMS properties present some limitations regarding not compatibility with high temperatures (PDMS degradation above 200℃)[91], challenging integrations with eletrodes on its surface, possibility to react and absorb hydrophobic molecules and tendency to adsorb proteins on their surface.[92]

Fluoropolymers are a good alternative to the conventional PDMS, glass or silicon devices. It present unique optical and dielectrical properties, flexibility and chemical inertness.[93,94] Initially, fluoropolymer films were exploited for the simple production of valves and pumps in glass microfluidic devices, similarly to PDMS counterparts.[95] Microcapillary film (MCF) is a novel microfluidic platform which exploit the low cost manufacturing process of fluoropolymer FEP-Teflon® and benefit of potential properties such as optical transparency, resistance to weathering, higher eletric conductivity, low friction and non-stick characterists, and withstand at extreme temperatures (FEP degradation temperature above 260-300 ℃).[96]

2.6.1. Fluorinated Microcapillary Films

Immunoassays can be conducted using a microcapillary film which is a novel and cheap engineered material made from fluorinated ethylene propylene (FEP Teflon®) by melt extrusion process.[97] Fluorinated ethylene propylene is a copolymer of hexafluoropropylene and tetrafluoroethylene which contains strong carbon-fluorinated bonds.[93] Microcapillary film was first presented as a cost-effective microfluidic immunoassay platform by Edwards et al.[97] It consists in a flat plastic ribbon containing 10 embedded capillaries (Figure 2.6) with mean internal diameter 206 ± 12.2 μm.[97]

MCF is manufactured by Lamina Dielectrics Ltd (Billingshurst, West Sussex, UK). The external dimensions of the MCF were 4.5 ± 0.10 mm wide and 0.6 ± 0.05 mm thick.

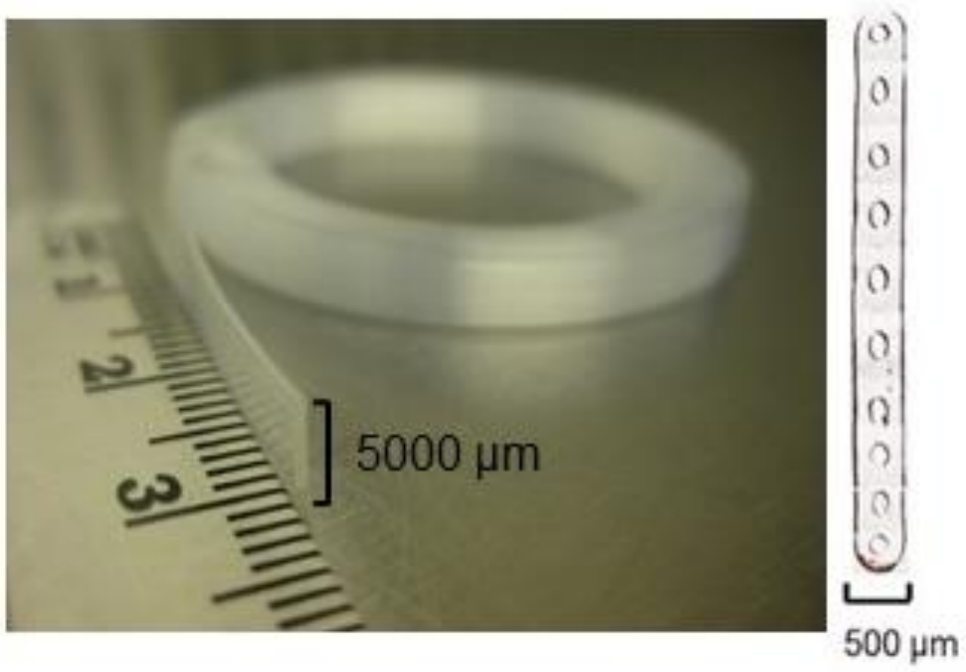

Figure 2.6 The MCF reel and cross section with ten 200 µm channels embedded in the FEP polymer. (Acknowledgemnt to Dr Ana Barbosa for providing this picture and with her permission)

The flat film geometry allows simple yet effective immobilisation of antibodies for immunoassays by passive adsorption on the plastic surface of the microcapillaries due their hydrophobic surface.[97]

Furthermore, MCF presents exceptional optical transparency with flat parallel faces providing a short path length through the wall with no curvature to refract the light. Similarly, the MCF has a refractive index of 1.338, very close to water (1.333).[97] This produces minimal optical refraction at the water-MCF interface allowing simple optical detection of colorimetric substrates, resulting in high signal-to-noise ratio (SNR) which is fundamental for sensitive signal quantitation. The MCF platform has demonstrated to be capable of performing up to ten different parallel microfluidic assays when dipped into a single sample whilst providing relevant optical information. It is possible to perform multiplex immunoassays and collect different reagents in each capillary, individual capillaries can be fitted with a fine needle and syringe.[25] MCF platform can provide flow, presents flexible signal detection able to be detected by cost effective equipment as smartphone, flatbed scanner or camera; is portable and therefore suitable for point-of-care diagnostics.

Moreover, its surface-area-to-volume ratio (SVR) allows the limit of detection to increase in comparison with MTP.[23,24,98] A clear example is the lab-in-briefcase concept for prostate cancer biomarker detection reported by Barbosa et al.[23] showing a major

capability from this material demonstrating 80 measurements at same time in less than 15 minutes due to the significantly reduced incubation times.

MCF provides affordability and portability which would be ideally suited to low resource health settings as measurements can take place outside the laboratory. On the other side, MCF enables to work with high concentrations of antibodies due to high surface area to volume ratio (approximately 200 cm^{-1}) in comparison to approximately 15 cm^{-1} a 96 well ELISA MTP well, given by Equation 2.8:

$$\frac{SA}{V} = \frac{4}{D_h} \tag{2.8}$$

where D_h is a diameter of each microcapillary, assuming each MCF strips is 30 mm long and MTP well with dimensions described in Figure 2.5.

The flow in microfluidic devices is generally laminar[99] and therefore characterised by low Reynolds number, described by equation 2.9, meaning the viscous forces are prevalent compared to inertial forces.

$$R_e = \frac{\rho.v.D_h}{\mu} \tag{2.9}$$

where ρ (kg/m^3) is the fluid density, v (m/s) is the velocity of the fluid, μ (Ns/m^2) is the fluid viscosity, and D_h(m) is the hydraulic diameter of the channel.

The flow in a pipe is laminar for Re < 2100, transient flow when 2100 < Re < 4000 and turbulent when Re > 4000.[100,101] The higher hydraulic diameter, which in a circular capillary is equal to its diameter, the lower is the Reynolds number at the same flow rate. The volumetric flow rate will also affect the flow regime in a pipe, as according to equation 2.10 affecting superficial flow velocity, where Q (m^3/s) is the volumetric flow rate, u (m/s) is the flow velocity, and A (m^2) is t*h*e cross sectional area.

$$Q = u.A \tag{2.10}$$

Laminar flow presents a typical velocity profile in tubes, showing maximum velocity in the centre and zero velocities at the walls of the tube (Figure 2.7). In laminar flow, molecules move parallel to each other (no-slip wall boundary) and no mixing occurs.

Another consideration to take into account in MCF is the molecular orientation of antibodies and their concentration on the surface area. Buijs et al.[102] suggested a relationship between the adsorbed amount and the molecular orientation on the surface, based on the dimensions of antibody molecules.

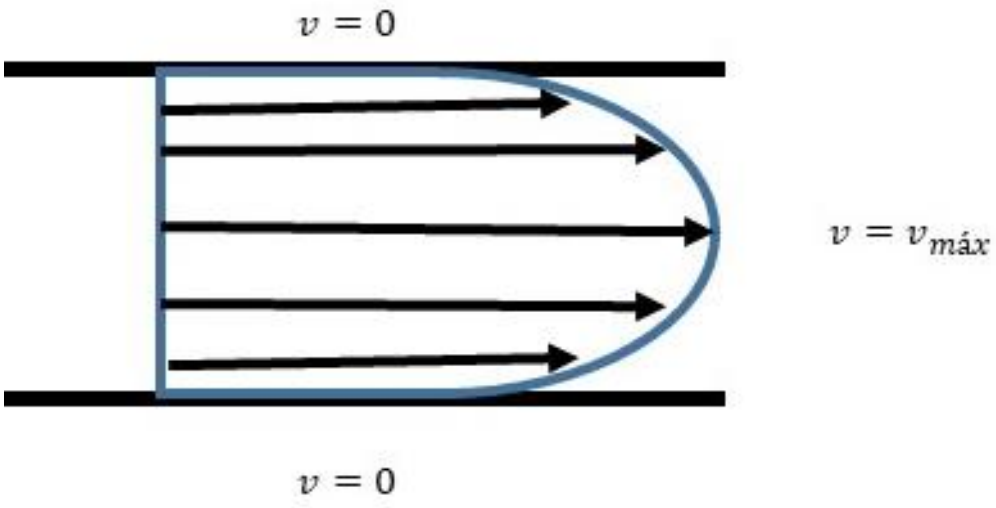

Figure 2.7 Velocity profile of a fluid in laminar flow regime with no-slip wall boundary.

Thus 200 ng/cm^2 would represent a monolayer with antibodies in a "flat-on" orientation, 260 ng/cm^2 in an "end on" orientation with Fab fragments in line, and 550 ng/cm^2 also in an "end-on" orientation with Fab fragments close together and parallel. According to Barbosa et al.[103], the antibody adsorption to FEP-Teflon was found to be similar to protein adsorption onto hydrophobic surfaces and other fluorinated surfaces.

A study characterizing antibody adsorption onto FEP-Teflon microcapillaries showed a maximum surface density of 400 ng/cm^2 at 40 µg/ml of IgG solution, demonstrating maximum binding capacity happened above half monolayer.[103] Therefore MCFs adsorption studies agreed with previous studies performed on other surfaces by Buijs et al.[102] demonstrating reliability for immunoassay development in point-of-care diagnostic.[103]

An *E. coli* cell has a diameter of about ≈ 1 µm, a length of ≈ 2 µm, and a volume of ≈1.3 µm^3 ($A = \pi r^2.(L - \frac{2}{3}.r^2)$) , considering a capsular shape[104]. Taking into account that MCF internal diameter is around 200 µm, in a 30 mm strip length, each capillary has a volume of ≈ 94200 µm^3 ($V = L * \pi * r^2$).

In conclusion, MCF can theoretically capture 72461 bacteria per strip however a fundamental study to understand bacteria flow distribution and attachment on antibody monolayer in MCF is needed and is presented in chapter 3 to enable assay optimization. High analytical efficiency is intrinsically related with the size of microfluidics platform. The Scatchard's model[25] (equation 2.1 from section 2.4.1) shows that higher concentrations of antibody favour the formation of antibody-antigen complex in an antibody-antigen binding reaction, so higher numbers of immobilised antibodies will capture more analytes

(antigens) in the microfluidic system. Although SVR is important for POC diagnostics, the total antibody immobilisation surface area is relevant for sensitive POC assay cost and portability.[45,105] Furthermore, microfluidic devices can be affected for different conditions such as the surface tension of the samples or biological fluids as blood or urine, the reduced volume on low concentration samples and the antibody-antigen kinetics.

2.7 Antibody immobilization and surface area

Surface chemistry is paramount for antibody immobilization and the key step in high performance of heterogeneous immunoassays.[42,51] Surface modifications include at first capture antibody immobilization and blocking (surface passivation) of the remaining available surface sites. Those steps influence tremendously the equilibrium antibody-antigen and prevent nonspecific binding.[58] Therefore immobilization technique can interfere in the density and distribution of capture antibody (capAb), that must provide proper antibody orientation, allowing CDRs availability in order to maximize affinity for bacteria target.[42,88]

In heterogeneous immunoassays, antibodies are usually immobilized either onto the surface of the channel walls or onto microbeads. Immobilization onto surfaces requires additional micro-fabrication processing steps and might be affected by low reproducibility and reliability. Immobilization onto microbeads is very often preferred due offer larger surface-area-to-volume ratio (SVR) and therefore more sensitive immunoassays.[106]

Immobilization of coatings depends on characteristics of microfluidic surface and the type of interaction antibody-antigen such as passive adsorption surfaces, covalent binding or surface attaching by 3D groups, (shown in Figures 2.8A, B and C respectively).[51]

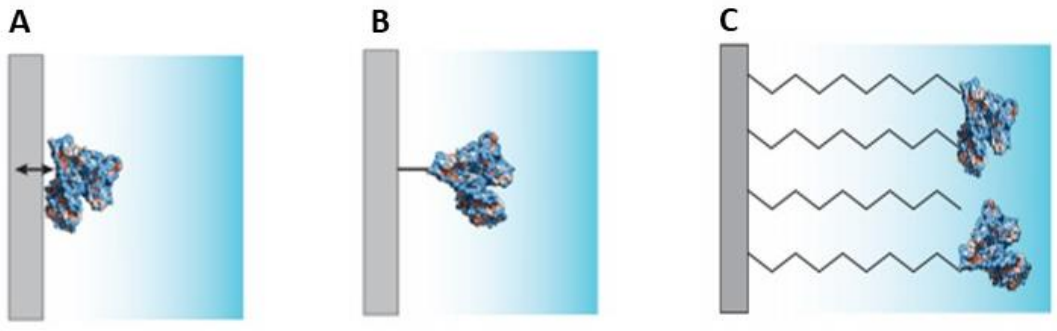

Figure 2.8 Antibody immobilization techniques. **A** Passive adsorption by intermolecular forces **B** Covalent bond **C** Surface-attaching head group by e.g. PEG (spacer it is often used for improving protein activity), adapted from Kim D. et al.[106] (with permission of PubMed Central)

The binding between capture antibody and antigen must be considered, in order to be strong enough in comparison to surface-antigen affinitty or surface-antibody affinity. Passive adorption is the simplest method where antibody interacts directly with surface without any external crosslink. Despite some reports suggest weak binding and random antibody orientation[107], passive antibody adsoprtion has been sucessfully applied in FEP-Teflon® microarrays[23–25,63,108], glass surfaces hydrophobised with Teflon®[109] and polysterene channels including MTP.[105] Passive adsorption is also exploited in chapter 3 and 4 of this thesis.

Covalent immobilization is very often applied into microfluidic surfaces, offering more stability, higher surface coverage and promote better antibody orientation, crucial for sentive immunoassays. Consequently there is an increase of complexity in manufacturing process by chemistries involved in surface modification. Majority of platforms (glass, silicone, polymeric) involve organofunctional alkoxysilane molecules as APTES, functional groups from proteins as epoxy groups from serine or threonine amino acids (-OH), NH_2 and COOH (amine) and glutaraldehyde (GA).[107,106]

Fluoropolymers present some challenges regarding surface modification and covalent immobilization of antibodies in comparison to silicon, glass or PDMS. Covalent immobilizitation in MCF plataform exploiting crosslinkers such as high-molecular weight polyvinyl alcohol (PVOH), NHS-ester groups, APTES, glutaraldehyde, and maleimide was successufully reported firstly by Reis et al.[110] and Pivetal et al.[94] This topic is discussed in more detail in chapter 5 and 6. When in presence of limited surface, antibody immobilization occurs with 3D groups attached on planar surfaces. Among these 3D structures, hydrogels such as polyacrylamide gel and polyethylene glycol (PEG) gel provide hydrophilic environments conducive to good protein stability and retained protein activity.[106,107]

2.8 Detection mode, enzymatic amplification and readout systems

In miniaturized systems, the detection and quantitation of low amount of analytes are fundamental for achieving sensitive assays. Detection mode systems are therefore an important step which at point-of-care demands portability and low costs without compromising performance. Lately, the big demand in miniaturized immunoassays aims to implement off-the-shelf technology, reducing usage of bulky equipment suchs as MTP reader which is, totally dependent on centralized labs. Moreover low resource settings need urgently sensitive, power free and inexpensive microfluidic POC test for healthcare.[11,111,112]

In heterogeneous immunoassays there is a trend for use optical detection systems to detect colorimetric, fluorescence or chemiluminescent signals. Fluorescence still the most widely applied since ensures more sensitive and specific assays[113]. Some examples were referred on Table 2.2 by Kokkinis et al.[4], Zhu et al.[39], Golberg et al.[67], Chang et al.[41], Wang et al.[80] and Yoo et al.[16].

Optical techniques present beneficial characteristics over electrochemical detection by their high sensitivity, high quantitative throughput, adaptability with bench-top protocols and multiplexed detection of several targets detection in a single sample.[114,115]

Cost effective readout systems such as smartphones, scanners and cameras present potential to supply all POC requirements, addressing portability and being power free enabling fluorescence readings by using additional materials as torch or LED to excite or detect fluorescence (only requires battery power but are not plugged in to electricity). [115] For instance, smartphone is a miniaturized device with internal memory, high quality camera lens, that can be easily connected to wifi and well spread worldwide offering similar and cheaper potential than analytical devices such as microscope or spectrophotometer.[116,117] Moreover, a smartphone is widspread among all ages, with more than 40 000 mobile health applications nowadays, representing an opportunity to increase acessibility to mobile healthcare diagnosis.[114,118,119] Indeed, the treatment of cancers, infectious or chronic diseases could be improved tremendously by the use of routine tests in impoverished areas.[120] In this way, smartphone (≈ £800/unit) or tablets (≈ £100/unit) would serve as a point-of-care diagnostic tool for the rapid detection of pathogens, reducing total costs of healthcare systems, providing portability and affordability.[115,118,119] Note, for example smartphone would be a portable device for analysis of several POC tests (≈ 1000), being easily transported between rural areas. An even more affordable option for fluorescent detection would be the implementation of a raspeberry pi (≈ £20/unit).

Prior to achieving sensitivity and throughput optical conditions, limited optical aberrations and incongruences from differential ambient light and transmitted light capture are still key points to evaluate.[8] Due to increasing POC testing needs, several prognostic approaches have been developed using smartphone technology such as blood test detecting glucose, haemoglobin levels, protein, virus, bacteria and drugs.[120–122] Zhu et al.[39] was the first developing a smartphone-based detection for visualising bacteria (Figure 2.9A). The systems consisted in a cost-effective bacterial detection platform with anti-*E. coli* O157:H7 antibodies immobilized on the interior surface of a capillary tube and attached to a cell phone. Proof-of-concept have demonstrated a LoD of 5–10 CFU/mL, in less than 2 h.

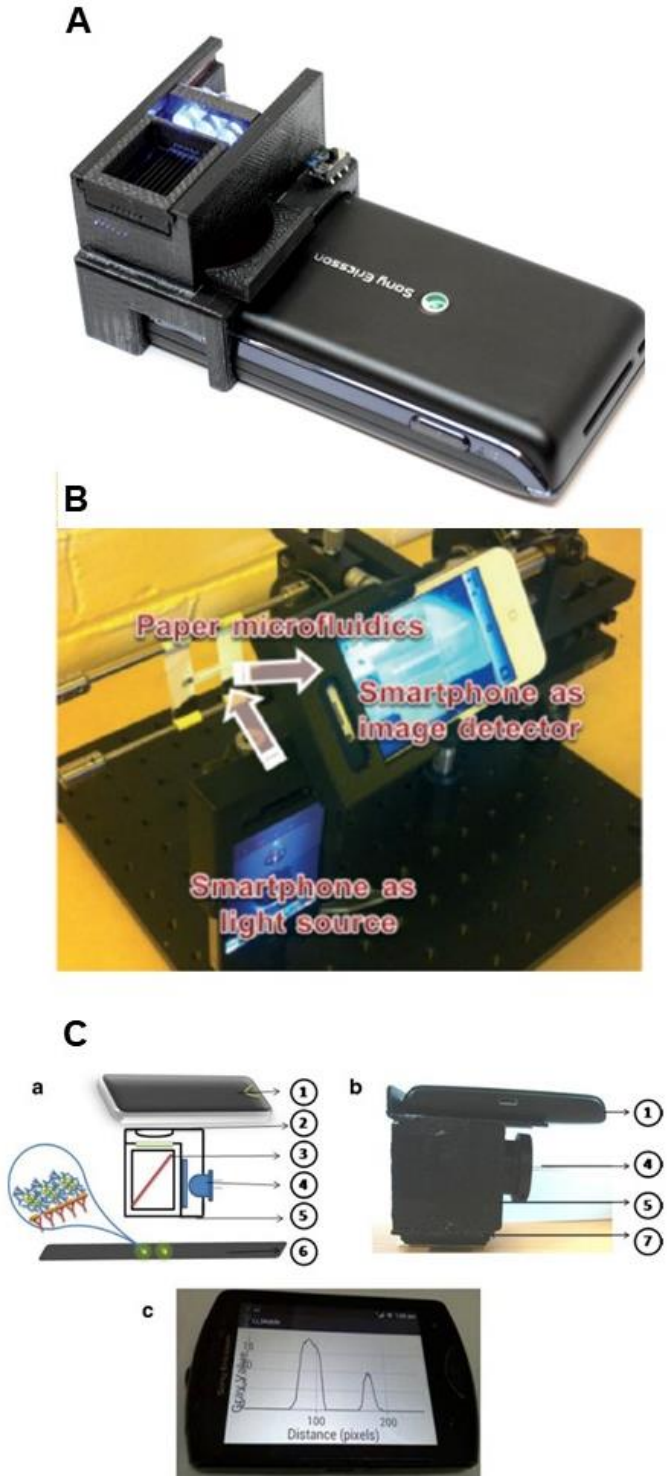

Figure 2.9 Microfluidic platforms for bacterial detection using smartphone as readout system. **A** Quantum dot enabled detection of *E. coli* using a cell-phone adopted from Zhu et al.[39] **B** Smartphone quantifies *Salmonella* from paper microfluidics adopted from Park et al.[112] **C** Smartphone based bacterial detection using biofunctionalized fluorescent nanoparticles adopted from Rajendran et al.[86] (with permission of Royal Society of Chemistry and Springer).

Cho and team[13] have reported a smartphone based μPAD conjugated with fluorescent antibody-conjugated particles to quantify *E. coli* from urine. They present a very rapid system with a LoD of 10 CFU/ml in urine of *E. coli* however human urine samples spiked with *E. coli* or *N. gonorrhoeae* were incubated for 5 min with 1% Tween 80. Park et al.[112] have developed a smartphone-based detection of S*almonella* on paper microfluidics pre-loaded with antibody anti-*Salmonella Typhimurium* conjugated latex microparticles and dried out subsequently (Figure 2.9B). Rajendran V. and coleagues[86] have developed a smartphone based bacterial detection using biofunctionalized fluorescent nanoparticles to detect *Salmonella sp*. and *E. coli O157:H7* (figure 2.9C). Despite being multiplexed, this system presents a LoD of 10^5 CFU/ml of *E. coli*. Shen et al.[117] have developed a point-of-care colorimetric detection approach with a smartphone to measure pH variation in urine. Coskun and team[123] have reported an albumin tester, running on a smart-phone that image and automatically analyses fluorescent assays confined within disposable test tubes for sensitive and specific detection of albumin in urine. Although very impressive LoD, all these assays still present big assay time (>2 h), aim to detect other *E. coli* strains not responsible for UTI's or demand additional steps of sample preparation to be conducted in synthetic or real samples. In an attempt to explore cost effective readout systems aiming portability for low resource settings, a rapid and sensitive bacterial detection assay was integrated with smartphone technology and is exploited in detail in chapter 4.

2.9 Manufacturing and fluid handling systems

Miniaturization of sandwich immunoassays demands simple fluid handling systems or automated steps in order to achieve accurate response. It remains challenging the delivery of cost effective tests whilst maintaining complex interactions for achieving sensitive tests and integration of cutting edge technology for high throughput.[124]

The starting point for manufacturing point-of-care microfluidic platforms is the capacity of those platforms being mass produced by cheap materials without compromising performance.[51] Nevertheless it demands non-opaque microfluidic materials compatible for low cost optical detection. Ultimately, design and geometry are key aspects for successful adoption and commercialization of microfluidic POC tests. Scalable manufacturing process at industrial replication requires adjusting all of the important geometrical parameters of a microfluidic structure for a successful functioning in the intended application.[125]

Microfluidic production still relies on gold standard techniques such as injection moulding whereas it allow to replicate by casting of soft elastomers such as poly-(methyl

methacrylate) and polycarbonate, poly(dimethyl siloxane). Most microfluidic pathogen sensing systems are based on those polymeric materials previously cited in section 2.6 due their low cost and fully optimized protocols for development of bioassays in parallel with glass or paper based devices.[14]

In addition, multistep assays demand multiple interactions achieved by external accessories as micro-pumps and micromechanical valves for increase automation which might increase costs drastically. Indeed, most research in this field is being directed towards eliminating or minimizing the need for external accessories and power and enhance performance of liquid driving systems. Nevertheless automation would offer a reduction of external accessories and costs of manufacturing and therefore minimizing human error, dead volumes and increasing reproducibility.[109,124,126] To implement that, fluidic operations in miniaturized devices can be operated by pressure driven, centrifugal forces, eletrokinetic, passive flow systems.[19,51]

Centrifugal based platforms are typically produced with a footprint disc shape containing channels and microchambers, relying on spinning frequency to drive fluid movements. Regarding sample analysis, some units are added to these lab-on-disks microfluidic platforms such as sample up-take, reagent supply, mixing and incubation sample. These compact disk (CD) devices are often applied in biomedical applications as biomarkers or infectious diseases detection (see Figure 2.10A).[77]

Lee and team[72] reported an innovative approach to detect antibody and antigen of hepatitis B virus. A whole blood sample is injected into device fully automated with a detector, motor and laser diode for valve control integrated.[72] Similarly, Olanrewaju and team[12] have developed Microfluidic capillaric circuit containing capillary pumps and micro valves for rapid *E. coli* detection. However CD based devices present shortcomings regarding environment conditions might affect negatively performance[127]. Temperature and humidity surroundings influence the migration speed of reagents and sample and recognition of antigen as well. Moreover, low concentration samples might be difficult due poor hydrophobic barriers, which might contribute to dead volumes and sample interference.[127]

Pressure driven are the most common and versatile method used in fluid control. Generally, it requires the external devices as flow or syringe pumps to deliver or stop flow according steps of immunoassays. Since those devices are easily connected to the microcapillaries, the flow is typically laminar due to small dimensions of platform handled. However, the use of pumps increases costs and demands power supply, compromising portability and suitability for low income settings.

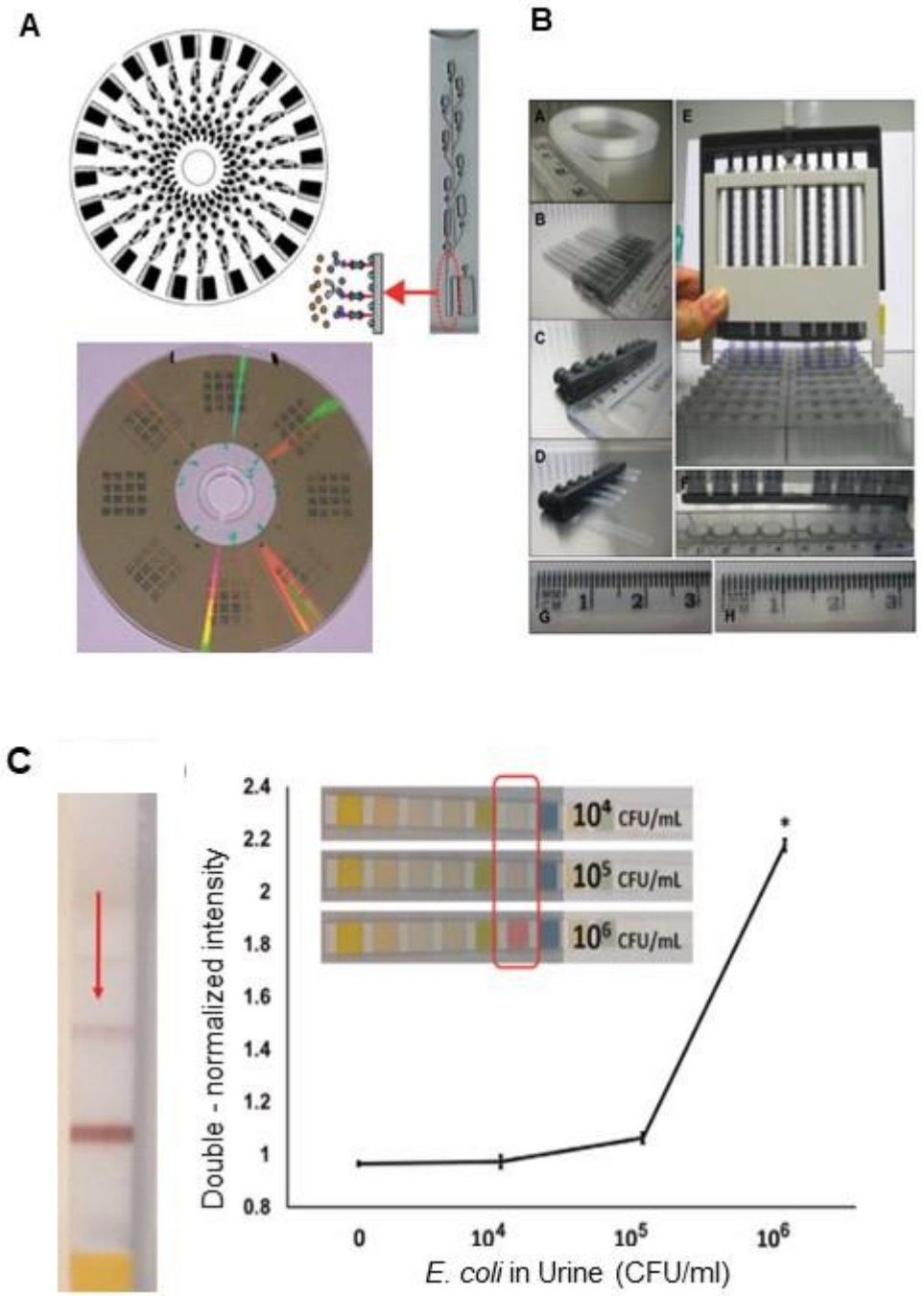

Figure 2.10 Fluid handling designs commonly used in microfluidic platforms. **A** Heterogeneous multiplexed immunoassay on a digital microfluidics platform, with 24 experiments on a centrifugal microfluidic platform. Adopted from Gorkin et al.[77] and Lai et al[73]. **B** MSA fully assembled, with a plastic frame, a syringe plug holder with a central knob allowing fluid aspiration by rotation through capillaries action adapted from Barbosa et al.[23] **C** Commercial urinalysis test strips were used with urine samples with 10^4,10^5 and 10^6 CFU/mL *E. coli* adapted from Cho et al.[13] (with permission of Royal Society of Chemistry and Elsevier).

Barbosa and team[23] have reported a cost effective microfluidic technology interface named Multiple Syringe Aspirator (MSA) capable of loading simultaneous 80 microarrays through 1 ml syringes using a simple rotation of a central knob (see Figure 2.10B). In addition Reis and team[110] have launched a gravity driven dipstick for one step assay, consisting in microcapillary films coated with PVOH. Pressure driven flow occurring due to the gravitational potential of the fluid's height is also exploited in chapter 5 and 6 of this thesis.

Magnetic forces exploit a magnetic field, where fluid actuation is performed driving multi step reagents into microfluidic devices.[109] For example Lab on a chip (LOC) devices using magnetic beads conjugated with antibodies for immunomagnetic separation (IMS) and impedance spectrometry (IS) techniques for capture, separation or detection of analytes.

Yang and team[128] have reported a LOC for separation of *E. coli* K-12 from synthetic urine in a chamber containing micro magnetic beads conjugated with anti-*E. coli* antibody, with an limit of detection of 3.4×10^4 CFU/mL . The LOC consists in a concentration and sensing chambers disposed in series and integrating an impedance detector. Clogging of channels is a limitation specially observed in bead-based microfluidic assays.[109,128]

Passive flow systems are independent of any external device or magnetic force, being the fluid transport driven by surface properties of microfluidic platform. Chemical gradients on surface, osmotic pressure, gravity and capillary action are some forces promoting the fluid handling. The big challenges of this method are related to control of flow rate, volume and incubation time. For instance capillary action has been used in dipstick assays for over 30 years in lateral flow pregnancy tests and colorimetric strip tests for urinalisys (Figure 2.10C).[51,88]

The first paper-based sandwich ELISA was developed to test for human chorionic gonadotropin (hCG) in a human pregnancy assay.[65] The commercial urinalysis test strips are a common example used to detect the presence of an UTI in urine samples.[13,40] Despite very simple to use and capable to identify an UTI infection very quickly, dipsticks present limitations in specificity of bacterial strain, are not quantitative and completely accurate giving false positives and being deeply dependent on the correct sample collection.

2.10 Bacteria capturing in microchannels

Bacteria migration within microchannels is fundamental to understand interactions with surroundings, evironmental stimuli and mechanisms of efficient capture relevant for pathogenic detection.[129–133] This is due flagella present in cell surface of 80% of bacteria

allowing to swim through fluids.[130,134] Motile organisms are capable of sensing and swimming towards favorable conditions in complex environments, through host cells and tissues and aggregate in antibiotic-resistant biofilms on surfaces.[135,136]

Several studies[134,135,144–152,136–143] have attempted the study to understand bacterial motility under several surfaces, however their migration within microchannels is not yet fully understood.[131]

In free solution, motile bacteria (e.g. *E. coli*) presents random diffusive migration patterns (Figure 2.11A), where bacteria such as *E. coli* have a small bias to persist in their direction of motion after tumbling, resulting in a nonuniform random turn angle distribution.[132,134,136,137,141]

An experimentally study conducted by Berke and Turner[135] have reported that motile bacteria trends to surface due a physical mecanisms of attraction between swimming bacterial cells and solid surfaces, i.e the hydrodynamic interactions with surfaces leads to a reorientation of the bacterial cells in the direction parallel to the surfaces and an attraction of the aligned cells by the nearest wall.

Nervertheless, those authors showed that the circular motion of *E. coli* near the surfaces of capillary that are larger than 50 μm in diameter is responsible for trapping the cells in the capillary assay. Jing et al.[153] and Tu et al.[154] have reported the importance of sedimentation regarding the highly efficient capture of pathogens as key parameter for development of rapid detection assays. Furthermore those authors mention the role of platform designs on promoting efficient capture

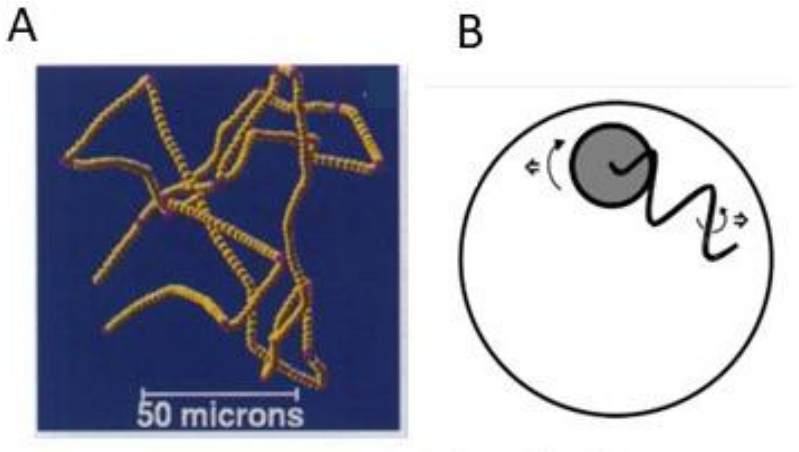

Figure 2.11 Bacterial motility**. A** Brownian motion of *E. coli* cell in a fluid free from surfaces, adopted from Frymier et al.[140] **B** Diagram about bacterial cell swimming in a narrow capillary when viewed behind the cell. Rotation of the cell body and the flagella are illustrated with curved arrows. The sideway forces due to wall effect are shown as double-line arrows. Adopted from Ping et al.[131] (with permission of Royal Society of Chemistry).

Therefore, tracking *E. coli* within MCF capillaries is fundamental to understand further mechanisms to enhance a rapid and high throughput capture, aiming sensitive immunoassays where sophisticated technologies are used, such as fluorescence labelling techniques with confocal microscopy for example.[155] Based on that, a deep study regarding migration of *E. coli* cells within FEP-Teflon® microcapillaries, aiming rapid miniaturized immunoassays compatible with POC format is exploited in chapter 3.

CHAPTER 3 | Immunocapture of *Escherichia coli* in a fluoropolymer microcapillary array

Abstract

This chapter presents novel experimental insights into the direct quantitation and immunocapture of bacteria cells in a fluoropolymer microcapillary array. *Escherichia coli* have been used as a model, a pathogen responsible for around 80% of urinary tract infections. In spite of the current clinical demand for sensitive tests for rapid identification and quantitation of pathogens in human samples, portable diagnostic tests developed to date lack the specificity, limit of detection and speed for effective implementation in bacteria detection at point-of-care. The 'open microfluidic' approach presented in this work directly addresses those challenges.

An evidence of immunocapture of bacteria using polyclonal antibodies immobilized on the inner surface of an inexpensive 10-bore, 200 μm internal diameter FEP-Teflon® MicroCapillary Film is reported by the first time with a limit of detection (LoD) of at just 20 colony forming unit (CFU)/ml of 0.01M PBS. In capillaries coated with less than a full monolayer of capture antibody, a first order equilibrium was observed, with bacteria captured (in CFUs/ml) linearly proportional to the CFU/ml in the incubated sample. It was captured up to 100% of *E. coli* cells, with clear evidence of immunospecificity as demonstrated by testing with a different bacteria specie (in this case *Bacillus subtillis*). It was noticed gravity settling of bacteria within the capillaries created a gradient of concentration which on the overall enhanced the capturing of cells up to 6 orders of magnitude beyond the theoretic full monolayer (~4×10^4 CFUs/ml), which washings having an unnoticeable effect. This data particularly highlights quantitatively the relevance of interrogation volume in respect to the miniaturisation of bacteria quantitation, which cannot be solved with the most sophisticated imaging equipment. A further set of continuous flow experiments at a flow rate of just ~1 μl/min (corresponding to a wall shear rate of ~101 s^{-1} and superficial flow velocity ~53 μm/s) showed a degree of flow focusing, yet the mobility, antibody affinity capturing and gravity settling of bacteria cells enabled successful capturing in the microcapillaries.

These results will inform the future development of effective microfluidic approaches for rapid point-of-care quantitation of bacterial pathogens and in particular the presence of *E. coli* in urinary tract infections (UTIs).

3.1 Introduction

Bacterial infections represent a significant burden to global health and economy. It is estimated that multidrug resistance 'superbugs' are responsible for around 25.000 deaths per year in Europe resulting annually in healthcare costs of €1.5 billion and significant productivity losses.[1] Although treatable, most diseases caused by bacterial infections including *Escherichia coli* (*E. coli*) are the cause of high annual mortality rate in both developing and developed countries. Difficulty in early identification of pathogens and inaccurate treatment remain the two major clinical challenges to be solved.[4,5]

Bacterial identification at point-of-care (POC) has proved particularly difficult, with no rapid and cost-effective tool yet available to identify and quantify pathogens with the high sensitivity and specificity required for clinical use. Identification of pathogens is currently done in centralised microbiology laboratories, involving complex logistics and long waiting times, typically between 20 and 72 h.[12,42] New diagnostics tools for rapid bacteria identification and quantitation are regarded essential for managing the over prescription of antibiotics and tackling antimicrobial resistance.[2,13,19] Consequently, microfluidic detection of pathogen is emerging as a new solution to tackle bacterial infections, offering high throughput combined with small fluid volumes and short assay time in a portable format compatible with POC requirements.[4,38,68] However, development of those devices remains mostly empirical, driven from an analytical chemistry perspective that is disconnected to the engineering challenges represented by e.g. the high-shear and focused flow of bacteria in microchannels or microcapillaries.

Methods currently available for bacterial detection are based on a variety of laboratory-based tests including microscopy[156], plate culture[42] and antimicrobial peptides[38] which are broad spectrum antibiotics peptides sequences which have the potential of permeabilize biological membranes, forming transmembrane pores or bind to intercellular molecules, killing the host cell. Other approaches would be immunoassays[19,42], nucleic-acid amplification[19,156](such as PCR), electrochemical impedance microscopy[19] (a method that measure the changes of the interfacial properties of the electrode after the interaction of bacteria target with their probes immobilized on electrode surfaces) and magnetic beads (functionalized with antibodies, enzymes or proteins and used in assays to increase surface reaction area)[156].

Though well established, some of those techniques present relevant drawbacks for application at POC such as complex sample preparation, expensive reagents, lack of specificity and sensitivity and/or demanding expensive readout systems only available in sophisticated centralized labs.[5,36,68,156] Microbiological identification of bacteria intrinsically relies on the doubling time and growth time of bacteria in agar-rich plates, which is set by

the nature of the microorganism and growth conditions. Immunoassays are highly sensitive bioanalytical tools that rely on the high antibody specificity and can be used in several applications including clinical diagnostics[4,12,68,157,158], environmental monitoring[68,159], bioterrorism[5] and drug kinetics[5,68] for pharmacology industry. They utilise enzymatic amplification for detection of very low concentrations of proteins or bacteria, so several authors have attempted detection of bacteria with immunoassays.[4,12,37,40,68,157–159] Miniaturization of bacteria detection tests presents the problem of reduced signal strength which demands very sophisticated detection and quantitation equipment. This is one of the biggest challenges for POC microfluidic devices.[68,69,160] Limitations reported for immunoassay detection of bacteria are the poor sensitivity, cross-reactivity, reproducibility and reduced limit of detection (LoD).[66,161] So far there has been no systematic study showing how the miniaturisation and immunoassay format affects the performance of an immunoassay aiming rapid POC bacteria quantitation.

In this chapter, optical imaging techniques such as Laser Scanning Confocal Microscopy (LSCM) and Scanning Electron Microscopy (SEM) were used to understand immunocapture (bioassay that use antibodies as probe to capture an analyte) of bacteria in plastic microcapillaries coated with a polyclonal antibody. *E. coli K12* fluorescently labelled was used to gather quantitative information about avidity of antibody-bacteria binding.[38,162] Plastic microcapillaries offer large surface-area-to-volume ratio (SVR), are inexpensive and enable larger volumes of sample to be used typical of 'open' microfluidics. A new cheap miniaturised immunoassay platform based on a 10-bore Microcapillary film melt-extruded from fluorinated ethylene propylene (FEP-Teflon®) was employed. MCF detection present optical characteristics that favour high signal-to-noise-ratio and simple optical detection with low-cost readout systems, essential for high performance detection in an affordable, portable format. The hydrophobic surface of FEP microcapillaries allows simple antibody immobilization by passive adsorption and avoids complex fluid handling.[97] The large SVR ratio of ~200μm microcapillaries (SVR of MCF is 14 times higher than microtiter plate, as explained in page 29) enabled a performance comparable to microtiter-based immunoassays with a >10-fold reduction in total assay time.[23]

These features were key to recent MCF developments: PSA biomarker detection using smartphone based system and screening from whole blood[23,24] multiplexed femtomolar quantitation of human cytokines (IL-1β, IL-6, IL-12 and TNF-α)[98]; Lab on a stick for multi-analyte cellular assays as antibiotic susceptibility and microbiological screening[110] and one-step quantitation of PSA using nanoparticles labels.[108]

3.2 Experimental methods

3.2.1. Reagents and materials

Unconjugated Rabbit Polyclonal Antibody Immunogen: O and K antigenic serotypes (all types) of *Escherichia coli* (# PA1-7213); LB Agar, Miller (# BP1425-2) and LB Broth, Miller (Granulated) (# BPE9723-2) were supplied by Fisher Scientific UK Ltd, Loughborough, UK). Phosphate Buffered Solution, 0.01M at pH 7.4 (PBS, # P5368-10PAK), washing buffer PBS with 0.05% v/v of Tween-20, Nunc maxisorp ELISA 96-well MTPs and SIGMAFAST™ OPD (o-Phenylenediamine dihydrochloride) tablets (# P9187) were sourced from Sigma Aldrich (Dorset, UK). Pierce™ Protein-Free Tris-Buffered Saline (TBS) Blocking Buffer (# 37584), LIVE/DEAD® BacLight™ Bacterial Viability Kit, for microscopy (# E2069) and High Sensitivity Streptavidin–HRP (# 21130) were supplied by Thermo Scientific (Northumberland, UK). Female Luer ¼ (# P-624) were obtained from C M Scientific (Silsden, UK). A 10-bore MCF material and push-fittings seals were provided by Lamina Dielectrics Ltd (Billingshurst, UK). MCF fittings were designed by Lamina Dielectrics Ltd and manufactured in-house. *E. coli K12* 'wild-type' (NCIMB 11290) and *Bacillus subtillis* (NCIMB 8054) were supplied by Loughborough University, obtained from NCIMB Ltd, (Aberdeen, UK).

3.2.2. Fluoropolymer MCF

A 10-bore MCF was used (see Figure 3.1A and B) which presents a parallel array of microcapillaries with a mean hydraulic diameter of 206 ± 12.6 μm and external dimensions 4.5 ± 0.10 mm width and 0.6 ± 0.05 mm thickness.[97] This material was manufactured by a novel melt-extrusion process from Teflon® FEP (Dow, USA).[24,97] The cost for pelleted FEP material is in range of £20/Kg, with a unit weight of 5 grams per meter of material, meaning the material cost for a 10-plex, 50 mm long MCF test strip is less than 1 pence. This excludes the cost of reagents, manufacturing and fittings required for carrying out immunoassays in the MCF. FEP was chosen for its excellent transparency resulting from refractive index matching with water, allowing good signal-to-noise detection with low cost readout systems[97] but also with sophisticated fluorescence imaging equipment such as confocal microscope.

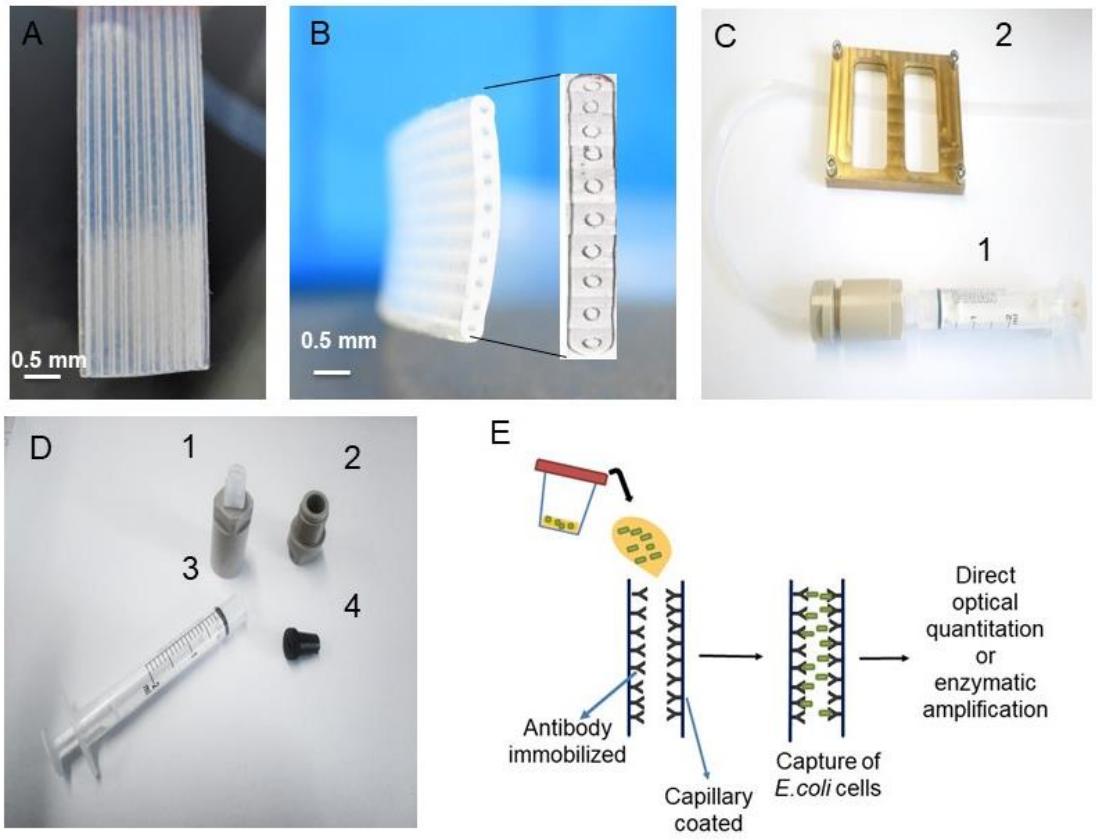

Figure 3.1 Fluoropolymer MCF platform and accessories used to carry out in-flow LSCM experiments. **A** Top view of MCF strips. **B** Cross section photograph of a 10 bore MCF. **C** MCF accessories used in LSCM: **1** - MCF fitting connected to the luer with lock syringe, **2** - MCF holder capable of holding several MCF parallel MCF strips. **D** MCF accessories to connect MCF strips to Harvard Pump: **1** - MCF fitting with female luer, **2** - MCF male fitting, **3** - Terumo Syringe 2.5 ml luer lock, **4** - Push-fit seal. **E** 'Open fluidics' design of microcapillaries that enable passing a large volume of sample through the microcapillaries with immobilized capAb.

3.2.3. E. coli sample preparation

''A colony of *E. coli K12* "wild type'' (NCIMB 11290) was inoculated in a 100 mL LB broth diluted in deionized water (Lysogeny broth composition according to supplier: Casein Peptone 10g, Yeast extract 5g, Sodium Chloride 10g) and incubated in a shaking incubator at 37 ºC overnight under sterile conditions. Afterwards the culture media was washed 3 times with PBS buffer and cells recovered after centrifugal separation (4,500 rpm, 20 min) and re-suspended in the original volume. *E. coli* sample aliquots were prepared in 2 ml Eppendorf tubes with an OD600 of ≈ 0.7 (to standardize samples for all experiments) and stored at -20 ºC. Every two weeks, this procedure was repeated. For

any experiment, the 2ml bacterial sample in Eppendorf was defrosted and serial dilutions were made from a volume of 0.1ml *E. coli* samples in PBS and spread onto LB agar plates at 37 ºC overnight for estimating the cells present in fresh media and assess the viability and concentration of bacterial cells used in experiments. Positive and negative control plates with 0.01M PBS and agar without *E. coli* were performed to assess any contamination at this stage. The same procedure was used to prepare *Bacillus subtillis* (NCIMB 8054) samples.''

3.2.4. Microcapillary *E. coli* capture and flow experiments using LSCM

Confocal microscopy experiments were carried with LSCM (Nikon inverted Microscope ECLIPSE TE300 with Bio-Rad RAD200 (scan head 60X-1.20NA objective lenses, excitation peak wavelength of 488 nm and emission peak wavelength of 530 nm) operating Laser Sharp 2000 software. Post-acquisition and particle tracking analysis were carried out using Image J.[163] For affinity capture of *E. coli* in the microcapillaries, *E. coli* was stained fluorescently with LIVE/DEAD® BacLight™ Bacterial Viability Kit according to supplier specifications for live cells.

For each experiment, a 80 cm long MCF strip was coated with 40 µg/ml of polyclonal anti-*E. coli* antibody (capAb) in PBS 0.01 M during 2 hours and Protein Free (TBS) blocking buffer for another 2 hours, being consecutively washed with washing buffer PBS with 0.05% v/v of Tween-20. Pushed-fit seals were used to connect MCF strips to a Terumo Syringe 2.5 ml luer Lock (Figure 3.1D) to promote a uniform filling of the microcapillaries. Flow experiments were performed using a PHD-ultra Harvard Pump syringe (Instech Laboratories, Inc., USA) and all MCF strips positioned flat in LSCM window with a built-for-purpose MCF holder (Figure 3.1C). Because of the small dimensions of the capillaries, flow was assumed laminar and therefore characterized by low Reynolds number described by Equation 2.9 and the volumetric flow rate,Q (m^3/s) calculated based on Equation 2.10, both in section 2.6.1 (page 29).

It can be shown the (maximum) wall shear stress, τ_w (Pa) and shear rate, $\dot{\gamma}$ (s^{-1}) are given, respectively by:

$$\tau_w = \mu \times \dot{\gamma} \tag{3.1}$$

$$\dot{\gamma} = \frac{\partial u}{\partial x} \tag{3.2}$$

where $\frac{\partial u}{\partial x}$ is the velocity gradient across the microcapillary.

3.2.5. Study of *E. coli* binding into MCF capillaries with SEM

A JSM-7800F Field Emission SEM was used to observe surface bound *E. coli* incubated in MCF strips with and without antibody coating. Polyclonal anti-*E. coli* antibody (40 µg/ml capAb) in PBS 0.01M was immobilized in a 50 cm long MCF strip and incubated for 2 hours and then further 2 hours with Protein Free TBS blocking buffer. Fluid aspiration was done with 1 ml syringes connected to the MCF via a 2 cm long silicone tube.

As controls, a 20 cm long MCF strip with the same concentration of capAb in PBS but without blocking buffer and a 20 cm long MCF strip with just Protein Free TBS blocking buffer were incubated during 2 hours without any capAb. Thereafter all strips were washed with PBS 0.05% v/v Tween-20 and trimmed into shorter, 10 cm long strips. Each strip was then incubated with 200 µl of a synthetic sample consisting of 10^9 CFU/ml *E. coli* in PBS for 20 minutes and then gently washed with 1 ml PBS 0.05% v/v Tween-20 buffer and dried at room temperature during 24 hours. One of the strips was incubated with 200 µl of 10^9 CFU/ml of *E. coli* in 2.5% w/v glutaraldehyde in 0.01M PBS and washed consequently. Before SEM imaging cell MCF strips were sliced through the middle of the capillaries aiming to expose the *E. coli* on the microcapillary walls. Samples were fixed to a pin stub with double-side tape and coated with 5 nm layer of gold using Au-Sputter Coater Quorum Q150T ES for 90 seconds.

3.2.6. Avidity of antibody-coated microcapillaries using agar plates

A 80 cm long MCF strip was first coated with 40 µg/ml of capture for 2 hours, followed by blocking buffer solution for another 2 hours and finally flushed with washing buffer and trimmed to produce individual 40 cm long strips. Each 40 cm long strip (having a total internal volume of 133 µl) was then gently flushed with 1.2 ml *E. coli* sample (rate of fluid flow estimated at 1200 µl in 20 seconds) and incubated for 20 min with a 10-fold serial dilution (from 0 to 10^8 CFU/ml) from 2 ml aliquots of *E. coli* samples in PBS. The solution from each strip was then fully recovered into a microwell by pushing the fluid out of the capillaries with a plastic syringe full of air attached to a 2 mm i.d. silicone tube and platted for CFU counting. The ratio between the CFU/ml in the recovered solution and the CFU/ml in the incubated solution enabled plotting the equilibrium curve (avidity of antiboy-bacteria) and computing the percentage of CFU captured in the MCF strips coated with capAb with a simple mass balance.

Assuming bacteria capture only occurred during batch incubation of the strips, it can be shown that in equilibrium conditions the CFUs/ml captured is given by the

difference between CFU/ml in the aliquot and the CFUs/ml in the solution withdrew from the microcapillaries. In order to understand the effect of washing on bacterial binding, similar experiments were repeated at same conditions but adding a final step of washing with 200 µL PBS with 0.05% v/v Tween-20. As CFUs/ml tested covered several orders of magnitude, results were plotted as $\log_{10}$ CFU/ml and $\log_{10}$ CFU/cm^2, the last based on an inner surface area of 25.84 cm^2 for 40 cm long strip. As a guideline, a full monolayer capacity of ~4×10^4 CFUs/ml was estimated assuming each *E. coli* cell has a footprint of 0.5 µm^2 when lying in a flat position (from the mass balance between SVR of MCF and SVR *E. coli* $\approx \frac{4}{0.2mm} = \frac{0.5\ \mu m^2.\ CFU}{0.001\ CFU.\ mm^3}$).

As antibody-cell interaction is likely to involve more than one antibody molecule, the equilibrium can be regarded as a representation of the binding avidity to capAb immobilized onto FEP-Teflon microcapillaries. Table 3.1 summarize calculations used to plot Figure 3.6, based on experimental protocol above described.

Table 3.1 Demonstrative example to calculate the amount of *E. coli* captured in microcapillaries.

a)	***Initial concentration of bacterial CFUs before incubation in MCF strips*** → ***C_i*** Log $_{10}$ *E. coli* in solution → 3 x 10^4 CFU/ml (value determined from counting plates) x 1.2 ml (initial volume incubated) = 3.6 x 10^4 CFU/ml **Log $_{10}$ *E. coli* in solution = Log $_{10}$ (3.6 x 10^4 CFU/ml) = 4.56**
b)	***Final concentration of bacterial CFUs after 20 min incubation in MCF strips*** → ***C_f*** 1 x 10^4 CFU/ml (value determined from counting plates after incubation overnight 37℃) **Log $_{10}$ *E. coli* captured** is calculated from the mass balance: (C_i x 0.133 ml) - (C_f x 0.133 ml) ↔ (3 x 10^4 CFU/ml x 0.133 ml) - (3 x 10^4 CFU/ml x 0.133 ml) =2.66 x 10^3 CFU →2.66 x 10^3 CFU → $\frac{2.66 \text{ x } 10^3 \text{ CFU}}{0.133 \text{ ml}}$ = 2 x 10^4 CFU/ml **Log $_{10}$ *E. coli* captured (CFU/ml) = Log $_{10}$ (2 x 10^4 CFU/ml) = 4.30**
c)	**Log $_{10}$ *E. coli* captured (CFU/cm^2) =** $=\text{Log}_{10}\left(\frac{2.66 \text{ x } 10^3 \text{ CFU}}{25.84\ cm^2\ (\text{inner surface of 40 cm length MCF}}\right)$ **Log $_{10}$ *E. coli* captured (CFU/cm^2) =** 2.01
d)	**Fraction *E. coli* captured (%)** = (1- $\frac{Cf}{Ci}$) x 100 % = (1- $\frac{1 \text{ x } 10^4 \text{ CFU/ml}}{3 \text{ x } 10^4 \text{ CFU/ml}}$) x 100 % =66.7%

3.2.7. Immunoassay detection of *E. coli K12* and *Bacillus subtillis*

To demonstrate immunospecificity of the immobilized capAb in respect to *E. coli* capturing, a colorimetric sandwich immunoassay was devised in the MCF strips inspired on immunoassay protocol previously reported by e.g. Castanheira *et al.*[98] for protein biomarkers. It was used the following work assay conditions: 40 µg/ml unconjugated polyclonal capAb in 0.01M PBS incubated for 2 hours; 1ml Protein Free TBS blocking buffer incubated for another 2 hours; 150 µl of *E. coli K12* or *Bacillus subtillis* diluted in 3% of BSA incubated for 30 min; 40 µg/ml biotinylated detection antibody incubated for 3 min; 4 µg/ml of HSS-HRP incubated for further 4 minutes; chromogenic substrate consisting of 4 mg/ml OPD in 1mg/ml H_2O_2. The antibody manufacturer reported the possibility of some cross reactivity with other bacteria in particular related enterobacteriaceae, in this case *Bacillus subtilis* was used for being a common, gram-positive bacteria available in our laboratory. Each data point represents the mean absorbance from the greyscale pixel intensity of 10 individual capillaries within each MCF test strip and error bars indicate standard deviation of these 10 replicate assays.

3.3 Results and discussion

3.3.1. LoD of bacteria is set by level of miniaturization

It was noticed the LoD of bacteria is intrinsically linked to the level of miniaturisation. The advantages of microfluidic bioassays are well understood and explained in literature, however detection and quantitation of bacteria is intrinsically more challenging in miniaturised systems because of the small volumes being dealt with. The volumes herein mentioned could refer to the sample volumes and/or interrogation volume. The most sensitive theoretical technique will allow detecting just 1 CFU, however this represents a minimum volume of 1 µL for a LoD of 1×10^3 CFUs/ml, typically the clinical threshold for Urinary Tract Infections (UTIs)[21]; note counting viable cells as CFUs is a norm in microbiology as it reflects the uncertainty connected to visual detection of a colony resulting from a single cell or group of cells. To illustrate this, plastic microcapillaries strips loaded with a serial dilution of fluorescently labelled *E. coli* in PBS were imaged into a confocal microscope. For optimum sensitivity and resolution, the interrogation window was set to be 200×200 μm^2, representing an estimated interrogation volume of just 62.5 nL for a 200 µm perfectly cylindrical capillary which is a fair approximation for the MCF.

Figure 3.2A shows a rapid drop of fluorescence signal as cells are diluted, suggesting it is not possible to directly quantify *E. coli* cells below 10^4 CFUs/ml even with a sophisticated microscope.

ImageJ was used to count the number of cells that could be detected in the interrogation window and established a relation to the theoretical number of bacteria expected to be found in that volume (Figure 3.2B). It was estimated a minimum $\log_{10}$ CFUs/ml of 5.20 required to have at least one CFU present in that small interrogation volume and that becomes experimentally visible.This finding shows that even the most advanced optical imaging equipment is unable to detect anything below 4-5 $\log_{10}$ CFUs/ml in a synthetic sample.

It was hypothesised the use of an 'open microfluidic' system as exemplified by Figure 3.1E like the MCF, enabling parallel replicas and cells capturing via immobilized high affinity antibodies, would offer the opportunity to combine within a single device capturing and quantification of bacteria cells with a level of amplification, enabling the use of large sample volume for yielding detection at reduced CFU/ml values.

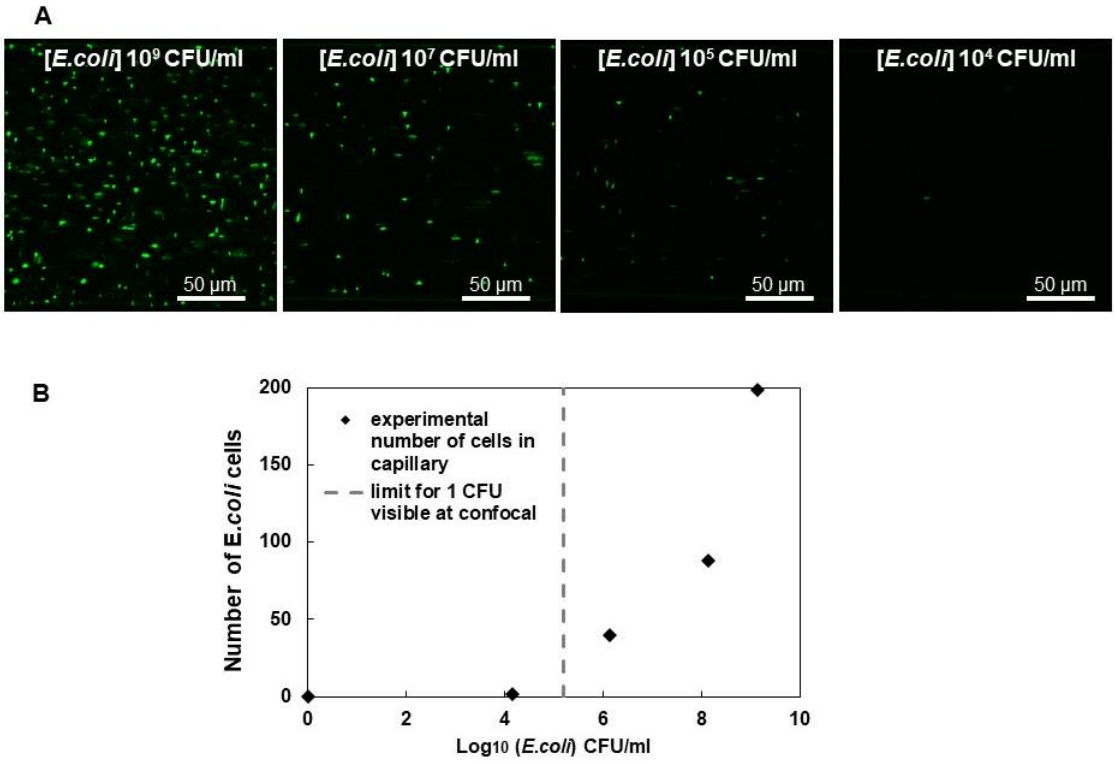

Figure 3.2 LSCM imaging of fluorescently labelled *E. coli* in a plastic microcapillary. **A** Serial dilution of *E. coli* in PBS imaged in a 200×200 μm^2 section of a 200µm i.d microcapillary. **B** Relationship between theoretical and experimental CFUs in interrogation volume (estimated as 62.5 nL).

3.3.2. SEM evidence of immune affinity of *E. coli* cells in microcapillaries

It was studied the capture of *E. coli* cells in microcapillaries coated with polyclonal antibodies by SEM and main results are summarized in Figure 3.3.

\All MCF strips were flushed with 1 ml of washing solution to remove any unbound cells before imaging. It was confirmed *E. coli* is unable to adhere non-specifically to raw, hydrophobic microcapillaries uncoated with capAb or in absence of blocking buffer (Figures 3.3A and 3.3B). Figures 3.3C-F revealed *E. coli* binding only occurred in microcapillaries coated with capAb, with Figures 3C and 3D showing detailed morphology between cells commensurate with the typical size for *E. coli*. This agreed with e.g. Chang *et al.*[38] who reported binding of *E. coli* DH5α and O157:H7 to the surface of the AMP-labelled beads with similar morphology and shape. The SEM study highlighted an important role of gravity in the capture of *E. coli* cells, with Figures 3.3E and 3.3F showing very distinct degrees of bacteria capture between the top and bottom parts for a given capillary cut along its length.

These optical observations of uneven *E. coli* capture in microcapillaries are original and to my knowledge not previously reported in the literature, yet they can have high relevance to the design of fluidic devices suited to efficient capture of bacteria cells. Note, the mechanical strength applied for slicing through the middle of the capillaries aiming to expose the *E. coli* on the microcapillary wall might contribute to the uneven distribution of bacterial cells. Conventional microfluidic devices are usually only coated with antibody in one surface, in contrast to the cylindrical microcapillaries. In spite of all cross section of capillaries being evenly coated with the capture antibody[23], settling created a gradient of concentration reducing density of bacteria in the top part of the capillary and consequently increasing efficiency of cells captured at bottom part of the capillary.

3.3.3. Study of *E. coli* capture with fluorescence techniques

LSCM experiments enabled studying the spatial and time-lapse immunocapture of fluorescently labelled *E. coli* (10^8 CFU/ml in 0.01M PBS) in the plastic microcapillaries. Initially MCF strips were used in the absence of flow (to avoid blurring microphotographs) and samples incubated between 5 and 20 min without any subsequent washing. Figure 3.4A shows a z-stack series of fluorescently labelled *E. coli* cells in a microcapillary at the middle, starting from bottom to the centre of microcapillary.

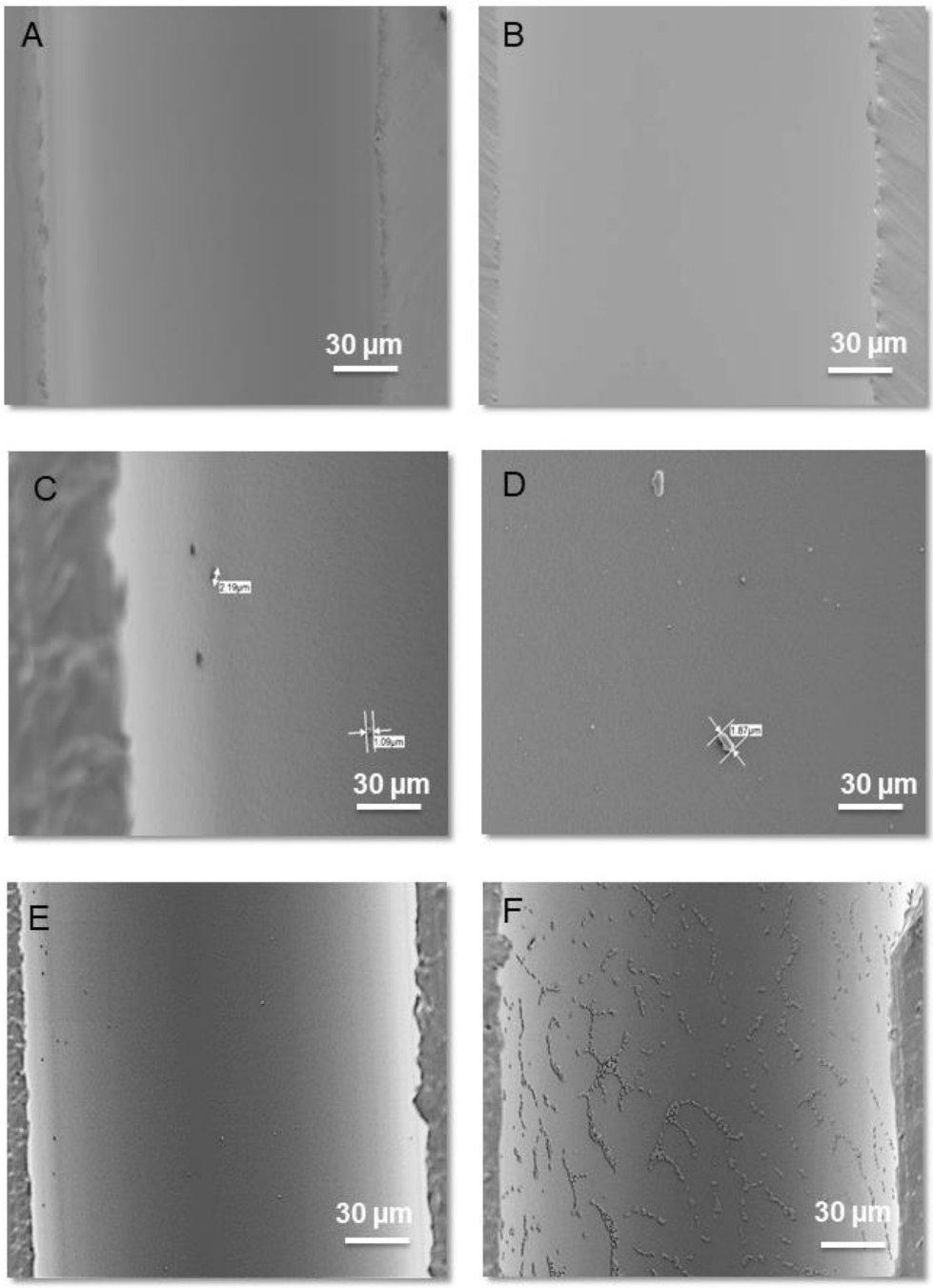

Figure 3.3 SEM microphotographs of inner wall of fluoropolymer MCF microcapillaries. **A** MCF strip coated with blocking buffer solution and then incubated with synthetic sample. **B** Uncoated MCF strip incubated only with synthetic sample. **C** and **D** MCF strips coated with capture antibody, blocking buffer solution and synthetic sample, showing size and morphology of *E. coli* cells. **E** and **F** Detail of top half and bottom half of the same microcapillary coated with capAb, blocking buffer solution and incubated with synthetic sample, revealing bacteria binding is not spatially uniform in horizontal capillaries.

A gradient of cells captured was noticed, with higher density of bacteria measured at the bottom part of the capillary in line with SEM data reported in section 3.2, as a result of bacteria settling during the incubation of *E. coli* sample (Figure 3.4C).

It was hypothesized gravity settling enhanced the overall capturing of cells within the microcapillaries. To validate this a series of in-flow capture experiments of *E. coli* at very low flow rate or 1 µl/ml were carried out. Note this corresponds to the total flow rate split between the 10-bore MCF strip, and assumed an even flow distribution between the 10 parallel microcapillaries.

Figure 3.4B (i) shows a time sequence at four different z heights. Image analysis were used to determine the fraction of *E. coli* cells that remained mobile between consecutive frames (i.e. cells not captured by capAb immobilized) and the fraction *E. coli* cells that remained static (therefore captured) by the coated microcapillaries, these are summarised in Figures 3.4B (ii) and 3.4B (iii), respectively. A decrease on the surface density of cells captured was observed with the increasing z position in the capillary, confirming the relevant role of gravity and suggesting cell capture is more effective at higher cell densities.

Park et al.[164] demonstrated a strip-based biosensor using ELISA and monoclonal antibodies as immunocapture probes to quantify *E. coli* O157:H7 diluted in PBS buffer after 30 min from a range CFU/ml of $1.8x10^3$-$1.8\ x10^8$. Jayamohan et al.[165] reported immunomagnetic separation (IMS) of *E. coli* O157:H7 in a range of 3-300 CFU per 100 ml of PBS buffer in 2 h, with 95 % extraction efficiency. Naja et al.[166] proposed capture and detection of *E. coli* suspended in PBS, using magnetic immune-nanoparticles. The immunoseparation was assured by attaching specific anti-*E. coli* polyclonal antibodies to the nanoparticles achieving an overall 82% yield. Wang et al.[167] validated a multiplex quantum dot-based immunoassay to separate foodborne pathogens (*E. coli* O157:H7, *Salmonella Typhiurium and L. monocytogens*) resuspended in PBS buffer with 82-90% capture efficiencies, however the immunoseparation process took 2 h overall for a bacterial level range of 10 to 10^3 CFU/ml.

Furthermore Tu et al.[154] emphasized the importance of sedimentation and motion of immunobeads in respect to improving the efficiency of bacterial capture, which is in line with the role of gravity settling for cells retained within capillaries in our approach. Although those authors have attempted the immunocapture/separation, they did not address the miniaturization challenges and presented complex and lengthy preparation steps not suitable for POC applications in contrast to our proposed approach.

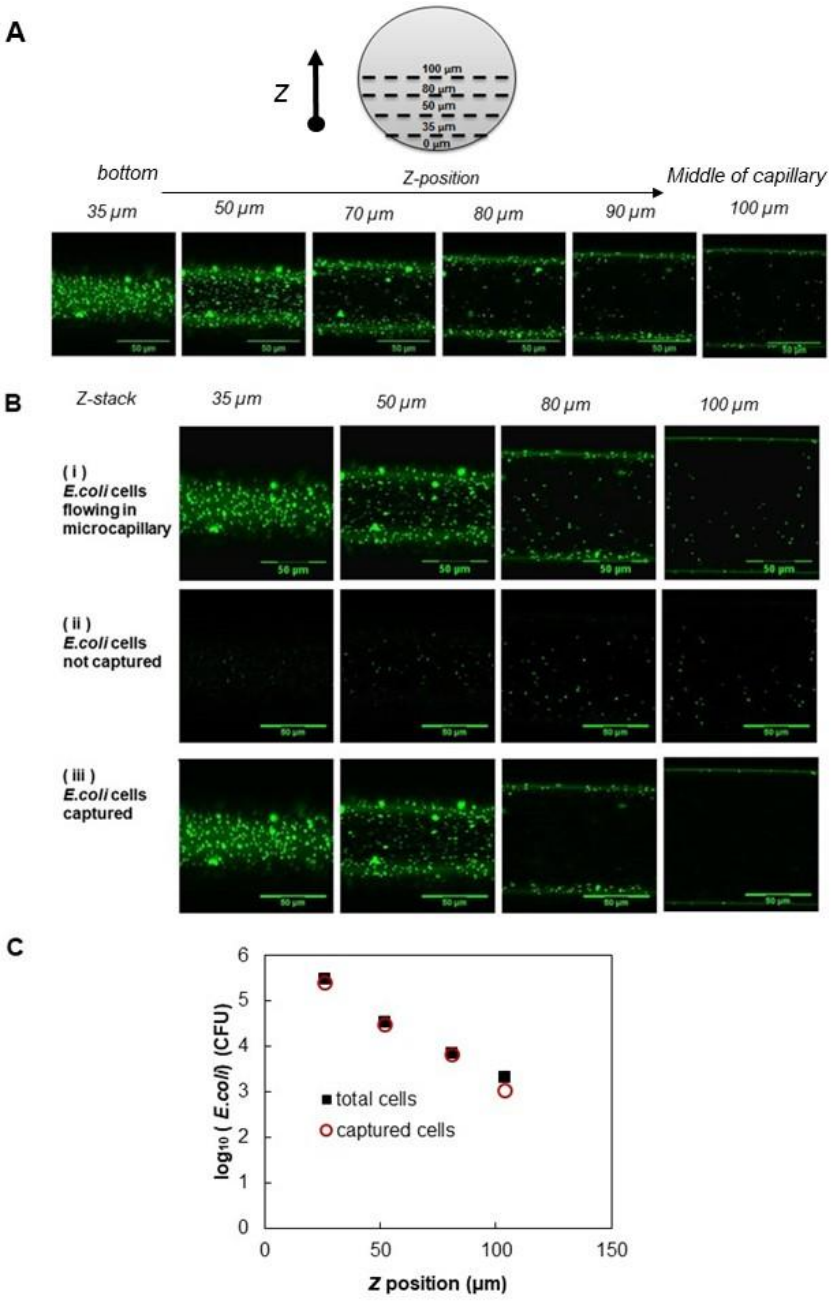

Figure 3.4 LSMC imaging of *E. coli* cells in plastic microcapillaries coated with polyclonal anti-*E. coli* antibody. **A** *z*-stack series of MCF strip coated with 40 µg/ml capAb and blocking solution, and incubated for 5 min (in continuous flow) with a synthetic sample of *E. coli* stained fluorescently in 0.01M PBS. Sequence shows confocal images from bottom of capillary, *z* position = 35 µm (left) towards the middle of capillary, *z* position = 100 µm (right). **B** In-flow capture of *E. coli* cells, total flow rate of 1 µl/min (for 10-bore MCF), (i) snapshot of time sequenced films imaged at 4 fixed *z* positions. Snapshot shows last frame in time sequence; for each stack two consecutive time frames were subtracted yielding in (ii) the cells that remained mobile (i.e. not captured by capAb) and in (iii) bacteria cells successfully captured. **C** $\log_{10}$ total cells and cells captured in interrogation window.

Note that immunocapturing of cells as presented in this work is unable to distinct between viable and dead cells in contrast to e.g. microbiological cells culturing. However clinical samples of active infections tend to have a very high fraction of viable cells (and in case of *E. coli* only live cells remain mobile). This disadvantage of our methodology based on capturing bacterial cells in plastic microcapillaries is surpassed by several advantages compared to other methods. For example, the gold standard method for diagnosis of UTI is entirely based on microbiological plate culture, requiring a trained microbiologist therefore totally limited to laboratory setting.[5,19,42]

Urine samples are presented with unknown cell density, requiring the need to plate a whole dilution series. The procedure can be cost-efficient but is very slow, requiring 2-3 days before CFUs can be counted.[4,12,42]

More modern procedures including enzyme amplification and polymerase chain reaction (PCR) are also complex in terms of fluid handling, requiring enriched samples and pre-selective steps[4,19,42,161], therefore financially un-attractive and restricted to analytical labs.

Fluorescence cell sorting or flow cytometry (bacterial cells or components are fluorescently labelled and analysed as they pass through the liquid stream in front of a laser so they can be detected. The fluorescently labelled cells are excited by the detectors, which therefore pick up a combination of scattered and fluorescent light. This data is then analysed by a computer that is attached to the flow cytometer using special software) is an effective method for counting cells yet it requires fluorescent labelling and separation of cells (which can be done with e.g. magnetic-activated cell sorting). However the method is complex and again limited to lab setting. Immunoassay methods based on plastic surfaces coated with specific capturing antibodies are widely accepted including at point-of-care and sensitive for bacterial detection.

All capillaries were imaged on a given MCF strip (results not shown) and in general observed a small variation (dh = 206 ± 12.6 μm) between the capillaries in the middle of the strips and those at the edges[97,168]. This is due to a 6% of variation on d_h for each capillary across the strip inherent from the melt extrusion fabrication process. According to Haggen-Poiseuille's equation pressure drop is proportional to $(d_h)^4$ a significant variation in flow distribution and mean residence time of the sample across all MCF strips.[168] Individual cells in the in-flow experiments of confocal imaging were tracked to determine the velocity profile of *E. coli* cells flowing along the straight microcapillaries (Figure 3.5). Note the magnification used in the confocal imaging aimed maximum resolution, therefore a small field of view of just 200×200 μm^2 was used.

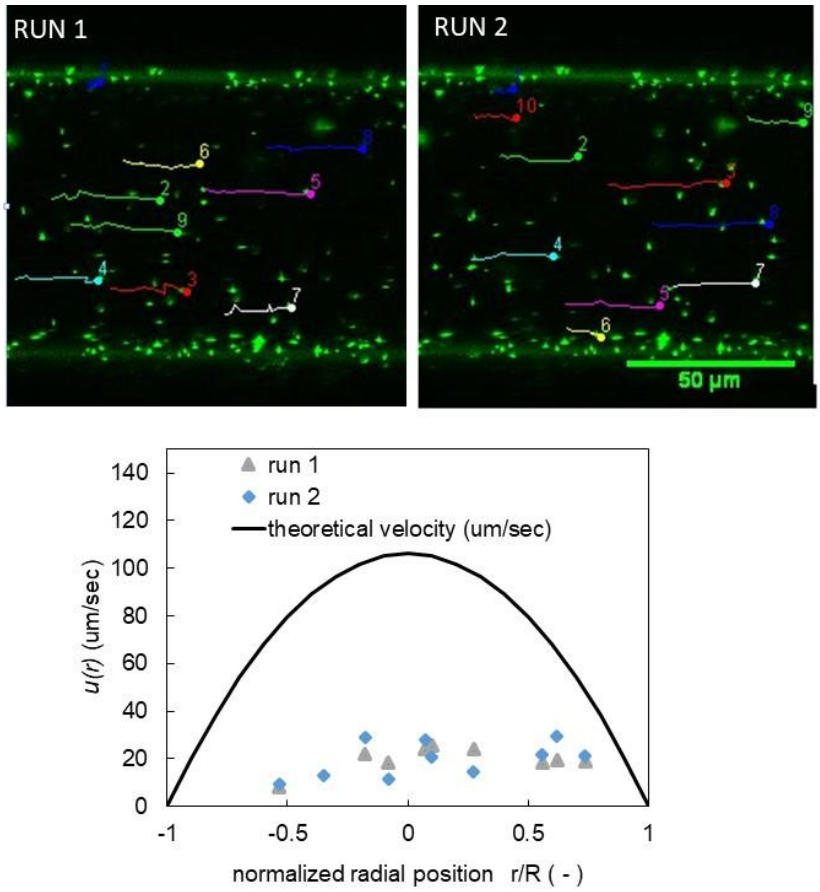

Figure 3.5 Velocity of bacteria flow in microcapillary number 5 versus normalized radial position, for rate of 1 µl/min in the 10-bore MCF. Individual *E. coli* cells were tracked in two separate runs (1 & 2) and the mean velocity plotted. Each dot is representative of one of the 10 lines shown in the individual runs.

All experimental data was collected assuming as reference capillary number 5 (at centre of MCF) and during a period of 20 min (lower than majority of assays presented in Table 2.3). It was noticed higher bacteria velocities at the centre of the capillary and negligible velocity as it approached the walls, agreeing with parabolic velocity profile characteristic of laminar flow in microcapillaries (Figure 3.5) and described by:

$$u(r) = u_{max} \times \left[1 - \left(\frac{r}{R}\right)^2\right] \tag{3.3}$$

where $u(r)$ (µm/s) is the superficial flow velocity at radial position r (µm) estimated, u_{max} (m/s) the maximum flow velocity achieved in centre of capillary, and R (µm) the radius of the capillary (assumed $R = \frac{d_h}{2}$), a maximum fluid velocity in the centre of the wall capillary of 53 µm/s and wall shear rate of 101 s^{-1} were estimated.

A degree of flow focusing was observed, with cells preferring to flow through the centre of the capillary, corresponding to streamlines with reduced shear rate therefore reduced resistance.

This focusing of cells in microcapillaries has a large implication in antibody capture of cells by reducing the probability of cells interacting with the wall and being captured by antibody immobilized at the wall, this observation is very relevant to any method relying on wall immobilization of antibody for quantitation and capture of bacteria. The maximum velocity of bacteria was always observed to be lower (on average 40 – 50 %) than the estimated core fluid velocity. This was consistent across three replicas and is presumably indicative of mobility of *E. coli* cells. According to Wioland et al.[169], *E. coli* trends to walls, however in presence of continuous flow they follow the orientation direction of fluid flow. Those are consistent with the LSCM observations presented in Section 3.3.1. Experimentally, the use of MCF adaptors might has influenced the lower flow rate imposed in MCF strips by the harvard pump.

3.3.4. Avidity of antibody-coated microcapillaries and immunospecificity of antibody-bacteria binding

The avidity of antibody- coated microcapillaries and efficiency of *E. coli* capture in MCF strips coated with immobilized capAb and incubated with *E. coli* samples for 20 min (Figure 3.6) according protocol section 3.2.6. All experimental runs were duplicated and values quantified with a standard deviation within 5%. Note that a capillary entirely coated with capAb presents a SVR ratio 4 times larger than the one obtained by coating a microtiter plate well, so the cylindrical shape of the microcapillaries offers larger surface for capturing cells but also helps pushing the equilibrium towards bacteria-capAb complex formation.

All independent experimental runs 1 to 3 (without washings) and run 4 (with washing) showed a great consistency with a cross-correlation coefficient of $R^2 > 0.9973$, with both CFU/ml and CFU/cm^2 increasing linearly with enhancing bacteria loading, up to 6 orders of magnitude beyond the CFU/ml estimated from a full monolayer (~4.6 log10 CFU/ml). The plot showed bacteria capturing as a first order process with no clear trend in respect to saturation of the surface in the whole window of concentration tested (up to ~10^{12} CFUs/ml).

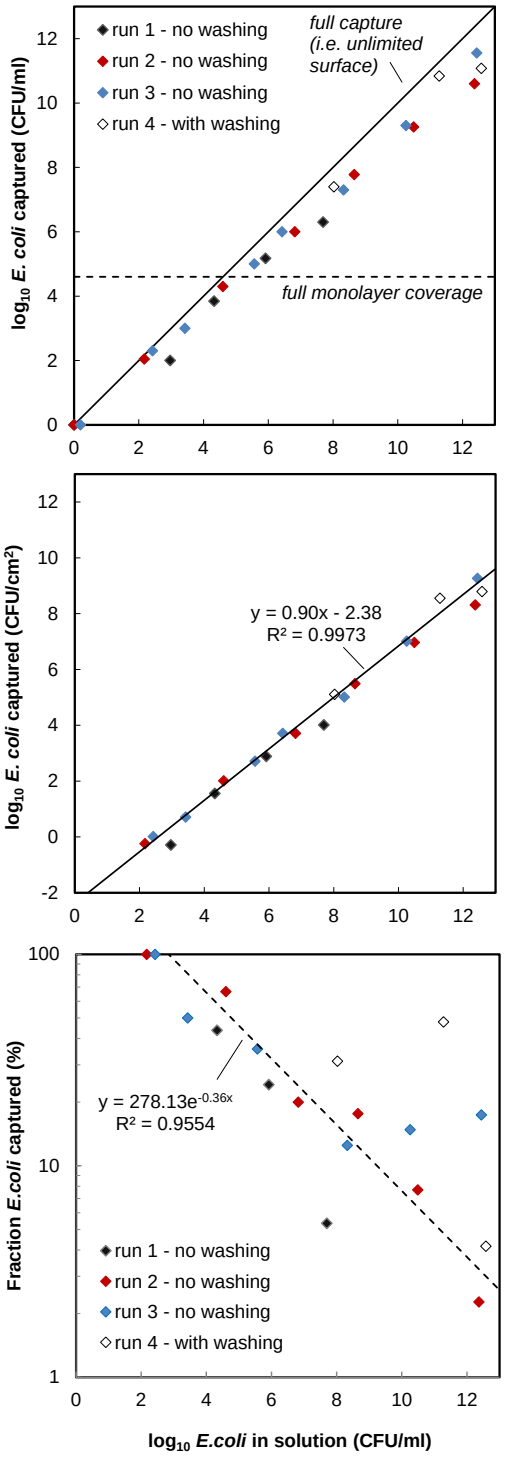

Figure 3.6 Avidity of *E. coli* capturing in the MCF coated with polyclonal antibody based on 3 independent, experimental replicates without (run 1-3) and with (run 4) sample washing. Full monolayer capacity was based on footprint of individual *E. coli* cells. Results are plots as CFU/ml and CFU/cm^2 and efficiency of capturing showing coated capillaries are particularly efficient capturing *E. coli* at low cell densities and washings had no detectable effect in reducing cells capture efficiency, validating immunocapture of polyclonal capture antibodies.

The efficiency for *E. coli* capturing was 100% for small values of CFU/ml (up to 2-3 log10) and followed an exponential decay with increasing CFU/ml in the incubated sample, however surprisingly it remained meaningful for the whole range of CFU/ml tested. For the range relevant to UTIs (up to 10^8 CFUs/ml), the capturing remained between 100 and 20% with just 20 min incubation, so in alignment with the capturing yields reported by e.g. Naja et al.[166] and Wang et al.[167].

The bacteria capturing resulted from a combination of immunoaffinity capturing by the immobilized capAb and gravity settling of cells within the microcapillaries. The later was especially noticeable at high cell densities and presumably linked to aggregation of *E. coli* cells which is widely reported in literature and in SEM microphotographs shown by Figure 3.3.[135,136,154]

Confocal imaging experiments discussed in section 3.3.3 showed settling of *E. coli* cells occurred within few minutes, and definitely within the 20 min incubation time used for these sets of experiments. Although the lowest CFUs/ml tested was 148 (equivalent to 2.15 log10), the plots in Figure 3.6 suggest the approach in this thesis (20 min) for immunocapturing of *E. coli* is 100% efficient at very low CFUs/ml, with a cross-correlation coefficient, R^2=0.9973. Based on the correlation presented for the CFU/ml vs CFU/cm^2 plot and considering the volume of MCF used (133 μl) and area of 25.84 cm^2, the best possible limit of detection would be 20 CFU/ml or 6 CFU/cm^2.

Run 4 aimed testing the effect of adding a washing step with 0.05% w/w Tween 20 in PBS for separating bound from unbound cells following incubation of sample with bacteria, and showed negligible effect of washing at higher cell densities (10^7-10^8 CFU/ml). Note, results were unable to demostrate influence of washing in lower concnetration of bacterial sample. In spite of a 62-fold difference in diameter for an IgG antibody molecule (160 Angstroms)[170] and *E. coli* cell (between 0.5 and 5 μm)[154], cells capturing revealed resistant to fluid shear given by equations (3.1)-(3.2).

Although a methodology for bacteria capturing relying on gravity as the one proposed in this work can sound unpredictable and inaccurate, the data from independent experimental runs demonstrate this method is very reproducible. It is however not possible at this stage to comment on whether this methodology shows any level of selectivity to enable its use for separation of cells or capturing of cells from mixed cultures. This would require further investigation (see chapter 7).

The immunospecificity of coated microcapillaries for *E. coli* capture was tested by carrying out a sandwich immunoassay amplification following a step of immunocapture of bacteria sample. Figure 3.7 shows the polyclonal antibody (specific to K and O serotypes

of *E. coli*) demonstrated specificity for capturing *E. coli* (gram-negative) when tested bacterial samples of *Bacillus subtillis* (gram-positive) suspended in PBS 0.1M buffer. Statistically, no significant difference was observed in the absorbance signal obtained for the sandwich immunoassays incubated with *Bacillus subtillis* and PBS buffer (negative control), however it should be noted that the immunoassays were carried at very high cell densities and the signal shown by *Bacillus sp.* will drop as cell density decreases. Also, *Bacillus sp*. are not present in UTI infections, however was a bacterial strain available in laboratory.

Sanvicens et al.[85] have used the same set of polyclonal antibodies for a quantum dot-based array for sensitive detection of *E. coli* O157:H7 and reported a negligible interference with pathogenic *S. aureus* (gram - positive) and *P. aeruginosa* (gram-negative) at low cell densities.

The cross-reactivity of the antibodies should ideally have been tested against all the most common bacterial strains present in urine samples, which according to the European guidelines for urinalysis[34] are *Enterobacter spp., Enterococcus spp., Klebsiella spp., Proteus mirabilis and Pseudomonas aeruginosa* (majority enterobacteriacea), however any limitations with cross-reactivity of antibodies can be solved by using more specific, monoclonal antibodies for capturing and/or detection stages.

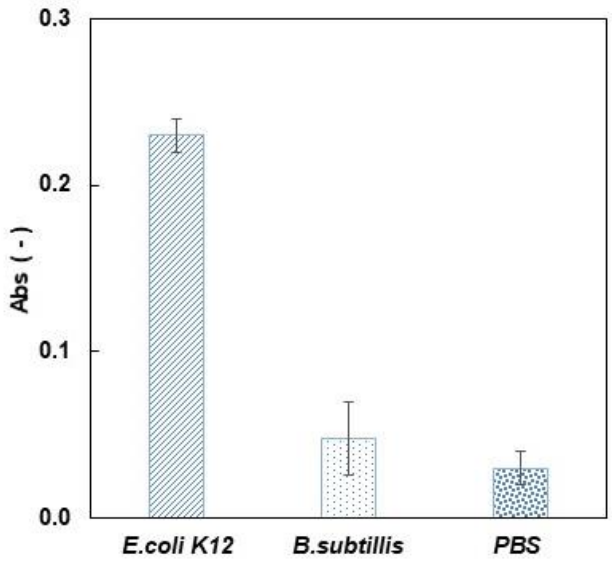

Figure 3.7 Colorimetric sandwich immunoassay showing immunospecificity of cells captured in microcapillaries using 10^8 CFU/ml of *E. coli* K12*, Bacillus subtillis* and buffer diluent (0.01M PBS).

Cross-reactivity of capture antibody with other species can actually be an advantageous feature for offering identification of multiple bacteria strains with a single capture antibody. A comprehensive cross-reactivity study will be the focus of future studies. It is common for some polyclonal antibodies to show cross-reactivity with other species, this will need to be fully examined using pure and mixed cultures before implementation of this method into an actual diagnostic test. Nevertheless, this new data related to immunocapturing is believed very useful for future developments of rapid test for UTIs, from clinical samples likely to contain pathogenic and non-pathogenic bacteria.

3.4 Conclusions

This experimental study has demonstrated efficient capturing of *E. coli* in plastic microcapillaries enabled by a combination of immunocapturing via an immobilized polyclonal antibody against *E. coli* and gravity settling, as evidenced by a range of optical imaging techniques. MCF platform showed immunospecificity for capturing *E. coli* K12 cells and high 'affinity' of capturing, with 100% capturing efficiency.

This study also highlighted the importance of interrogation volume in respect to the minimum CFUs/ml that can be detectable which intrinsically sets the limit of detection and the development of rapid miniaturised immunoassays based on affinity capturing of bacteria. Washings are an important feature in high-performance heterogeneous immunoassays (utilising immobilized antibodies), therefore the washing resistant cell capturing herein reported open up the opportunity to integrate cells capturing with antibody and enzymatic labelling for quantitation of cells in future works.

These new insights into microfluidic capture of *E. coli* are believed to be a major step towards the development of rapid immunoassay-based POC tests for quantitation of *E. coli* and other microbial pathogens. This method for capturing bacterial cells can certainly be applied to capture and eventually separation of other bacteria strains, to be the subject of future studies.

CHAPTER 4 | Microfluidic smartphone quantitation of *E. coli* in synthetic urine

Abstract

The current lack of rapid diagnostic tools for identification and quantitation of *E. coli* and other pathogens is regarded as the biggest bottleneck in the fight against the spread of antimicrobial resistant bacterial strains.

This chapter reports for the first time an optical, smartphone-based microfluidic fluorescence sandwich immunoassay capable of quantifying *E. coli* in buffer and synthetic urine in less than 25 minutes without any sample preparation nor concentration. A limit of detection (LoD) down to 240 CFU/ml, commensurate with the cut-off value required for UTIs (10^3-10^5 CFUs/ml) was achieved. Replicas of full response curves performed with 10^0-10^7 CFUs/ml of *E. coli* K12 in synthetic urine yielded recovery values in the range 80-120%, assay reproducibility below 30% and precision below 20%, therefore comparable to high-performance automated immunoassays. The unrivaled LoD was mainly linked to the 'open fluidics' nature of the 10-bore microfluidic strips used that was enabled by passing through large volume (1 - 2 mL) of samples.

The new smartphone based test has the potential of being a rapid, point-of-care test for reliable identification and quantitation of *E. coli* infections that are responsible for around 80% of UTIs, leading to an accurate prescription of antibiotic and avoid its prescription in situations caused by viruses.

4.1 Introduction

E. coli presents concerning resistant levels to the last generation of antibiotics[2], however the current point-of-care microfluidic devices for bacterial detection struggle to quantify low limit of detection with high sensitivity and specificity to enable the early detection of such infections.[2,13]

There is a current gap in available diagnostics to quantify directly *E. coli* in biological samples. Lateral flow assays, colorimetric strips to detect presence of nitrite and microfluidic paper analytical devices (μPADs) are the available approaches for a quick screening of UTIs, but lack specificity and provide non-quantitative information. The most accuracy diagnosis of UTIs is totally dependent on clinical sample culture in a centralized laboratory facility, which requires minimum 2 - 3 days[12,42] and hence is not suitable for POC diagnostics.

According to the European Urinalysis Guidelines, the limits for symptomatic UTI from midstream urine caused by *E. coli* is 10^3 CFU/ml[34]. This is intrinsically difficult to achieve in a conventional 'dip stick' test, due to very small sample volumes used. Therefore, finding new, portable and straightforward approaches for simple signal detection and effective quantification with affordable readout systems, fluid handling and on-chip reagents storage are essential for POC diagnostics commercialisation at a global scale.[10,76] The prevention and early identification of bacterial infections raises the potential for new cost-effective, sensitive, specific and rapid devices to tackle antimicrobial resistance.

Microfluidic based devices are the emergent tools to develop a new generation of simple to use POC tests bridging a gap between high precision laboratory equipment. They enable integration of multiple steps in one-step handling assay, offering portability, sample and reagent volume reduction, increased automation, lower power consumption and hight throughput.[24,64,160] There is a broad application of microfluidic devices, covering fields including chemical synthesis, bioanalisys, protein cristallization monitoring and POC diagnosis.[10,76] Nevertheless, miniaturization presents some drawbacks mainly by expensive manufacturing costs and reduced sensitive signal demanding sophisticated readout systems.[2,6]

Smartphones as portable biosensors offer a tremendous potential in expanding the new POC diagnostics for several point-of-need applications outside a centralised lab.[120] Portability, wide availability and low cost offered for these smart electronic devices integrated with a wide range of optical based methods as absorbance, reflectance, fluorescence, surface plasmon resonance, bio-chemiluminescence and

electrochemiluminescence.[120] The preferable approaches in microfluidic immunoassays are based in fluorescence and chemiluminescence due to their excellent sensitivity.[42,45]

In an attempt to address the misdiagnosis of bacterial infections, some microfluidic platforms integrated with smartphones were reported and listed in Table 2.2 of chapter 2.

In this chapter It is presented a sensitive and rapid optical sandwich fluorescent immunoassay to detect and quantify *E. coli* K12 in less than 25 minutes in synthetic urine without the need of sample preparation, with the assistance of a smartphone camera. The new sandwich immunossay presents several advantages, such as: 1) affordable off-the-shelf immunoassay reagents, 2) rapid (takes less than 25 min), not relying on doubling-time of bacteria, 3) requires no sample preparation and 4) uses inexpensive microfluidic strips with good optical transparency for smartphone interrogation. Proof of concept was validated integrating a smartphone as optical readout device, achieving a LoD of 240 CFU/ml, from a range of 10^0-10^7 CFU/ml. This immunoassay for bacterial detection and quantification was developed in microfluidic platform, namely Microcapillary Film fabricated from FEP-Teflon®.

4.2 Materials and methods

4.2.1. Reagents and materials

A set of O -monoclonal uncojugated antibodies (# MA1-7029) was used as capAb and biotinaled with biotin to be used as detAb, purchased from Fisher Scientific UK Ltd. As blocking buffers It was tested the followings products: StartingBlockTM Buffer (# 37538), Protein Free (TBS) & blocking Buffer (# 37584) from Thermo Scientific (Northumberland, UK); 3% w/w Bovine Serum Albumin lyophilized powder, free of protein (BSA) (# A3858) from Sigma Aldrich (Dorset, UK) in 0.01M PBS; Elisa Synblock (# BUF034A) and Elisa Ultrablock (# BUF033A) were acquired from BioRad (Hertfordshire, UK); JSR Micro B-3001 and JLSP blocking buffers were donated by JSR Micro (Leuven, Belgium). SIGMAFASTTM OPD (o-Phenylenediamine dihydrochloride) tablets (# P9187), synthetic urine (# S019), hydrogen peroxide (# 289132), and phosphate–citrate buffer tablets, pH 5.0 (cat. no. P4809) were sourced from Sigma Aldrich Ltd (Dorset, UK). High sensitivity streptavidin– horseradish peroxidase (HSS-HRP) (#21130) were supplied by Thermo Scientific (Northumberland, UK). Enzyme and substrate for fluorescent immunoassay consisted of Alkaline Phosphatase (AP) enzyme substrate supplied by Cambridge Biociences (AnaSpec, # 71101-M) and AttoPhos(R) AP Fluorescent Substrate System (# S1000) purchased from Promega UK (Southamptom, UK). As washing buffers, 0.05% v/v Tween 20 diluted in 0.01M PBS (Sigma-Aldrich, Dorset, UK) and alkaline

phosphatase KIT wash buffer (AnaSpec #71101-M) (Cambridge Bioscience, UK) were used. *E. coli* serotype O44 (NCTC9702) was purchased on Culture collections from Public health England and *E. coli K12* (NCIMB 11290) donated by university of Nothingham.

Remaining reagents used in this Chapter were described in section 3.2.1.

4.2.2. *E. coli* sample preparation

The procedure to prepare *E. coli* K-12 (NCIMB 11290) and *E. coli* O44 (NCTC9702) was the same and it is described in section 3.2.3.

4.2.3. Microcapillary Film strips

The microfluidic platform used is a 10-bore microcapillaries, as described in Section 3.2.2. The development of a colorimetric and fluorescent sandwich ELISA in microcapillary strips was demonstrated by Figure 4.1A.

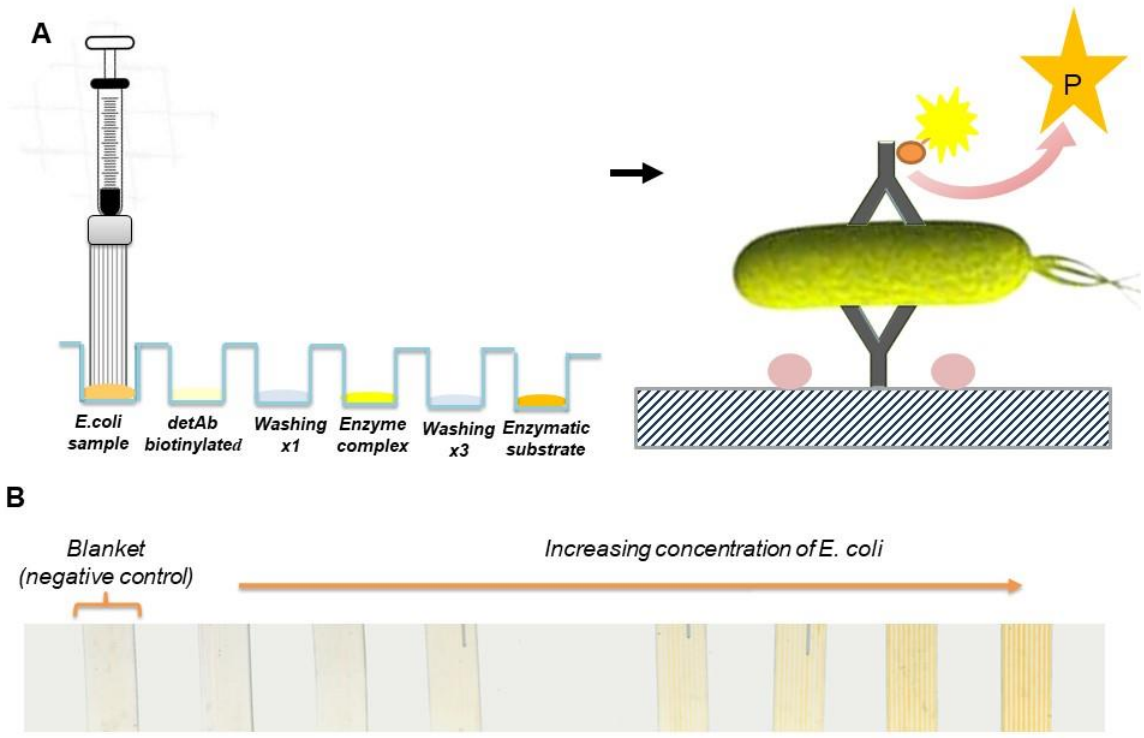

Figure 4.1 Development of a sandwich ELISA in microcapillary film. **A** Immunoassay steps and **B** Scanned MCF strips from an *E. coli* quantitative colorimetric immunoassay strips using MSA, after 5 min of OPD converted (4 mg/mL OPD in 0.1 M phosphate-citrate buffer (pH 5.0) with 1 mg/mL H_2O_2).

4.2.4. Optimization of a colorimetric *E. coli* immunoassay

The immunoassay performance optimization was developed using a fluid handling system, named multi syringe aspirator (MSA) and firstly reported by Barbosa et al.[23](Figure 2.10B), being broadly adapted to several biomarkers assay development in MCF platform.[97,98] The experimental protocol was similar to the procedure used by Barbosa[23] and Castanheira[25] and lately adapted for the fluorescent sandwich immunoassay described in section 4.2.5 and conditions explained in Table 4.1.

The first parameter studied was the ideal concentration of capAb. A 50 cm MCF strip was trimmed into 3 cm pieces and individually coated with a range of capAb concentration: [0, 20, 40, 80, 100, 150 & 200] µg/ml polyclonal capAb in 0.01M PBS and incubated for 2 hours. Following this, each strip was incubated with 3% BSA blocking buffer diluted in 0.01M PBS and incubated for another 2 hours. Afterwards, strips were attached to the MSA and all following reagents preloaded to the custom multi well plate as described by Table 4.1 i): (dilution buffer, 0.5 µg/ml polyclonal biotinylated detAb in 0.1M PBS, washing buffer, 4 µg/ml HSS-HRP, 3x washing buffer and the enzymatic substrate (OPD, 4 mg/mL in 0.1 M phosphate-citrate buffer (pH 5.0) with 1 mg/mL H_2O_2[23]).

Table 4.1 Comparison of time and volume of reagents used previously and after the optimization of *E. coli* immunoassay.

MCF Test	Bacterial assay in MCF strip	Previous Time (min)	Time (min)	Concentration	Volume (µl)	
					MSA setup	MS setup
Bacteria Assay	*E. coli* Incubation	30	12	$[10^9 - 10^1]$ CFU/ml	150×4	350×4
	DetAb incubation	30	3	40 µg/ml	150	250
	Washing	-	-	-	150	300
	Enzyme incubation	30	4	4 µg/ml Alkaline Phosphatase or HSS-HRP	150	250
	Washing	-	-	-	150×3	300×3
	Enzymatic substrate Incubation	1-10	1-5	0.6 mg/ml Atthophos or OPD	150	150
Total assay time (min)		90-100	20-25			

An optimization study was carried on to access the maximum signal-to-noise-ratio and the maximum absorbance signal. To achieve the best assay performance, experimental tests were based in a set of strips, respectively the control strip loaded with dilution buffer (and 0.01M PBS or 3% w/w BSA) and strip loaded with 10^8 CFU/ml of *E. coli* K12 or *E. coli* O44 respectively. The washing buffer in all tests was 0.05 % tween 20 in 0.01M PBS and using 200 µl of reagent solution in each step.

At the end of immunoassay steps, the whole set of 8 strips attached to MSA were laid down in a HP Scanjet G4050 scanner with 2400 dpi resolution in transmittance mode and scanned every minute over the 10 min of incubation.

The RGB images were analysed using ImageJ software, from which the absorbance presented for each individual MCF strip was determined from the baseline grey scale peak height (I_0) in the split blue channel at the peak height (I) at the center of each capillary, where Abs could be directly determined according:

$$\text{Abs} = -\log(\frac{I}{I_0}) \quad (4.1)$$

4.2.5. Fluorescent *E. coli* sandwich immunoassay

The manual incubation of each reagent was performed by 1 ml syringes connected with a silicon tube (i.d. 20 mm) to promote uniform filling of microcapillaries. A concentration of 40 µg/ml unconjugated polyclonal capture antibody (all serotypes) in PBS 0.01M was aspirated to a 200 cm length MCF strip and incubated during 2 hours at room temperature in a petri dish, to avoid evaporation. Afterwards 2 ml of protein free (TBS) blocking buffer was incubated for another 2 h at room temperature. The MCF strip was then washed by 0.05% Tween 20 in PBS and trimmed into small strips of 40 mm each. However, the need to load large amounts of reagents (> 100 µl - < 1000 µl) onto MCF strips, led to use manual syringes, free of aspiration support providing bigger reagents volume handling in several steps as shown in Figure 4.1B.

Volume of sample and incubation time (total 25 min) of each step using MSA or manual syringes are detailed in Table 4.1. Serial dilutions of *E. coli* K12 [range of 10^8 to 10^0 CFU/ml] in 3% w/w BSA or synthetic urine were loaded into a Nunc maxisorp microplate 400 µl well and 3% w/w BSA used as negative control. The strip and syringe were then moved to a new well with 40 µg/ml biotinylated polyclonal detection antibody (detAb) and washed with 0.05% w/w Tween 20 in 0.1M PBS. Consequently, it was incubated with 4 µg/ml of alkaline phosphatase diluted in tris-buffered saline (TBS), pH 7, then washing buffer (AnaSpec) three times and AttoPhos® AP fluorescent was finally

added for enzymatic substrate conversion in fluorescence product as described in Figure 4.1C. In the end of the assay, MCF strips, 96-well plate and syringes were disposed.

4.2.6. Fluorescence signal quantification and Image processing

MCF strips of fluorescence immunoassay developement in buffer were imaged with a BioSpectrum 810 UVP System (AnalytikJena, Cambridge, UK) with 2 seconds of exposure time. Full response curves in synthetic urine were performed by imaging strips with a smartphone, as shown in Figure 4.2A.

A Super bright 9 LED powered by 3 AAA torch purchased from (Mapplin UK) was used as excitation light and integrated in a black hold manufactured in-house. The low background signal for sole fluorescence emission collection was minimized by 50 mm square dichroic additive amber filter provided from Analytik Jena AG (Jena, Germany) between the MCF strip and the smartphone camera to reduce regions of a spectrum lower than 430 nm. For the signal collection, it was used a 60x magnification lens and attachment purchased from Amazon (Slough, Berkshire) for iPhone 6S. Dark conditions were assured to minimize background from fluorescence emission as demonstrated in Figure 4.2B. RGB pictures collected were analysed by ImageJ[163] software in green channel mode (see Figure 4.2B i). It was measured the fluorescence intensity (FI) of each individual capillary I_{int}, for each grey scale plot produced (Figure 4.2B ii), and to minimize the variability originated by camera settings, normalized by the mean intensity peak of reference strip $I_{int,ref}$ or by exposure time of camera settings.

As previously described by Barbosa et al[24], the fluorescence intensity ratio (FR) is given by the equation:

$$FR = \frac{I_{int,sample}}{I_{int,ref}} \tag{4.2}$$

AttoPhos® substrate was converted by alkaline phosphatase resulting in an enhancement in fluorescence signal. This is due to increased quantum efficiency, fluorescence excitation and emission spectra that are shifted well into the visible region, according to the manufacturer. We selected AttoPhos® as it presents an unusual large Stokes' shift of 120 nm, which leads to lower levels of background fluorescence and higher detection sensitivity according to the supplier (Promega). FI values were normalized by dividing it with the exposure time of smartphone camera, according to:

$$FI = \frac{I_{int,sample}}{exposure\ time} \tag{4.3}$$

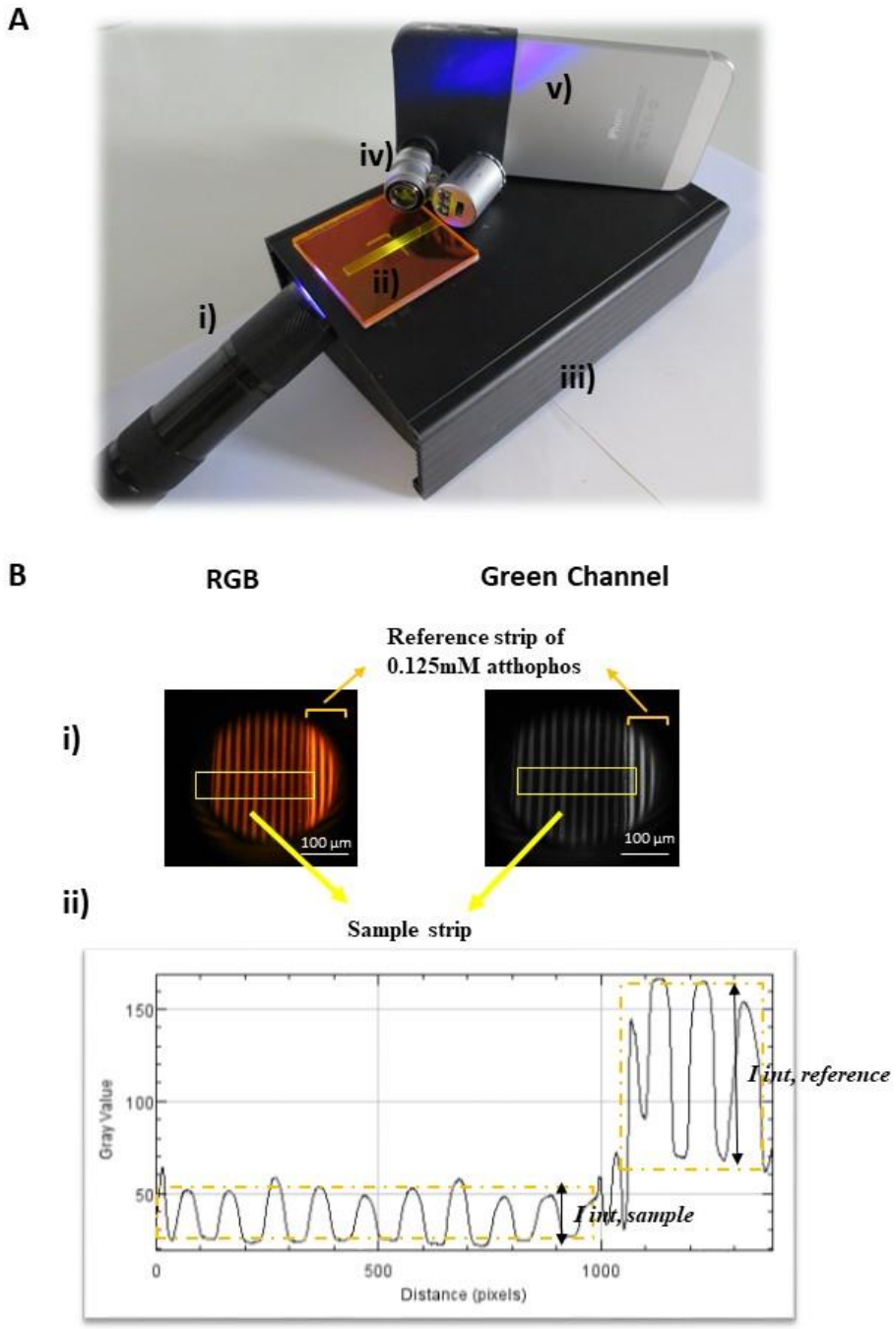

Figure 4.2 Smartphone components used for *E. coli* quantitative fluorescent immunoassay and signal image analysis. **A** Smartphone set up and accessories to coupled *E. coli* fluorescence immunoassay (i) Super bright 9 LED torch, (ii) dichroic additive amber filter (iii) MCF support (iv) integrated magnified lens (v) smartphone (iPhone® 6S, 12 megapixels camera); **B** fluorescence signal quantitation (i) RGB and green channel image (with reference strip of 0.125 mM Atthophos) and strips incubated with bacterial sample, (ii) correspondent grey scale analysis.

Each data point represents the mean fluorescence intensity of 10 individual capillaries within each MCF test strip, and error bars indicate standard deviation of these 10 replicate assays. All immunoassay response curves were fitted with a theorethical 4 parameter logistic model (4PL) and the LoD determined as the minimum concentration yielding as negative control plus 3 times the standard deviation of the blank, which means a minimum signal-to-noise (SNR) of 3 estimates the LoD. Therefore, the LoD is intrinsically related to SNR providing the relation between signal streght and signal stability. By analogy, the limit of quantification (LoQ) was calculated as the lowest concentrations of analyte (blank) plus 10 times the standard deviation[15,51]

4.2.7. Variability studies of fluorescent immunoassay in buffer and synthetic urine

Variability of the immunoassay were determined by replicating on three different days the same assay in buffer (3%v/v BSA) and synthetic urine, and results translated in inter- and intra-assay variability. The measure of the variability of the signal in the same sample is termed precision or variability and expressed by the coefficient of variation (CV), which is obtained by the ratio of the average signal and the standard deviation multiplied by hundred.[15] When it is evaluated in the same assay run is named intra-assay and between different runs and/or samples is called inter-assay variability.[15,51]

In order to evaluate these parameters, three full replicates of smartphone fluorescence *E. coli* immunoassay response curves were performed on different days using different aliquots with the same initial concentration of bacteria. From the same experimental data, % of recovery was calculated based in the ratio of fluorescence intensity (FI) by Equation 4.3 in 3% w/w BSA to the FI signal in synthetic urine sample multiplied by 100%.

4.3 Results and discussion

4.3.1. Optimization and development of an inexpensive *E. coli* immunoassay

Identification and quantitation of pathogens remains time consuming, and still relies on microbiological tests[12,13,34] with enriching medium that have been around for many years or decades. The speed of detection is naturally limited by the initial CFU/ml and doubling-time, which limits their use to rapid, point-of-care (POC) testing. It was taken

an immunossay detection approach to the quantitation of bacteria in a liquid sample, using *E. coli* as working model, a pathogen responsible for around 80% of UTIs. Due to the considerable size of bacteria (between 0.5 and 5 μm)[5], a sandwich immunoassay has the additional advantage over small protein quantitation of enabling the use of a single antibody for both detection and labelling of the captured *E. coli* cells, by simply varying the conjugation with biotin or other molecule according with the fluorescent or colorimetric signal.[5,68,171]

There are at least two major drawbacks identified in immunoassay detection of bacteria that explain the very limited success in development of rapid immunoassay tests for bacteria detection. Firstly, bacteria cells display different morphologies with many surface epitopes (proteins, glycoproteins, lipopolysaccharides, and peptidoglycan) that can lead to nonspecific signal interaction with the sensor surface.[172] Secondly, the washing steps essentials for separating removing unbound detAb and enzyme and reducing the background (which sets the limit of detection, LoD) add shear which potentially displaces the bacterial cells captured with the capAb.[173] It is known sensitive and specific assays are easily achieved by monoclonal antibodies. Nevertheless, it was noticed the absence of immunoassays developments to detect *E. coli* using monoclonal antibodies in the literature, being the exception in *E. coli* O157:H7 detection, or when the antibodies production was performed *in situ* according with specific strains for each study.[158]

Previously to the data reported in this chapter, a set of monoclonal antibodies was selected from Fisher to develop an *E. coli* immunoassay. It was found many companies unable to supply monoclonal antibodies denoting a lack of options for this project and in specific for *E. coli* K12. Based on supplier specifications, the monoclonal antibodies used in this study were reactive with a number of *E. coli* serotypes including: O18, O44, O112 and O125. For this reason, an *E. coli* O44 strain was also purchased purposely and tested. Experimental tests were performed and monoclonal Abs were unable to detect the maximum concentration of *E. coli* O44 and K12 (10^8 CFU/ml) with a signal to noise lower than 1 (see Figure 4.3A), validating the technological challenges in this field (lack of specific probes and therefore specificity) reported in the literature.[5,171]

Based on that, experimental study was continued with polyclonal antibodies. It was noticed that the optimised conditions for the *E. coli* sandwich immunoassay (summarised in Table 4.1 and further detailed in Figure 4.3B) were similar to those reported previously for protein biomarkers quantitations in the same microfluidic platform.[23,24,98] Figure 4.3B shows effect of capAb concentration in colorimetric *E. coli* assay performance with respectively signal-to-noise ratio.

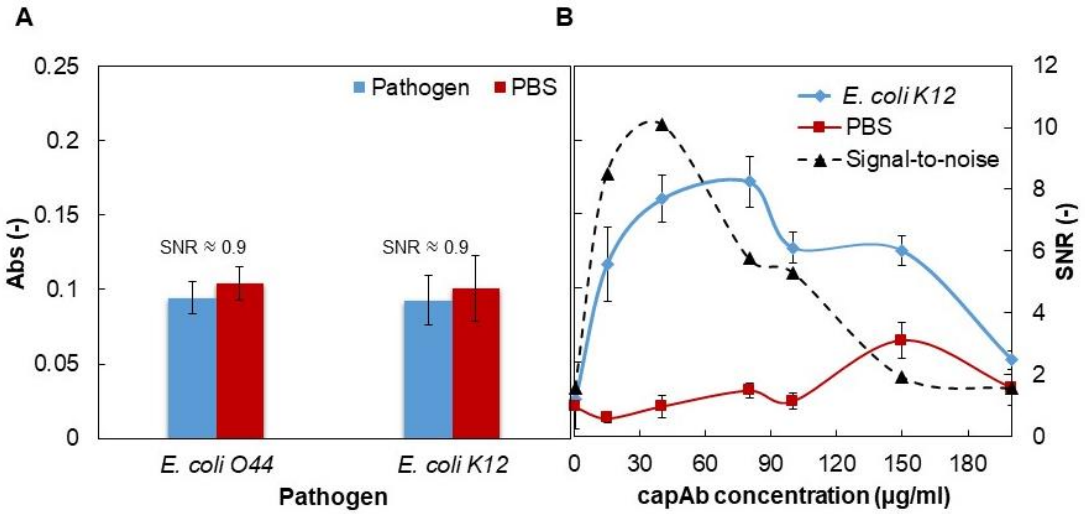

Figure 4.3. Initial study to understand antibodies set to develop *E. coli* immunoassay. **A** Colorimetric sandwich immunoassay test to detect *E. coli* using monoclonal antibodies. **B** Effect of polyclonal capAb concentration in *E. coli* assay performance with respectively signal -to-noise ratio.

A concentration of 40 µg/ml of capAb demonstrated to be the most sensitive (maximum SNR obtained from all concentration of capAb tested) to develop *E. coli* immunoassays in MCF.

Those findings were consistent with characterization results of antibody adsorption onto FEP-Teflon microcapillaries reported by Barbosa et al.[103] suggesting a maximum surface density of 400 ng/cm^2 at 40 µg/ml of IgG solution, meaning 40 µg/ml of capAb is ideal concentration to provide the best oriented position ‘’end on’’ to capture *E. coli* in microcapillary film. Above this concentration there was an increase of background with consequent reduction of SNR and below 40 µg/ml of capAb was produced a reduced signal.

The blocking buffer was the second parameter being studied as fundamental to minimize the nonspecific binding (i.e. the background). All sandwich immunoassay procedure described before was repeated, but coating MCF strips with 40 µg/ml for 2 hours and afterwards incubating in each set of strips a different panel of blocking buffers: Starting Blocking, Super Blocking, Protein Free (TBS) blocking, Elisa Synblock, Elisa Ultrablock, JSR Micro B-3001, JLSP and 3% BSA. Figure 4.4A demonstrated the best SNR achieved was using Protein Free (TBS). Following the same procedure, dilution buffer, concentration of detAb and enzyme concentration were the next parameters assessed.

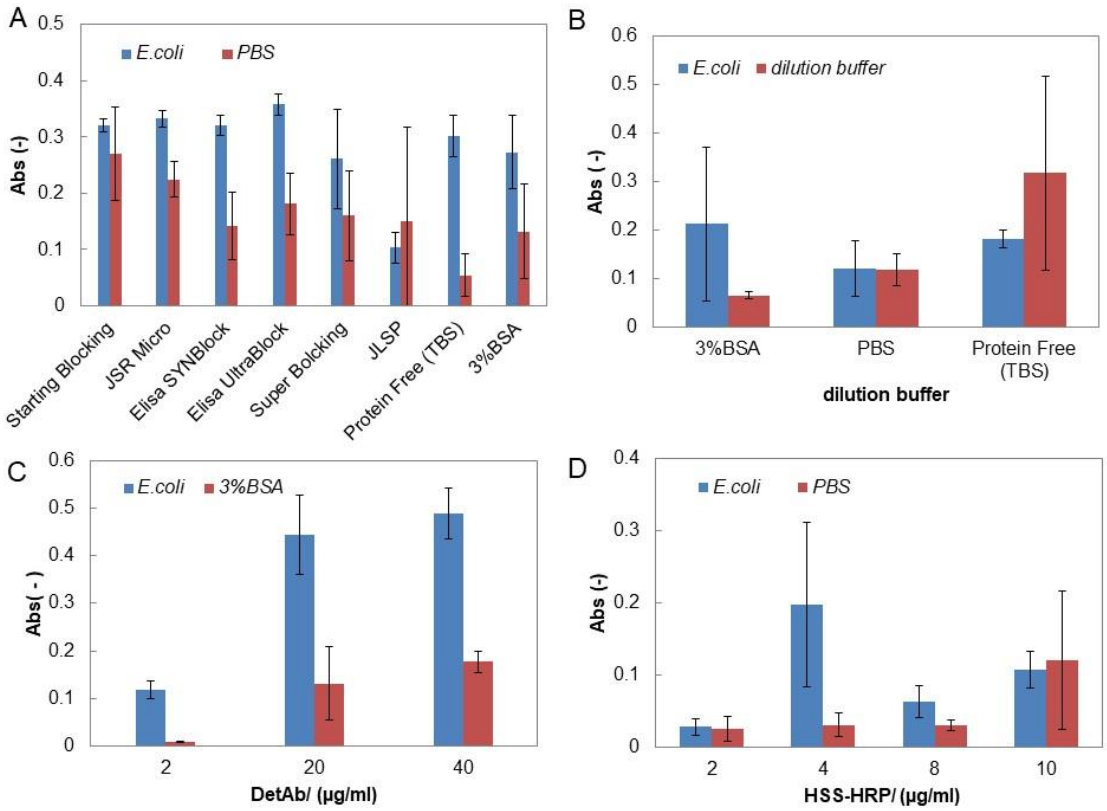

Figure 4.4. Optimization of immunoassay parameters in order to enhance sandwich immunoassay performance. All images analysed were gathered at the end of 5 minutes of enzymatic substrate conversion. **A** Effect of blocking buffer. **B** Effect of different buffer. **C** Effect of detAb. **D** Effect of enzyme HSS-HRP concentration.

Experimental data in Figure 4.4B shows an improvement using 3% BSA as dilution buffer of sample and detAb, keeping capAb and HSS-HRP diluted in 0.01M PBS. Alongside it was noticed an increase of assay performance using 40 µg/ml of detAb (see Figure 4.4C).

This can be related to the binding equilibrium principle stablished by Scatchard's model[25], where excess of detAb favours the binding complex of capAb-bacteria-detAb at the inner surface of 10-bore plastic microcapillaries. Furthermore, this fact matches what many authors reported in literature where they used the same concentration of capAb and detAb for bacterial detection purposes using sandwich immunoassays.[171]

Nevertheless, Figure 4.4D showed concentration of 4 µg/ml of HSS-HRP strength bacteria quantification signal without any increment in background. This fact highlights detAb concentration was paramount to increase proportionally the background of the assay overall with little effect of enzyme complex. In order to improve sensitivity with maximum SNR, incubation times were fundamental to decrease background allowing to

aim a full response curve to detect *E. coli* using a colorimetric immunoassay in less than 25 minutes as specified in Table 4.1 and Figure 4.5. The immunoassay works with a polyclonal antibody, that has the advantages of being strain-specific of a few *E. coli* O- and K- serotypes with higher affinity according to supplier informations. By having multiple bores, 10-replicas on each strip were performed, however, it would be possible to coat each capillary with a different capAb and hence use this system to detect a range of bacterial strains within a single assay.

A

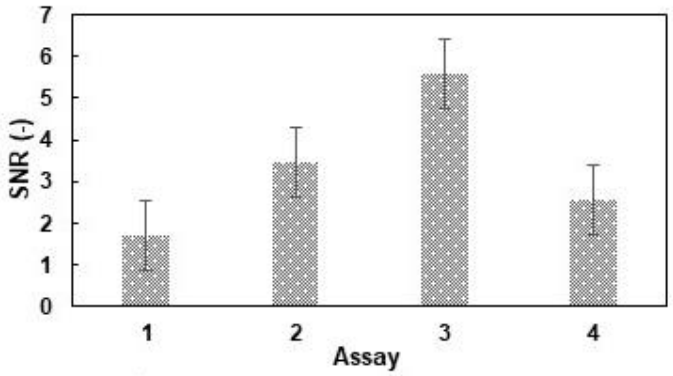

Assay	1	2	3	4
Sample	3x 4min	3x 5min	4x 3min	4x 3 min
DetAb	5 min	3 min	3 min	4 min
Enzyme	5 min	5 min	4 min	4 min
Washings	4x	4x	3x	3x

B

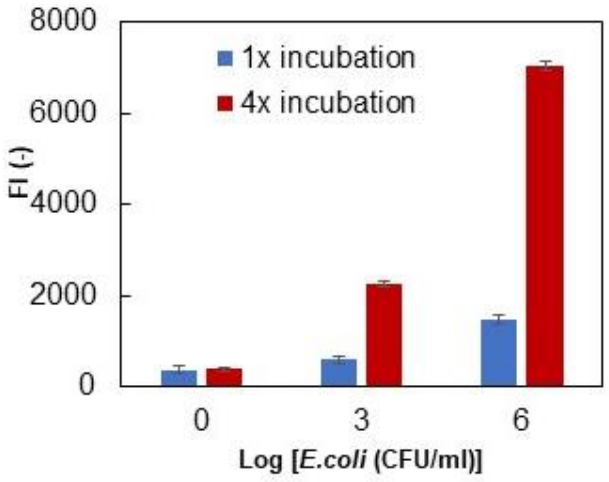

Figure 4.5 Optimization of *E. coli* sandwich immunoassay in MCF platform. **A** SNR performance testing four different sets of time incubations. **B** Comparison of a single incubation sample of 12 min and 4 incubations times by 3 min each.

Note, the 10-bore microcapillaries of a MCF strip can be coated with different concentrations of reagents: (antibodies, enzymes, buffers) or loaded by different bacterial samples using a small syringe needle, as demonstrated by Castanheira et al.[25] However it is not possible to impose different flow rates in the different capillaries (for example using a pump), being the control of flow dependent of manual incubation by syringes.

E. coli immunoassay development demonstrated similar performance concentrations of detAb and capAb used in development of PSA assay[23] and the multiplexed cardic cytokines assay[25] in MCF, paramount to achieving the best performance. The concentration of 40 µg/ml capAb and deteAb was the effective range validated for this *E. coli* sandwich immunoassay and 4 µg/ml the best concentration of enzyme HSS for colorimetric signal as shown by Figure 4.3, 4.4C and 4.4D.

The sample incubation study odserved by Figure 4.5A showed higher SNR by assay 3 (based on incubating the sample for 3 min 4 times followed by 3 min incubation with detAb, washing step, ezyme incubation 4 min with consecutive 3 washings and finalizing with atthophos conversion). The use of multiple incubations revealed a beneficial increase of signal as seen by Figure 4.5B and it will be discussed in detail in section 4.3.2 with further data.

4.3.2. Enhancement of assay performance and sensitivity increased by free volume range

During optimization of the colorimetric *E. coli* assay described in the section 4.2.4, it was noticed a lower performance (regarding the standard value of 10^3 CFU/ml for the diagnosis of UTI)[34] was given by an LoD of 10^4-10^5 CFU/ml with a few reproducibility issues. Fluorescence immunoassays are widely recognized by achieving higher sensitivity in comparison to colorimetric assays.[24,174]

Following similar colorimetric steps used, It was adopted immunoassay procedure to fluorescence quantification using Alkaline Phosphatase, using the same concentration of 4 µg/ml and AttoPhos®. It was noticed an improvement of overall performance and mainly a 1000 fold increase in LoD. Reproducibility of the assay remained variable triggering some technological issues to validate the lower LOD of this assay.

Therefore, it was attempted an ‘open microfluidic approach’ allowed by the microfluidic design of MCF film, passing a large volume of sample through the capAb coated microcapillaries using manual syringes. This multi-incubation strategy enhanced the capacity of coated microcapillaries to capture *E. coli*, being similar to the chromatography principle (where a mobile phase,bacterial samples flow through a

stationary phase, antibodies immobilized in the MCF inner surface, leading to the separation of bacteria cells that are captured by antibodies) by strength the interaction between probe and antigen.

On the other hand, 200 µm internal diameter capillary has a surface-area-to-volume ratio about 16 times higher than a 96 well microtiter plate with 100 µl of solution that benefits the formation of complex capAb-bacteria-detAb. It was attempted to reproduce the same principle over MCF coated strips with capAb (see Figure 4.6A), passing large volumes of sample to increase the concentration of antigen available and promote the capture. Nevertheless, this strategy can be easily applied for efficient diagnosis of UTI , since large volumes of urine are disposed of daily by each human being.

In order to understand the influence of sample volume with time and sensitivity of the assay, a few experiments were carried out using a free range of sample volume using manual incubation (MS), illustrated by Figure 4.6A and related assay performance using MSA (which limits sample volume to under 200 µl in only one step and total volume of assay steps for 1 ml). The full response curves illustrated by Figure 4.6B were obtained in only 19 min of assay plus 2 min of AttoPhos® conversion.

It is evident by the left shift on full response curve the dramatic increase of sensitivity in more than 100 fold, resulting in a LoD of 510 CFU/ml in free range in comparison with an LoD 1.3×10^4 CFU/ml of assay performed in MSA. The analytical sensitivity is the capacity of differentiate two very close bacterial concentrations and is usually given by the slope of the curve. Nevertheless, sensitivity does not consider the non-specific signal while LoD demonstrate the minimum *E. coli* concentration that this test can quantify with a specified precision and reproducibility.[15,51]

A positive improvement in assay variability was noticed using a free volume sample with manual syringes, being precision values below than 20% overall as shown by Figure 4.6C. At same time signal-to-noise ratio increased with free range of volumes, observing a positive increment of 1.5 times of the curve slope as seen by the left shift in Figure 4.6D. The ability of exploit multiple incubations and therefore only possible with a free volume sample offered by manual incubation is related to the improvement of assay variability. This effect was demonstrated by (Figure 4.5B) where SNR from a single incubation of *E. coli* spiked in 3% BSA by 12 min is compared with 4 consecutive incubations of same bacterial sample by 3 min each. An increase of 3-fold a middle concentration of response curve is observed and a further approximately 6 fold intensification of signal is noted for higher concentrations of *E. coli* without any negative impact on non-specific signal.

There is an urgent need to develop POC devices capable of processing biological samples and overcome the matrix effects (the effects of several constituents in real

samples that might influence quantitation of *E. coli* in urine) without sample preparation and minimizing the speed of the assay.

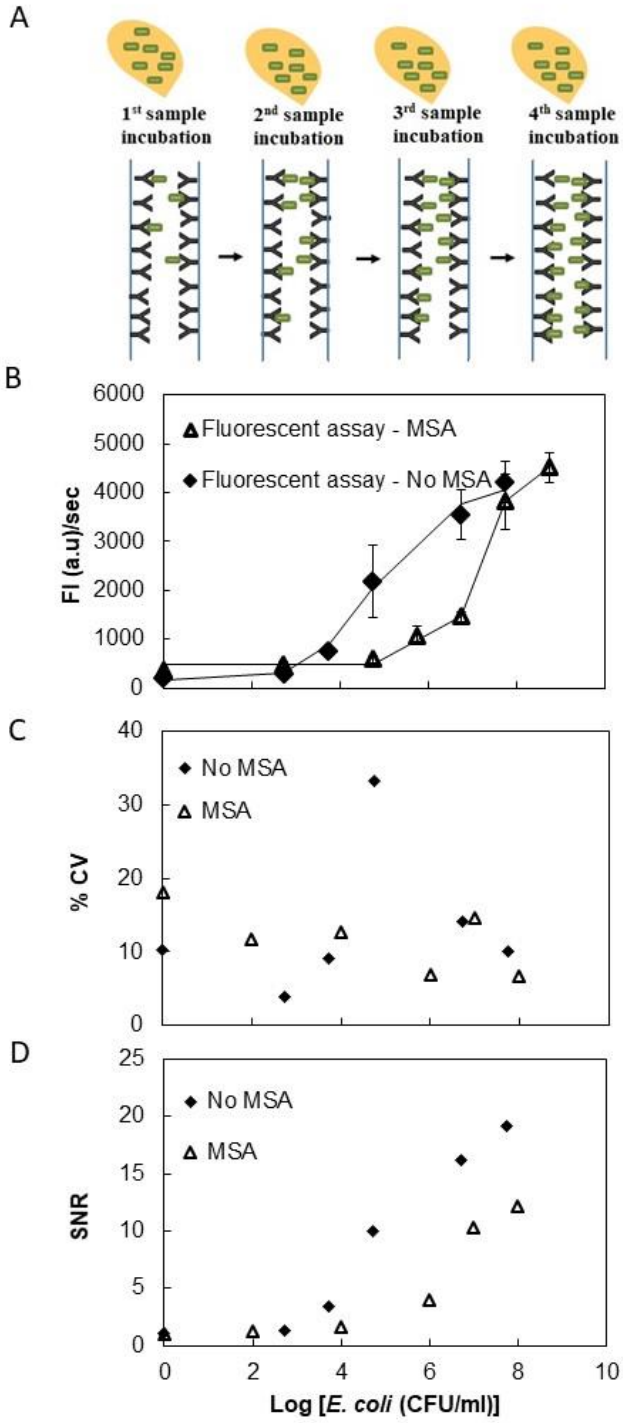

Figure 4.6. Comparison of *E. coli* fluorescence immunoassay performance in buffer (3% BSA) using multi syringe aspirator and free range of volumes with single syringes. **A** Principle of chromatography used in MCF coated to enhance sensitivity. **B** Full response curves. **C** Precision range achieved in all *E. coli* concentration tested. **D** Signal-to-noise-ratio comparison between assays.

Table 4.2 Performance of fluorescence immunoassay determined from full response curves for a *E. coli* concentration of 10^0-10^7 CFUs/ml.

Sample	Fluidics	Imaging device (fluorescence)	Data correlation with 4PL model (R^2)	LoD (CFU/ml)	LoQ (CFU/ml)	Assay time (min)
Buffer	MSA	Gel scanner	0.999	136×10^3	572×10^3	< 25
Buffer	MS	Gel scanner	0.995	473	1300	
Synthetic urine	MS	Gel scanner	0.998	191	575	
Synthetic urine	MS	Smartphone	0.996	240	1527	

Prior to the development of the rapid and sensitive *E. coli* immunoassay using a smartphone as a readout system, the validation of assay performance in synthetic urine was performed in UVP.

Experiments in Figure 4.6 B showed a sensitive performance of fluorescent *E. coli* quantification assay using synthetic urine without any detrimental effect on background. Table 4.2 present the comparison of all fluorescent assays in buffer or synthetic urine, runned in less 25 minutes showing 4PL correlation value, LoD and LoQ respectively. The fluorescent immunoassay running in synthetic urine provided a significant improvement in 2.5 fold the LoD of buffer, presenting a LoD of 191 CFU/ml and a LoQ of 575 CFU/ml with an R^2 of 0.998, matching a high sensitivity of clinical threshold for an UTI caused by *E. coli*, when compared with previous conditions. Very often, biological matrix effects can interfere in the equilibrium capAb-bacteria-binding. This remarkable finding can be explained by the surface-area-to-volume-ratio of FEP microcapillary platform that is 4 times larger than any other surface in a microchannel with same internal dimensions. Therefore antibody–antigen binding is favoured by the increased concentration of free binding sites of capAb on the microcapillaries surface, which results in higher assay sensitivity.[98,54]

Urine pH can varies in a range between 4.6 and 9.0 with, where the urine of an healthy person presents normally a pH of 6.0. Individuals with an UTI present alkaline urine with pH values above 6.[175,176] Nevertheless synthetic urine presents a neutral pH (6-7) that favours antibody activity, promoting the binding with antigen[21].Further studies to

understand influence of real samples would give a complete overview of assay performance as mentioned in Chapter 7.

4.3.3. Proof-of-principle of portable smartphone quantification of *E. coli* in synthetic urine

In order to perform the fluorescence *E. coli* immunoassay using a smartphone camera as readout system, the optical detection of fluorescent substrate was first studied. The environment, light source, right angle and design are factors interfering in the accuracy and sensitivity of a smartphone camera's ability to measure fluorescent signal.

Experiments were conducted in a dark room to avoid interference of light in fluorescence signal and minimize background. For the same reason, a homemade dark polyethylene box was used. Other possibility would be the use of a black card box to simplify the set up and environment conditions in a POC setting. A super bright 9 LED torch was used to illuminate the whole 4 cm MCF strip, where the LED light (filtered by a square dichroic additive amber filter) was scattered and transmitted enabling to detect the fluorescent signal by smartphone coupled with 60x magnification lens. Smartphone images were collected observing the top part of the MCF strip displaced horizontally along assay (from the first sample incubation till the last Atthophos step incubation). Note LED torch and smartphone require battery power but are not plugged in to electricity which matches the power free requirement.

A series of 1:2 dilutions of 1 mM of Atthophos converted, according supplier information and represented by Equation 4.4, were loaded into eight 4 cm MCF strips and placed individually into the smartphone set up seen in Figure 4.2A.

$$Attophos\ Substract\ (BBTP) \xrightarrow{Alk\ Phosphatase} BBT\ anion + P_i \qquad (4.4)$$

where substrate (2´-[2-benzothiazoyl]-6´-hydroxybenzothiazole phosphate $(BBTP)$ is cleaved by alkaline phosphatase to produce inorganic phosphate (P_i) and the alcohol, 2´-[2-benzothiazoyl]-6´-hydroxybenzothiazole BBT).

At this stage it was determined that the best position of the super bright 9 LED torch was to hold this at the front of the homemade dark polyethylene box performing a 45° with base, hence allowing the light to penetrate along the length of the channels rather than across them. This resulted in sharp rather than blurry images. The control of environmental light is often hard, producing sometimes a few inconsistent results with increased signal noise, so a reference strip with converted Atthophos was imaged at same

time of the experiments to ensure normalization of the fluorescent signal. These normalized light conditions improved the image quality capture caused by exposure time variations. Figure 4.7A and B shows the experimental data regarding smartphone fluorescent *E. coli* immunoassay in synthetic urine.

Values of LoD and LoQ are described in Table 4.2, proving the high performance of fluorescent bacteria test in microcapillaries platform, achieving a LoD of 240 CFU/ml and a LoQ of 1327 CFU/ml in less than 25 min.

Despite this value matching the sensitivity for an UTI a slight decrease of this parameter in comparison to the test performed in UVP is noted.

This loss is intrinsically related to the 'digital capture' of smartphone camera and light environment surrounded. Some authors have attempt microfluidic fluorescence assay for UTI diagnosis which performances are regarding *E. coli* detection and quantitation in buffer, synthetic urine or urine but their assay times are typically longer, require more sample preparation or do not achieve such a low LoD.

For example, Yoo and colleagues[16] reported a LoD of 10^3 CFU/ml of *E. coli* in PBS using a microfluidic fluorescence assay with total assay taking 30 min plus 45 min of staining. Yang and Team[128] reported an LoD of 3.4×10^4 CFU/ml of *E. coli* in synthetic urine with total assay taking 100 min. Safavieh and colleagues[17] developed a microfluidic loop-mediated isothermal amplification (LAMP) with electrochemical detection presenting an LoD of 48 CFU/ml of *E. coli* using filtration of urine as pre-sample treatment and total assay taking 60 min.

Therefore, intra-assay and inter-assay variability are represented respectively by Figure 4.7C. With the exception of three values between bacterial range log 2 and log 4, the overall precision of the three assays remained below 20%, as shown by Figure 4.7C i). Signal-to-noise-ratio presented in Figure 4.7C ii) shows a slight decrease, around 0.5 times, when compared to the values achieved for assay in buffer (Figure 4.6B). This difference is mainly noted in the high concentrations of *E. coli* quantified when the fluorescent signal is proportionally stronger or saturated and harder to be quantified due to limitations of the camera settings.

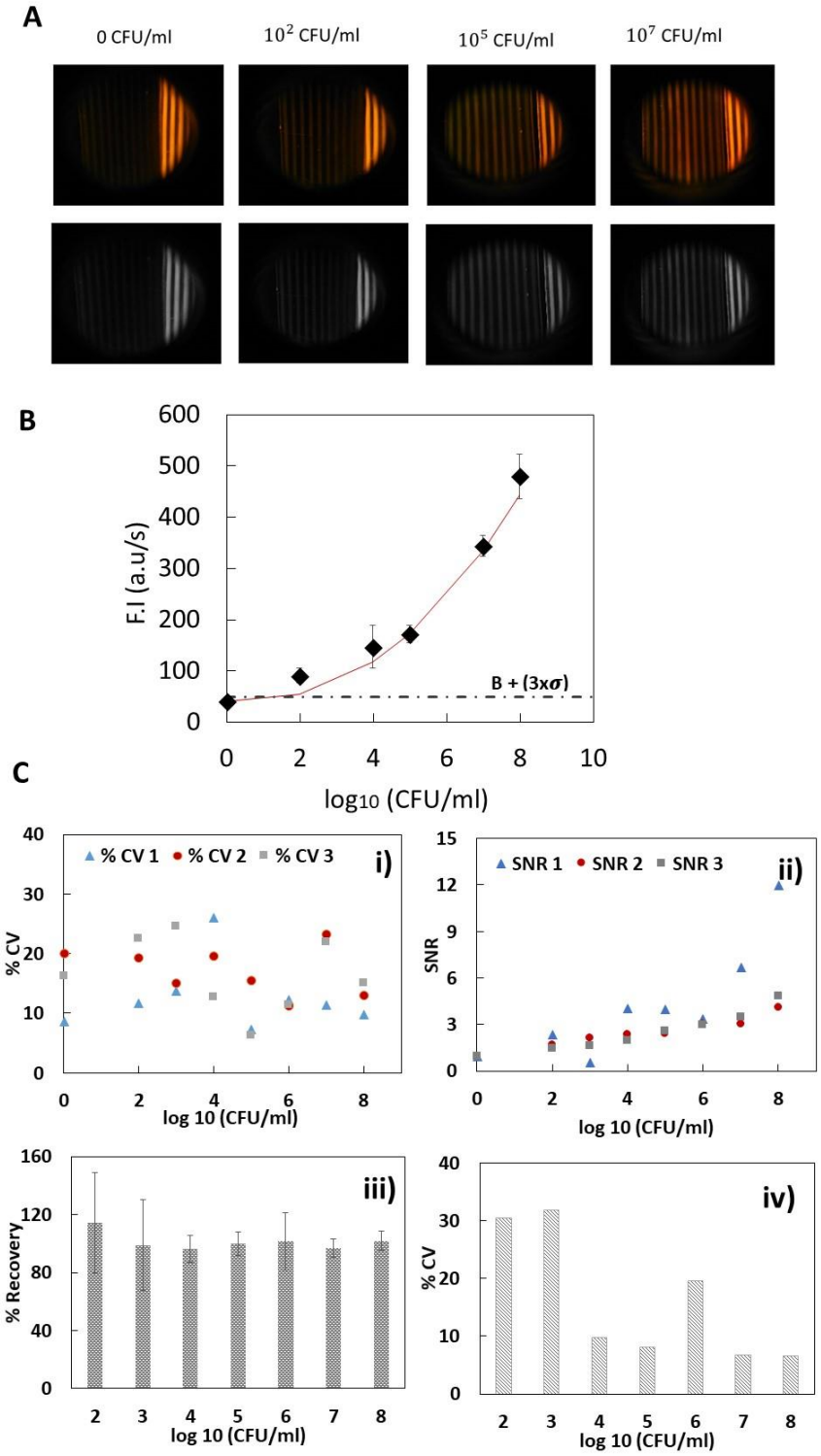

Figure 4.7 Smartphone fluorescence detection of *E. coli* in synthetic urine. **A** RGB and Green channel images of MCF phone quantitation. **B** Full response curve at 2 minutes of Atthophos conversion. **C** Inter-variability study showing the precision range (i) and SNR overall (ii). Intra-variability study for a triplicate quantitation of *E. coli* in 3 different days showing the percentage of sample recovery in (iii) and precision intra assays in (iv).

Recovery values for each concentration showed very linear and consistent within ranges 80-120% (see Figure 4.7C iii)), what is desirable for immunoassays. Furthermore, intra-assay precision was also evaluated and is displayed in Figure 4.7C iv). All values are below 30%, being higher in lower concentrations of *E. coli* in urine. However according to Ederveen[177] and Suresh [43] this value is still under acceptable limit due to cumulative error effect during different steps. This ultimately demonstrates the fluorescent *E. coli* immunoassay coupled with smartphone as an efficient test for *E. coli* quantification in urine, overcoming the matrix sample complexity without additional steps of sample preparation for POC.

Future developments will be focused in develop new microfluidic designs driven by gravity to load liquid samples and minimize detrimental shear stress on capture of bacterial cells caused by manual incubation. To further boost the reproducibility of this microbiological test, a portable light detector will be developed by simple accessories that create a mini dark box around the photo camera, preventing ambient light from interfering with the test's light signal.

4.4 Conclusions

This work demonstrated proof-of-principle for a new affordable, optical microfluidic test integrated with a smartphone camera able to perform a fluorescence immunoassay for *E. coli* quantification. Full response curves performed in both buffer and synthetic urine yielded a LoD of up to 240 CFUs/ml in less than 25 minutes (lower than 85% of assays presented in table 2.1), which is compatible with clinical cutt-off for UTIs caused by *E. coli*.

The ability to pass a large volume of sample through the 'open' microfluidic strips was revealed as key to yielding >100-fold improvement on LoD. This is believed to be linked to increased number of bacterial cells captured by the immobilised capture antibody before addition of immunoassay reagents. The recovery values and inter- and intra-variability data shown demonstrates the bioassay is simple yet robust and reproducible, and comparable to high-performance protein immunoassays. Future work will report strategies for power-free reagents loading and improvement on smartphone fluorescence interrogation.

This affordable immunoassay-smartphone based strategy for rapid identification of *E. coli* strains is relevant for a more accurate prescription of antibiotics worldwide, particulary in low income countries where patients have limited access to centralised microbiology and pathology labs. A single device (holder without MCF strips) coupled with a smartphone can be reused thousand times with disposable MCF strips coated with capture antibodies and easily transported between clinical settings.

CHAPTER 5 | Hydrodynamic characterization of two new power free microfluidic devices

Abstract

Diagnostics are the key device to increase life expectancy. Nevertheless power free quantitative diagnostics would benefit low resource settings.

This chapter presents for the first time two new high throughput microfluidic designs capable of performing multi-step point-of-care sandwich immunoassay detection, using just gravity, named ‘’MCF-funnel’’ and ‘’MCF-siphon’’. The latest is the first ever microfluidic device to solely perform by siphon action. They integrate eight Microcapillary Film strips each with 60 mm and 54 mm length respectively (with 10 capillaries i.d 200 µm). The inner surface of the hydrophobic of FEP-Teflon® were coated with PVOH and both devices have been characterized by injecting a consecutive step change of dyes and washes for hydrodynamic flow characterization by residence time distributions (RTD). The distributions were then compared with an axial dispersion model. The siphon design have demonstrated a more consistent and reproducible flow presenting the lowest standard deviation of residence time ≈ 3-5% along hydrodynamic acessement. Despite MCF-funnel design have presented lower residence time (< 15 s) in comparison to siphon (< 58 s), the last showed negligible levels of backmixing with effective dispersion axial coefficient lower than 5 x 10^{-6} m^2/s between eight strips per step. Dimensionless dispersion number showed a plug flow closer to ideal (< 0.02) without detectible contamination of dyes and washes resulted by the dead volumes observed in MCF-funnel.

This chapter provides the foundations of an affordable, automated and power free device which could be combined with an inexpensive readout system to produce an extremely powerful power-free diagnostic tool for future point-of-care diagnostics.

5.1 Introduction

Microfluidics platforms are driven by the desire to achieve the highest practical degree of miniaturisation, although the employment of such platform as biosensors, as micro-total analysis systems (μTAS) and lab-on-a-chip formats has exploited a continuous innovation and development in the design of new devices[178,179] for pharmaceutical industry[90], environmental monitorization[180,181] and biomedical applications.[178,179,182,183] The promising advantages of portability, fast and efficient analysis of using this miniaturized technology represents a clear trend towards growing this market.[181,180] Despite the several advantages, the automation of multi-step sample processing, reaction and detection remains challenging.[181] Solving the problem of expensive manufacturing process of microfluidic platforms, fluid handling and limited-resource settings will require innovative approaches to increase effectiveness in performance of low cost devices.[8,182,180]

Contrary to prevailing methods of microfluidic chip fabrication, 3D printing is a versatile and effective alternative for manufacturing devices that contain these microchannels, as they can be manufactured quickly at a relatively low cost with minimum labor work.[183]

To this end, more design concepts implying sequential fluid delivery and exploiting further engineering technologies to ensure power free, portability and reliability are receiving major consideration for POC applications. For example, Hosokawa et al.[184] developed a power-free injection method for a microfluidic immunoassay to detect protein-reactive C (CRP) by air evacuation. Juncker and team[185] reported an autonomous microfluidic capillary system to transports aliquots of different liquids in sequence by capillary phenomena and it therefore does not require any external power supply or control device. Laksanasopin and team[186] reported a full laboratory-quality immunoassay to detect HIV and syphilis without requiring stored energy based only in a smartphone dongle. Nevertheless microfluidic paper analytical devices (μPADs) are growing in the market of POC, being based on capillary action without need of external power sources to pump fluids through a device. Examples are the commercial strips for urine analysis[175], detection of human chorionic gonadotrophin in pregnancy tests[65,175] and glucose assay.[187]

Novel pressure driven designs can launch a new generation of automated and power free devices integrating the inexpensive Microcapillary Film platform. The surface modification of inner FEP-Teflon® microarray is a significant step for implementation and full performance of this new design approaches, yet not trivial regarding optimized surface modification of standard microfluidic devices as glass or PDMS.[110,94] Reis and co-authors[110] reported for the first time the one-step microfluidic bioassays, named ‘’Lab on a stick’’ with MCF bulk coated with a hydrophilic crosslinked PVOH layer. Pivetal and

colleagues[94] studied by the first time the covalent immobilisation onto FEP films by introducing a diverse panel of functional groups such as glutaraldehyde, polyvinyl alcohol (PVOH), PVOH via NHS-maleimide solution, PVOH using glutaraldehyde and (3-aminopropyl) triethoxysilane (APTES) - coated PVOH for sensitive and quantitative immunoassays.[94] Despite high-background as result of surface modification, they showed inert and hydrophobic fluoropolymer microfluidic strips effectively coated with PVOH were sensitive and rapid to quantify IL-1β in a relevant range for cardiac diagnosis.[94]

Herein, It is presented for the first time two new design approaches: MCF-funnel and MCF-siphon which uniquely combine the reagents and sample loading in sequence solely driven by gravity to perform power free immunoassays in the MCF. These two designs were manufactured using 3D-printing technique and integrate affordably manufactured MCF strips with their inner surface wall coated with crosslink PVOH. Consequently this work exploit automation in delivering fluids which increase repeatability, eradicate human error and enables increased throughput, mainly by this new sophisticated multi step assay performance. MCF-funnel and MCF-siphon were designed and studied to ultimately address some drawbacks pointed out previously in chapter 3 such as the need to work with lower shear stress flow and exploit gravity settling of bacteria within capillaries and the need to improve fluid handling system of chapter 4. Thus, funnel and siphon present key features that intend to: minimize the disruptive effect of shear stress caused by loading reagents promoting lower flow rates and increase residence times; minimize dead volumes (important in volume precision mainly in low analyte concentration) and decrease cross contamination of reagents to improve reliability; be power an battery free, be practical for easy access in low resource settings and user friendly; be off-the-shelf design with ability to integrate inexpensive readout systems as camera or smartphone, reduce assay time by reducing diffusion distances, cost effective manufacturing process and provide quantitative fluorescent or colorimetric assays due exceptional optical characteristics of FEP-Teflon microarrays.[97] From our knowledge, MCF-siphon is the first ever microfluidic point-of-care platform where the whole device relies on the siphon effect.

Residence time distribution of a flow into microcapillaries is a useful information for clarifying for instance the presence or not of an ideal near flow response, visualizing homogeneity flow and access overal performance. Injection pulse methods are reocurrent in chemical, biological systems as biomedical applications as well, with signal measurements can be based in fluorescent, colorimetric or radioactive probes. Heymann and team[188] have reported blood flow measurements with radionuclide-labeled plastic microspheres to detect anomalies in cardiac valves and the presence of shunting through various organs. Mao and colleagues[189] have introduced a novel fluid manipulation

technique named ‘‘microfluidic drifting’’ performing an hydrodynamic acessment with 50 mM fluorescein and measuring signal output via epifluorescence microscopy. Ultimately, Hornung and Mackley[190] have characterized the flow performance of a 19 parallel thermoplastic microreactor system with diameters around 230 µm using optical micro-probes and assuming plug flow model superimposed by axial dispersion open-open boundary. Also Reis and Li Puma[168] have measured the fluid behaviour in a 10-bore Teflons FEP MCF with different mean hydraulic diameters (aproximatelly 103 and 159 µm).

In point-of-care diagnostics aiming to achieve sensitive immunoassays, the understanding of fluid flow performance can be paramount to standardize fluid shear of reagents loading and maximize interactions between probe and antigen. Repeatable and consistent flows are also qualities evaluated in this new MCF designs leading to more reliable assays and better quality imaging. This only can be achieved through capillaries homogeneously filled with a consistent flow rate, free from air bubbles and lower backmixing. Moreover costs of point-of-care diagnostics can be reduced by designs where low sample and reagents volume and small MCF lengths with antibody immobilized are needed.

5.2 Materials and methods

5.2.1. Reagents and materials

Digital ABS RGD 515 (cat. no. 5117-12-4) and RGD 531 (cat. no. SDS-06152) for 3D printing MCF gravity devices, support material SUP 705 (cat. no. 57-55-6) were purchased from Stratasys Ltd. (Derby, UK). The MCF-siphon reservoirs were made from clear cast acrylic (cat. no. 490-995) from Technology Supplies Ltd. (Lancashire, UK). Screws and bolts in stainless steel, grade 316 and pro white PTFE tape 12mm x 5m x 0.2mm (cat. no. 231-964) were sourced from RS (Nottingham, UK). Polyvinyl alcohol (PVOH) (MW 146000–186000 g mol^{-1}; 99+% hydrolysed; cat. no. 363065), Tween®20 (cat. no. P1379), ProClin™ 300 (cat. no. 48912-U) were purchased from Sigma-Aldrich (Dorset, UK). MCF fittings were designed by Lamina Dielectrics Ltd and manufactured in-house connected to a female Luer ¼ (# P-624) obtained from CM Scientific (Silsden, UK). Nunc maxisorp ELISA 96-well MTPs (#10547781) were sourced from Sigma Aldrich (Dorset, UK). Blue and red tracers were food dyes obtained from Sainsbury's supermarket. Optical conditions were assured using a 12V LED tube light (cat. no. LEDTSMD201) from BeamLED, UK and a 50 cm Photography Studio Soft Light Box Photo Tent Cube 4 Colour

Backdrop purchased on ebay, UK. Images were taken using the USB 2 uEye XS industrial camera by IDS Imaging (Obersulm, Germany) with the accompanying IDS software suite.

All image analysis was processed by ImageJ bundled with 64-bit Java 1.8.0_112 (NIH, USA).[163]

5.2.2. Microcapillary Film strips

This miniaturized microarray film was presented in section 2.6.1 and 3.2.2.

5.2.3. Coating Teflon-FEP microcapillaries with crosslink PVOH

The hydrophobic inner surface of microcapillaries was modified for hydrophilic surface adding the crosslinker molecular weight PVOH. The influence of capillary rise was studied using three different solution concentrations: 0.10; 0.15 and 0.20 mg/ml prepared from a stock solution generated by dissolving 0.2 g of the PVOH in 100 ml ultra-pure water. The solution was heated by a hot plate at a constant temperature of 85°C till complete dissolution of PVOH and mixing with a magnetic stirrer. Due to evaporation, ultra-pure water was added to ensure accurate solution concentration. Proclin™ 300, which is a diagnostics grade preservative, was added at 0.05% (w/w) concentration to avoid any microbial growth.

Afterwards, the solution was diluted in 0.01M PBS to produce the desired concentrations. Hydrophilic coating was made by injecting each concentration of PVOH solution into 100 cm length MCF strips with support of MCF fittings and female leur connected to a luer lock 2 ml syring and leaving for incubation overnight at room temperature. Hydrophilic MCF strips were then washed with 0.05% Tween®20 and dried by blowing air using silicon fitting (i.d. 2mm). The inner surfaces of the hydrophobic MCF were coated with 0.10; 0.15 and 0.20 mg/ml of PVOH to measure liquid rise. Previous studies carried on by Reis and team[110] suggested the inner surface modified by PVOH reduced the contact angle from 122.4 ± 3.15 degrees to 74.9 ± 1.80 degrees.

5.2.4. Manufacturing and fluid handling operation of gravity driven devices: ‘’MCF – funnel’’ and ‘’MCF – siphon’’

Gravity driven microfluidic devices were manufactured using a mixture of Digital ABS RGD 515 and RGD 531 3D with SUP 705 as support material and printed by an Objet Connex260 3D. MCF-funnel design is able to integrate a 60 mm MCF strip and waste

reagents are collected by a Nunc maxisorp ELISA 96-well MTPs, as seen in Figure 5.1. For effective sealing of funnel, 6 screws and bolts were used to tighten the structure and PTFE used to seal the top part of the strips. MCF-siphon was designed to assemble a 54 mm length MCF strip, according Figure 5.2, with sample reservoirs made by clear cast acrylic (Figure 5.2E). Both approaches are driven by gravity due inner surface modification of microcapillaries described in 5.2.3. An 8-pipette channel was used to load 80 µl of liquid in each reservoir on the top of the funnel. MCF-siphon is totally pippette, pump or any external device free.

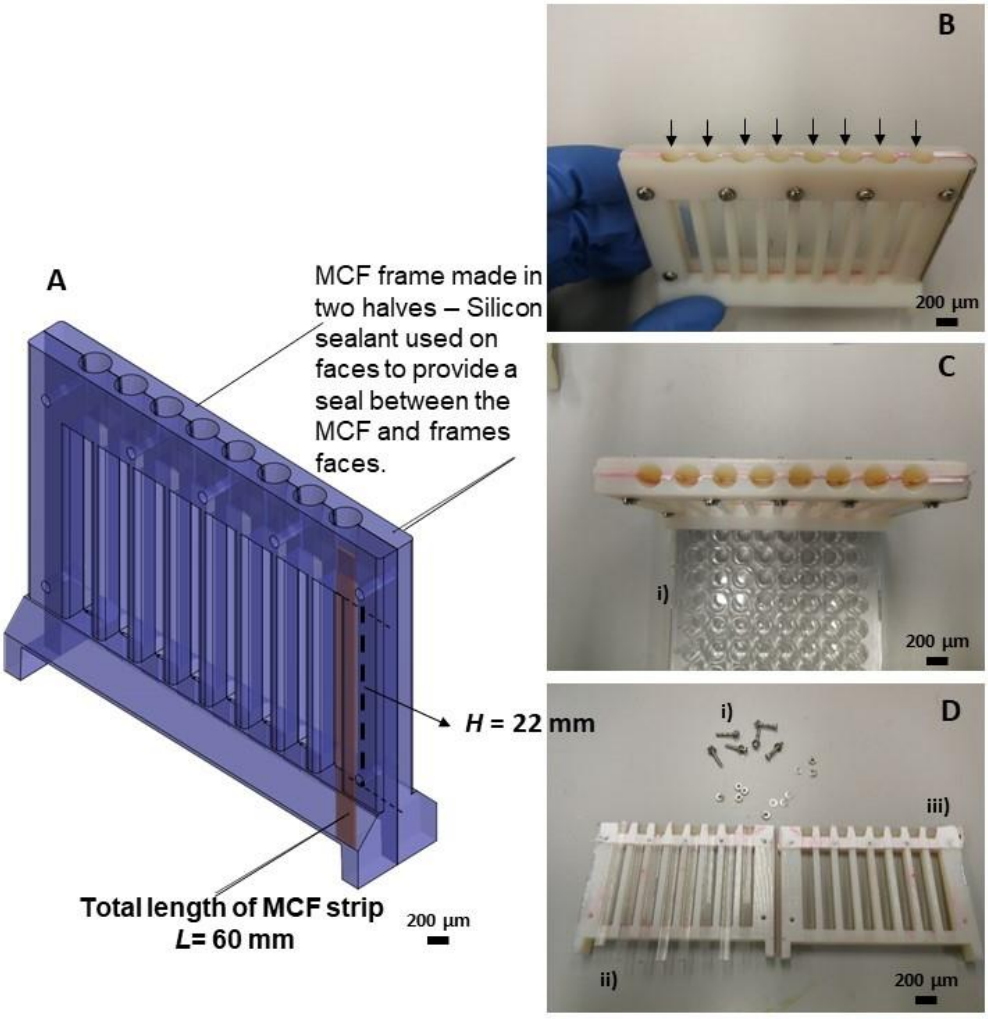

Figure 5.1 3D printing design and structure of MCF gravity driven denominated ‘’MCF-funnel’’ manufactured by 3D printing. **A** 3D printing draw **B** MCF-funnel manufactured by digital ABS assembled in two halves integrating 8 small funnel entrances to load 60 mm length MCF strips. **C** Funnel coupled to nunc maxisorp ELISA 96-well MTPs in i) to collect reagents waste to assess hydrodynamic characterization. **D** Individual structures of funnel before assembling, i) 6 screws and bolts in stainless steel, ii) 8 MCF flat films and iii) white PTFE film for sealing.

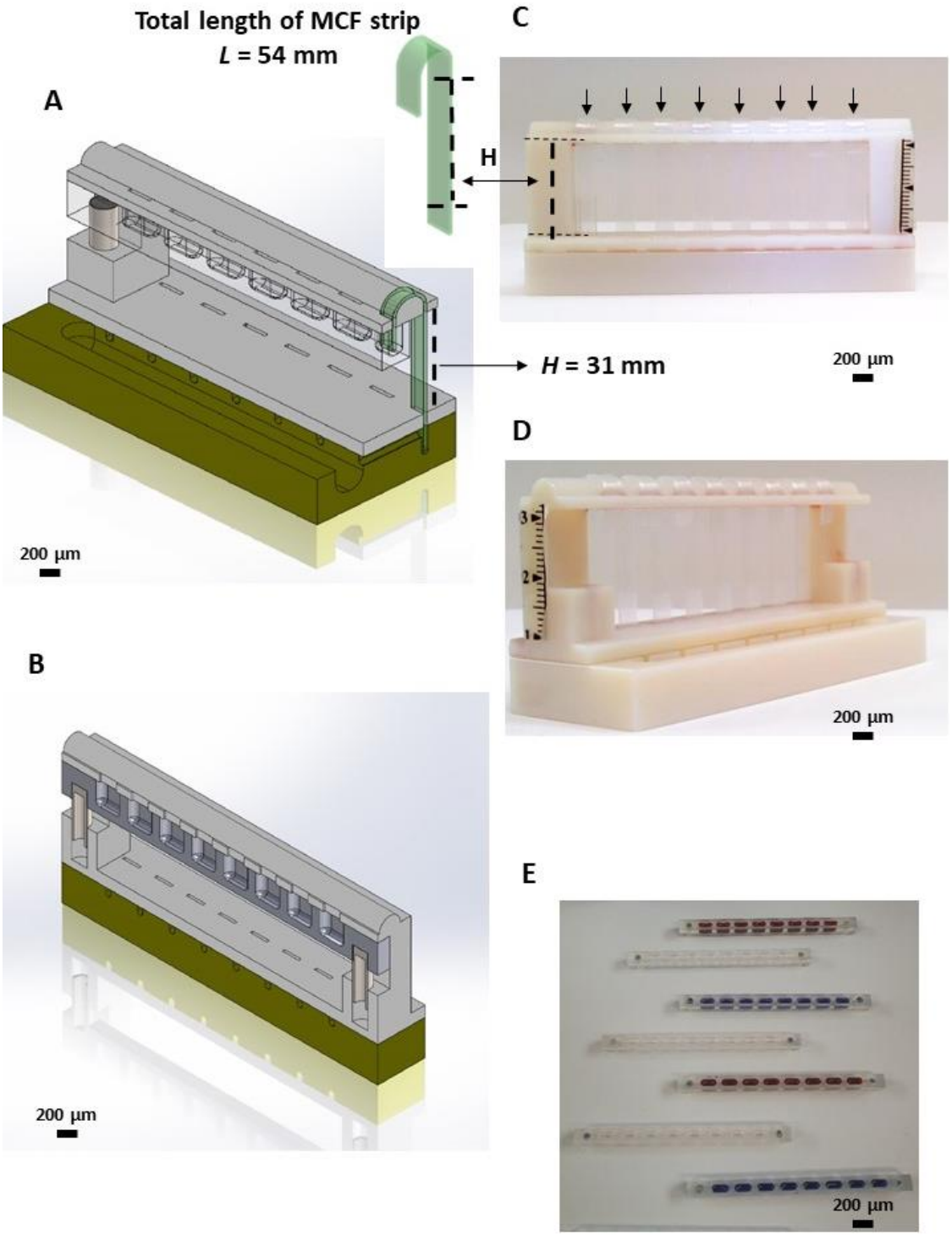

Figure 5.2 3D printing design and structure of ''MCF-siphon''. **A** 3D printing drawings with collecting reagents chamber assembled. **B** Cross-section of whole structure of MCF-siphon device. **C** Front view siphon manufactured by digital ABS integrating 8 MCF strips with 54 mm each with i.d. 200 µm. **D** Backwards view of MCF device where it is assembled each reservoir by 2 magnets in the top of the structure. **E** Individual reservoirs made in clear cast acrylic capable of maximum volume of 100 µl with two magnets allocated in the top extremities of each structure.

5.2.5 Residence time distribution assessment of dye-tracers in plastic microarrays MCF

Residence time distribution (RTD) of flow into microchannels can provide information about a reaction rate, fluid flow nature and geometry of microchannels by determination and fitting parameters as flow dispersion.[191,192] This hydrodynamic characterization started by imposing a positive step, changing from zero to 10 v/v % tracer-dye concentration and being recorded by real-time during 10-15 minutes. After a steady state condition at full dye concentration at the outlet of the MCF strips was reached, a washout was initiated by introducing washing solution, changing the input concentration from full to zero. The measured absorbance is calculated based on Equation 5.1, using the average of the mean grey values of the 10 capillaries and then converted as a concentration curve, $C(t)$, removing noise from background, assessing the normalised in- and outlet responses curves.[190,192]

5.2.5.1. Hydrodynamic characterization of dye-trace flow in ''MCF-funnel'' and ''MCF-siphon''

Red and blue trace solutions were prepared with a concentration of 10 v/v % in ultrapure water. In MCF-funnel, 8 dried MCF strips with 60 mm length, previously coated with 0.15 mg/ml PVOH and washed were assembled. In this way, the MCF strips could be filled simply by capillary action (‘dipstick’ mode). A PTFE film was cutted according to the design of slots at top part and added to avoid leakage of liquid. Both structures of MCF-funnel were assembled and perfectly secured by 6 screws and bolts. Funnel frame was positioned vertically to a Nunc maxisorp ELISA 96-well MTPs and then lowered to fully immerse the tip of the eight strips in the wells at once. The residence time distribution was performed by adding 80 µl of dye solution into each strip using a multychannel 8 tip pippette interleaved by a washing step with pure water by the following order: (red dye, washing, blue dye, washing, red dye, washing, blue dye, washing). In MCF-siphon eight dried MCF strips with hydrophilic coating of 54 mm length were assembled. Each clear acrylic reservoir was loaded with respective dye or washing solution (pure water).

The residence time distribution was performed by after plugged the reservoir (containing 80 µl of liquid in each well) to the siphon strip neck by a magnet, where liquid was loaded solely by surface tension liquid-air and then liquid-liquid without any pippetting. It was consecutively performed removing the previous empty reservoir and adding a new

one with respective solution following the same procedure as in funnel. In both microfluidic characterization, image analyis was executed as outlined in section 5.2.5.3.

5.2.5.2. Image Analysis

Experiments were recorded by the uEye XS USB camera positioned on the field of view with the set up to observed whole length of 8 microarrays. To ensure consistent lighting conditions It was used a white background provided by a 50 cm photography Studio Soft Light Box Photo Tent Cube 4 Colour Backdrop with a 12 V LED tube light. Avi files collected were analysed by ImageJ software[163] and according to dye color, the mean pixel grey scale was converted in the blue or red chanel. The absorbance signal of the trace was normalized, quantified by Beer Lambert's law[192]:

$$Abs = \varepsilon I_p C = -log_{10} \frac{I_p}{I} \quad (5.1)$$

where C is the trace concentration (g/ml), I_p is the light path distance (m), ε is the wavelength-dependent molar absorptivity coefficient (M^{-1} cm^{-1}), I_0 is the intensity of incident light beam entering the optical box taken as grey scale of baseline and I is the intensity of the light emerging out of the box taken as grey scale of baseline. The absorbance background for each strip was also quantified for signal normalization, resulting the RTD-curves. Each data point represents the mean absorbance from the greyscale pixel intensity of 10 individual capillaries within each MCF test strip and error bars indicate standard deviation of these 10 replicate assays.

5.2.6. Analysis of RTD results

The study of fluid elements passing through MCF capillaries is given by residence time distribution by a trace and wash steps consecutively.[193] This stimulus response curves can reveal which type of flow has ocurred and information about homegeneous flow distribution, molecular difusion, backmixing and dead volumes.[191,193,194] For instance, it is essential ensure an homogeneous distribution of flow reagents across entire MCF capillary radius for the development of accurate imunoassays. Undesirable backmixing can lead to contamination and further cross reactivity of reagents during immunoassay procedure, decreasing reproducibility and performance of the bioassays.[191,193,194]

Ideally it is aimed to achieve perfect plug flow which implies that each fluid element passing through the microcapillary has the same reaction and residence time, which

means that the entire reaction occurs under equal conditions. The fluid mechanisms within a capillary are governed by dimensionless Reynolds number showed by Equation 2.9 in section 2.6.1 (page 29).

Reis and coleagues[110] introduced a modified equation of Young-Laplace's of microcapillaries, since they have an elliptical shape and a 6% variation of d_h due melt-extrusion process, for each capillary across the film, which is a more accurate represented by Equation (5.2):

$$H = \frac{\gamma\, cos\theta}{\rho g}\left(\frac{1}{a} + \frac{1}{b}\right) \tag{5.2}$$

Typically the flow in MCF is laminar (Re below 2100) with a parabolic profile meaning it is faster in centre of a capillary than at the edges. This shows the system relies on molecular difusion given by Fick's law[191]:

$$N = D\frac{\partial^2 C}{\partial x^2} \tag{5.3}$$

where N is the difusional flux to the concentration gradient assuming steady state mass transferance, D is the difusion coefficient and C the concentration of analyte in a difusion distance x. The gradient of analyte concentration in time, it can be represented by Fick's second law (Equation 5.4), where *t* is the diffusion time.[191]

$$\frac{\partial C}{\partial t} = D\frac{\partial^2 C}{\partial x^2} \tag{5.4}$$

MCF capillaries have the advantage to present reduced diffusion distances by the small channels which allows significantly reduction of incubation times and high reaction rates crutial to develop rapid bioassays.

For the funnel and siphon, a trace dye-wash was applied consecutively 4 times to show the step input and output of the system. In each experiment, one frame was captured per second and total of 365 and 755 frames, for funnel and siphon, respectively (Figure 5.3). The output response was assumed close to ideal and given by $F(t)$ curves, where concentration is measured by absorbance (Abs) by Equation 5.1. In each individual washout, at any time $t > 0$ was given by:

$$W(t) = \frac{C_{out}\,(t)}{C_0} \tag{5.5}$$

with $C_{out}\ (t)$ the outlet concetration of the trace at time t and C_0 the initial concentration of the trace. The cumulative distribuction function, $F(t)$ is correlated to the washout function, represented graphically by a gaussian shape where area under the curve is given by normalized equation:

$$F(t) = 1 - W(t) \tag{5.6}$$

The normalised time θ is given by the ratio of diffusion time and the mean residence time, $\bar{t}$, given by the area above the $F(t)$ curve, according Equation 5.7,

$$\theta = \frac{t}{\bar{t}} = \frac{u}{L} = \frac{Q.t}{V} \tag{5.7}$$

Here, u is the mean flow velocity, V is the strip volume, L the total strip length, H the strip height (see Figure 5.1 and 5.2 for clear understanding of L and H) analysed and Q is the flow rate through a single capillary as described using the no-slip Hagen-Poiseuille equation given by :

$$\Delta P = \frac{128\mu LQ}{\pi d^4} \tag{5.8}$$

with d_h, ρ, g described previously in equation 5.2. The Hagen-Poiseuille equation describes the pressure drop of an incompressible Newtonian fluid, flowing under laminar flow in a cylindrical pipe of constant cross section.

It assumes the length of pipe is much greater than the diameter, like those found in the MCF and the fluid is at constant velocity. Under gravity driven flow and siphon action, the pressure diference is given by:

$$\Delta P = \rho g H \tag{5.9}$$

As the MCF strip consists in 10 microcapillaries and assuming the flow rate in each microchannel was constant, the total flowrate through the MCF strip, Q, is given by Equation 5.10.

$$Q = 10 \times \frac{\pi d^4 \rho g H}{128\mu L} \tag{5.10}$$

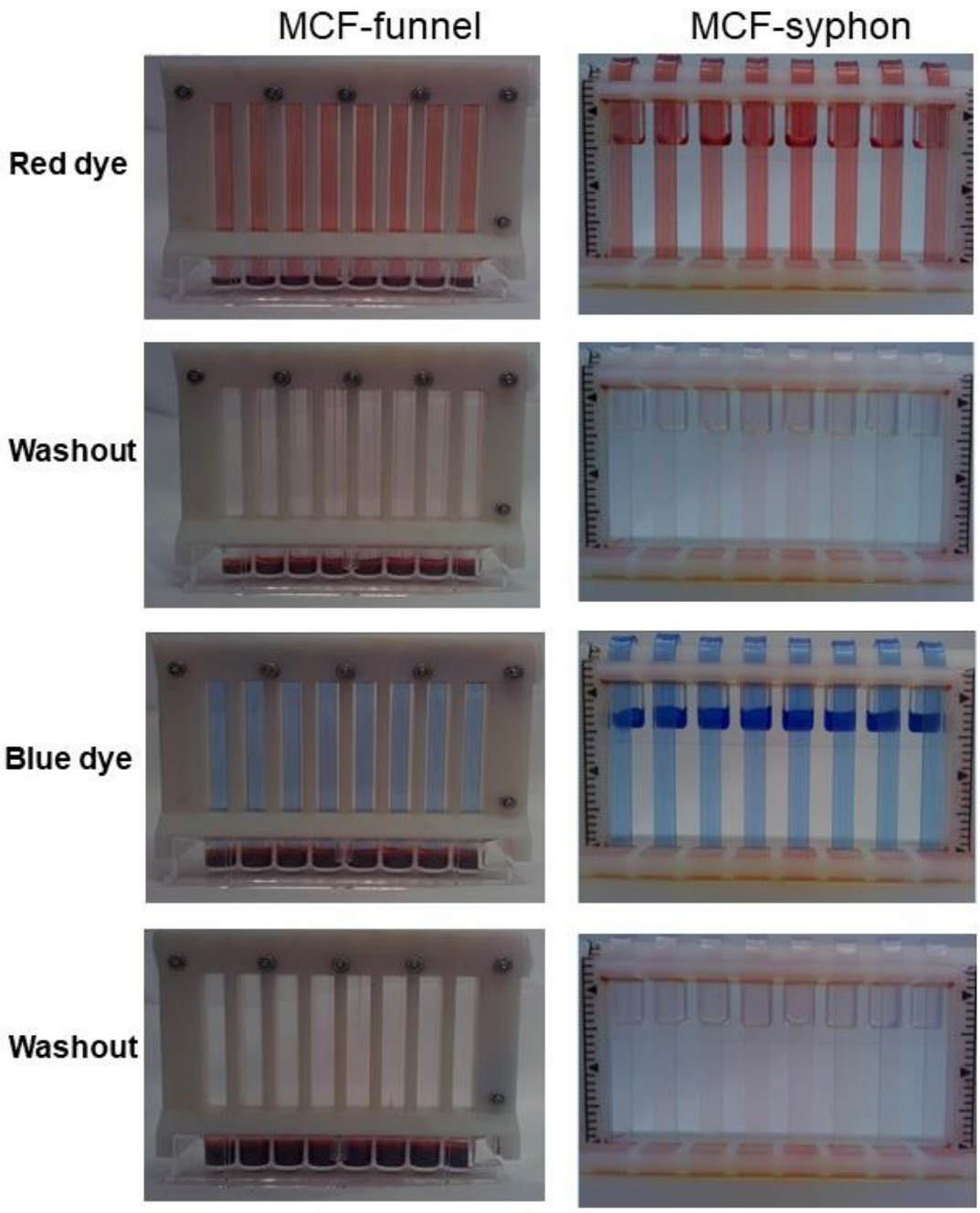

Figure 5.3 Dye trace and washout inlet at steady state conditions, for funnel and siphon in consecutive steps.

5.2.7. Modelling axial dispersion

The dimensionless axial dispersion coefficient, D/uL was estimated by fitting the experimental data $F(t)$ to plug flow velocity profile with the axial dispersion model with open-open boundaries with through the wall measurement proposed by Levenspiel[191]. The flow behaviour typical for a plug flow reactor, with maximum values of D/uL is about 3.2-

fold larger in the smaller bore MCF.[168] This is due to the shorter time for radial diffusion in smaller diameter capillaries, being proportional to the square of the distance according to the Stokes–Einstein equation (5.11) for molecular diffusion D of spheric particles in a fluid with low Reynold number.

$$D = \frac{K_b\, T}{6\, \pi\, \eta r} \tag{5.11}$$

where K_b is boltzmann constant, T the absolute temperature, η is viscosity and r the spheric radius.

Microdluidic systems exploit the miniaturization advantage in reduce diffusion distances and maximizing the flux of reaction rate. This is also called Taylor dispersion, common for many microfluidic systems[193], when a laminar flow in pipes or tubular systems pass through small channel diameters, a viscous velocity profile is developed across the tube leading to a molecular diffusion. The backmixing degree or deviation of plug flow inside the channels is quantified by the dispersion coefficient D from the axial dispersion of the trace, what means the ideal trace inpulse diffuse over the capillary superimposed by an axially spreaded plug flow.[99] From the following diferential equation it is possible determine the dimensionless axial dispersion group D/uL and effective dispersion axial coefficient D (m^2/s), respectively:

$$\frac{\partial C}{\partial \theta} = \left(\frac{D}{uL}\right)\frac{\partial^2 C}{\partial z^2} - \frac{\partial C}{\partial z} \tag{5.12}$$

with C being the concentration of trace and $Z = \frac{x}{L}$ is dimensionless length L and x the axial position (m) and $\theta \geq 0$, given by Equation 5.7. The absorbance, Abs, was calculated using Equation (5.1) and using a smoothing filter in excel (to reduce background in absorbance signal) and normalized (ratio of the mean grey values of the 10 capillaries and the average of the background, both at middle position of H) to produce the output to the step input, $F\,(t)$ curves. The residence time age distribution for a perfect pulse can be represented by $E(t)$, which represents the volume fraction of fluid having a residence time between 0 and t for constant velocity (u).

$$E\,(t) = \frac{u.C_{out}\,(t)}{\int_0^\infty u.C_{out}\,(t)} \tag{5.13}$$

A ideal plug flow occurs when $\frac{D}{uL}$ presents a lower value between 0.01-0.02[99,191] and can be calculated from the analitycal expression $E(\theta)$ for an ideal pulse input with open-open boundaries[191] (Equation 5.13).

$$E(\theta) = \left(\frac{1}{\sqrt{4\pi(D/uL)}}\right)\exp\left[-\frac{(1-\theta)^2}{4(\frac{D}{uL})}\right] \quad (5.14)$$

Integrating Equation 5.13, the shape of $F(\theta)$ model curve is obtained and fitted to the the RTD experimental data. The best numerical fitting is achieved using *Excel's Solver tool* and by the least square minimization method and converting according (Equation 5.14 and 5.15).

$$F = \int_0^\infty E\,dt = \int_0^\infty E\,d\theta \quad (5.15)$$

5.3 Results and discussion

5.3.1. RTD of gravity driven funnel and siphon

The capability of achieving near plug flow behaviour by any system is crutial for reproducible and sensitive power free immunoassay diagnostics. To access that in both gravity driven platforms, a series of experiments were feeded consecutively with a dye trace (charge) and a wash (discharge) to provide a step change of color concentration was carried out.

The experimental configuration is shown by Figure 5.3, where normalised steady state concentration is achieved for dye (from 0 to 1) and wash (from 1 to 0) respectively. The dye-trace and wash response curves were recorded continuously by camera and concentration of the tracer measured by the mean grey values of the 10 capillaries and the average of the background from ImageJ[163], according Equation 5.1 (see snapshots sequence of dye and wash in Figure 5.4).

Absorbance values of red and blue dye plus wash were normalised using the ratio of experimental absorbance and background to reduce noise and obtain $F(t)$ for funnel and siphon (Figure 5.5). There is a clear change in concentration of dye over the 8 consecutive steps, visible by the diference of the greyscale absorbance measured, noticing small irregularities in MCF-funnel device. The RTD response curves for MCF-siphon are very close to a perfect step, showing a more consistent pattern flow than in the funnel.

The cumulative $F(\theta)$ curves for tracer and washing steps, according to Equation 5.13 are shown in Figure 5.6. Siphon shows 8 similar shape and closer curves, with dye and washing after with only small deviations. Funnel presents less consistent curves with trace and washout steps showing diferent residence times, for example step 3 takes less than double time than remaining steps, while siphon takes in average aproximatelly 120 s per step. Nevertheless, curve shapes confirmed irregularities of flow seen in Figure 5.5 and suggesting the siphon device produced a more reliable and homogeneous flow.

In order to achieve more sensitive immunoassays, microfluidic design needs to ensure an homogeneus filling of microcapillaries in a consistent flow. So any fluid containing bacterial antigen or assay reagents will interact effectively with the whole eliptical surface of microcapillary, promoting effective binding. Nevertheless, results in chapter 3 highlighted the effect promoted by horizontal strips in the capture of bacterial cells deposited on the bottom surface of the coated capillaries. Thus, the gravity driven devices benefits from the vertical operation of MCF strips enabling to exploit throughout surface area to volume ratio of microcapillaries, in contrast of previous findings.

Comparing Figure 5.3 and Figure 5.4, contamination was noticed after the wash steps in the funnel design. It is perceived a slight purple color in a few capillaries of strips in MCF-funnel, which was not observed in MCF-siphon. A similar issue to this, also occured at top of the MCF where droplets were formed due to surface tension. This is caused by remnants of dye on the top of funnel entrance after each step, observed during experiments performance and denominated dead volumes.[124–126] Conversely, in siphon this issue is minimized since the head of MCF is inserted in the reservoir, where it is constantly changed in each step to avoid dead volumes of dye.

The siphon design benefits from the fact each reservoir is easily assembled and changed in comparison to funnel design, where the fluid entrance is the same for each step. This phenomenon is validated in Figure 5.7 by the sharper shape of outlet response curves, where curves in funnel show small discrepacies between individual steps, being more remarked by washings after blue trace. Contamination and remnants in Funnel might be correlated with dye viscosity. In fact, viscosity measurements showed a variation between the two dyes used, where the blue dye is more viscous as seen in Figure 5.8.

Note, urine samples from patients diagnosed with UTI presents a viscosity at room temperature between 1.05 and 1.15 x 10^{-3} Pa.s, being similar to viscosity presented by water or red dye.[195] Therefore, it is expected achieved a more consistent and homogeneous flow with urine as observed with red dye. Regarding MCF-siphon these curves (Figure 5.7) present similar trends for the 4 consecutive washings and each of 8 individual strips. Dead volume and cross-contamination are major disadvantages noticed in funnel performance, since the first factor reduces the accuracy caused by the lack of

volume precision handled. In terms of bacterial samples, the loss of sample volume can lead to a variation of concetration of analyte, sacrificing the reliability of any immunoassay conducted in the device.

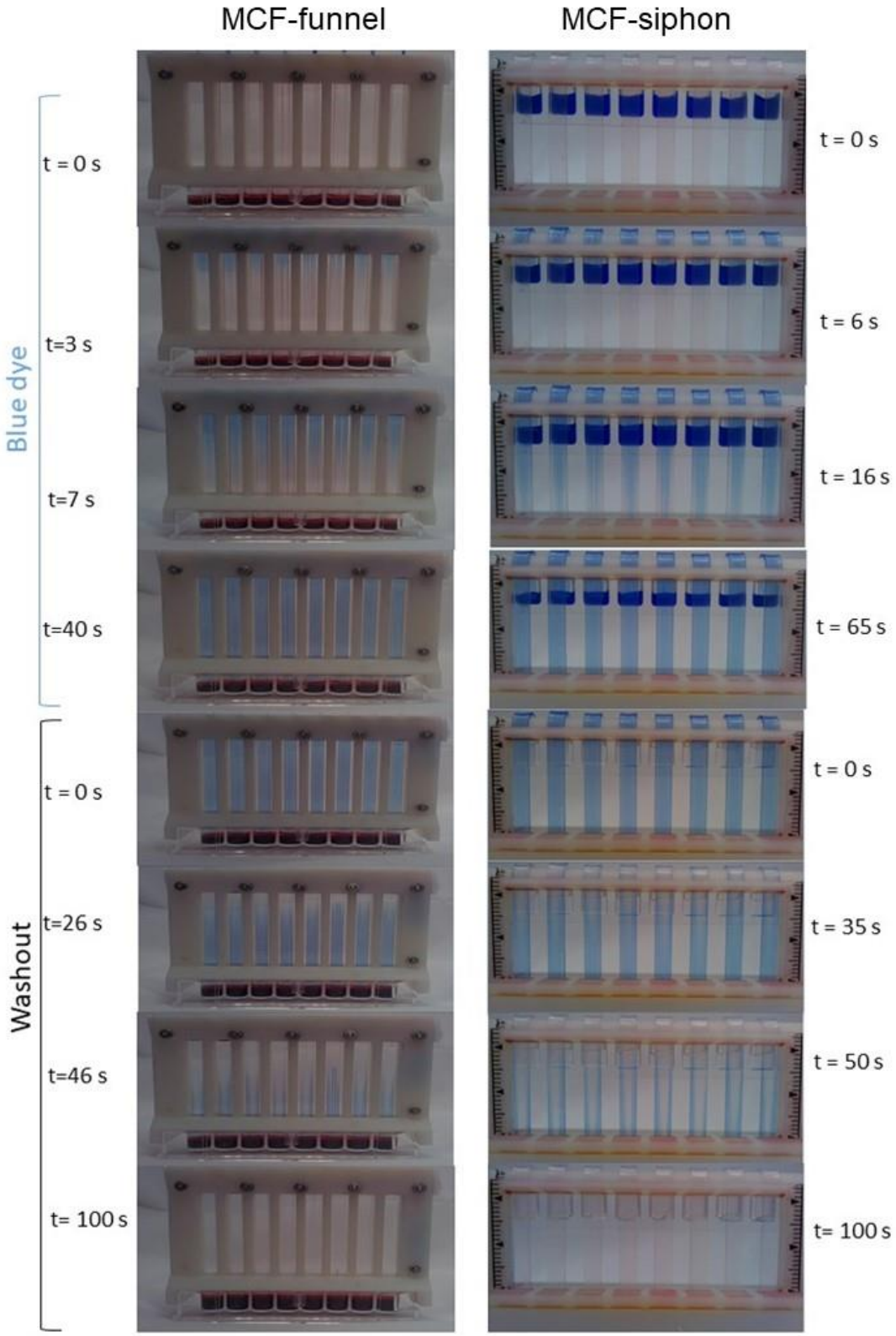

Figure 5.4 Snapshot of stimulus response curves in MCF gravity driven devices.

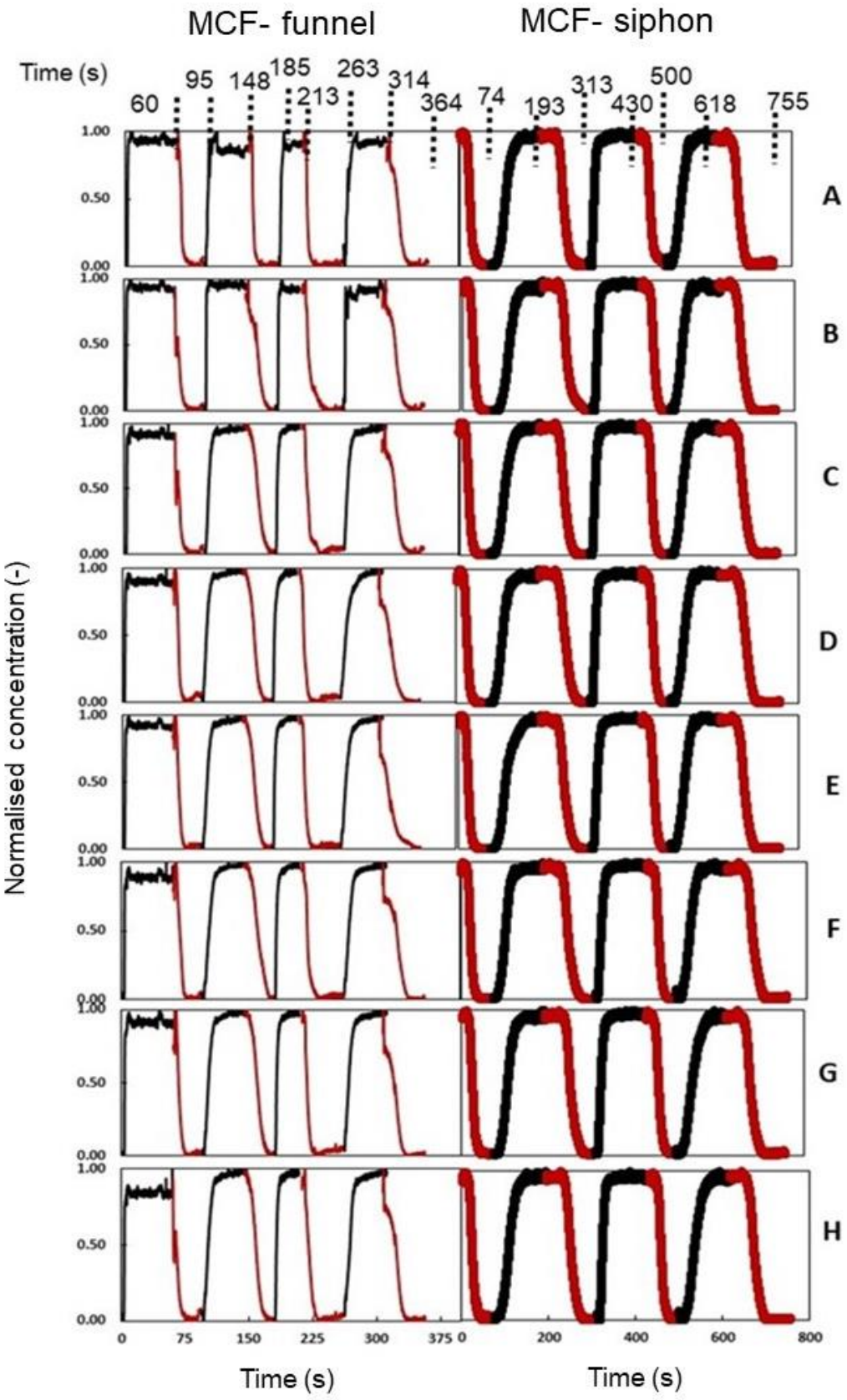

Figure 5.5 RTD experimental curves in MCF-funnel and MCF-siphon for each individual MCF strip, respectively (**A-H**). Tracer impulse is represented by black lines (**—**) and washout step represented by red lines (—).

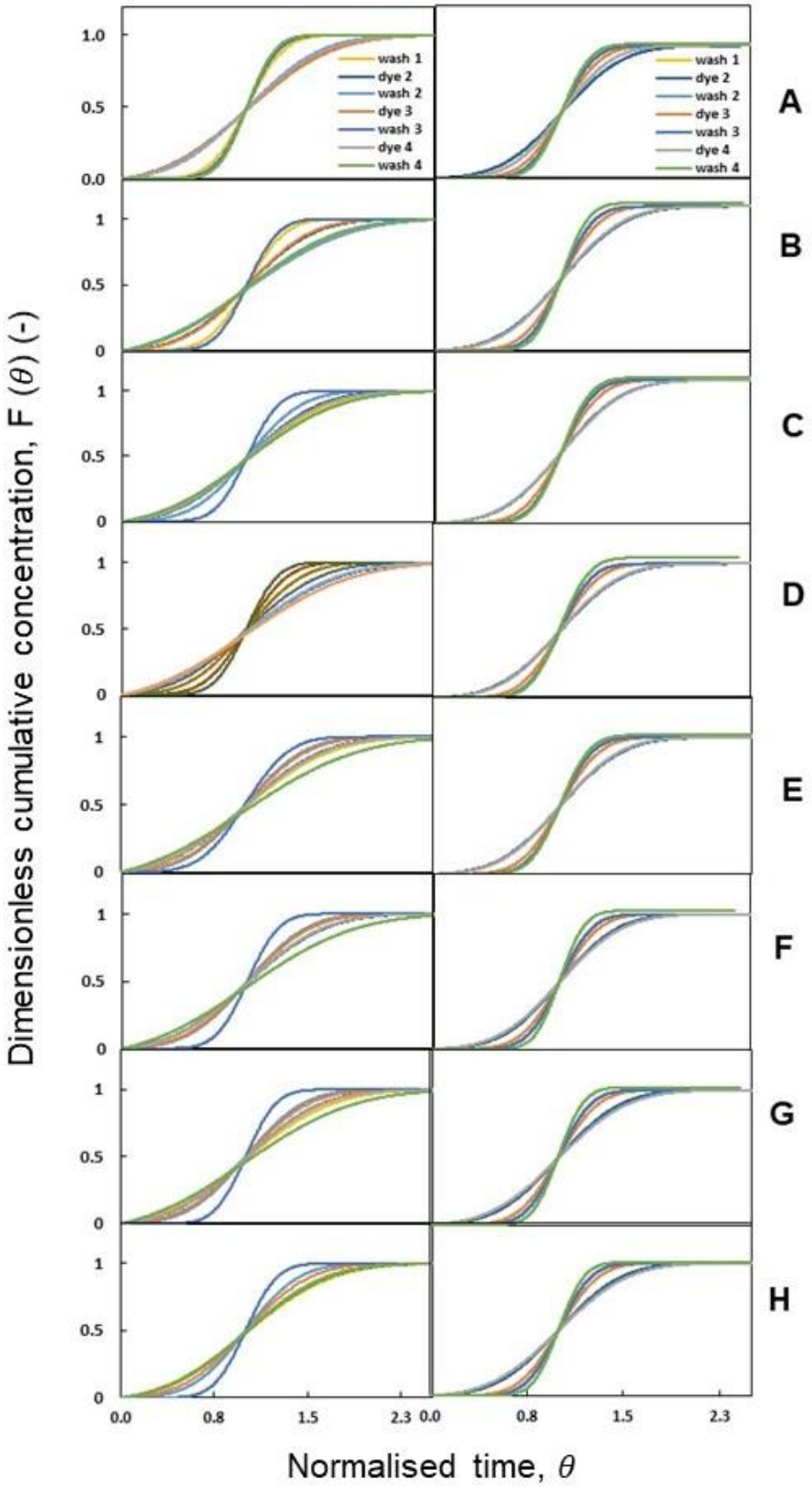

Figure 5.6 Dimensionless cumulative concentration *F (**θ**)* curves in funnel (left side) and siphon (right side), for each individual strip represented from **A-H**.

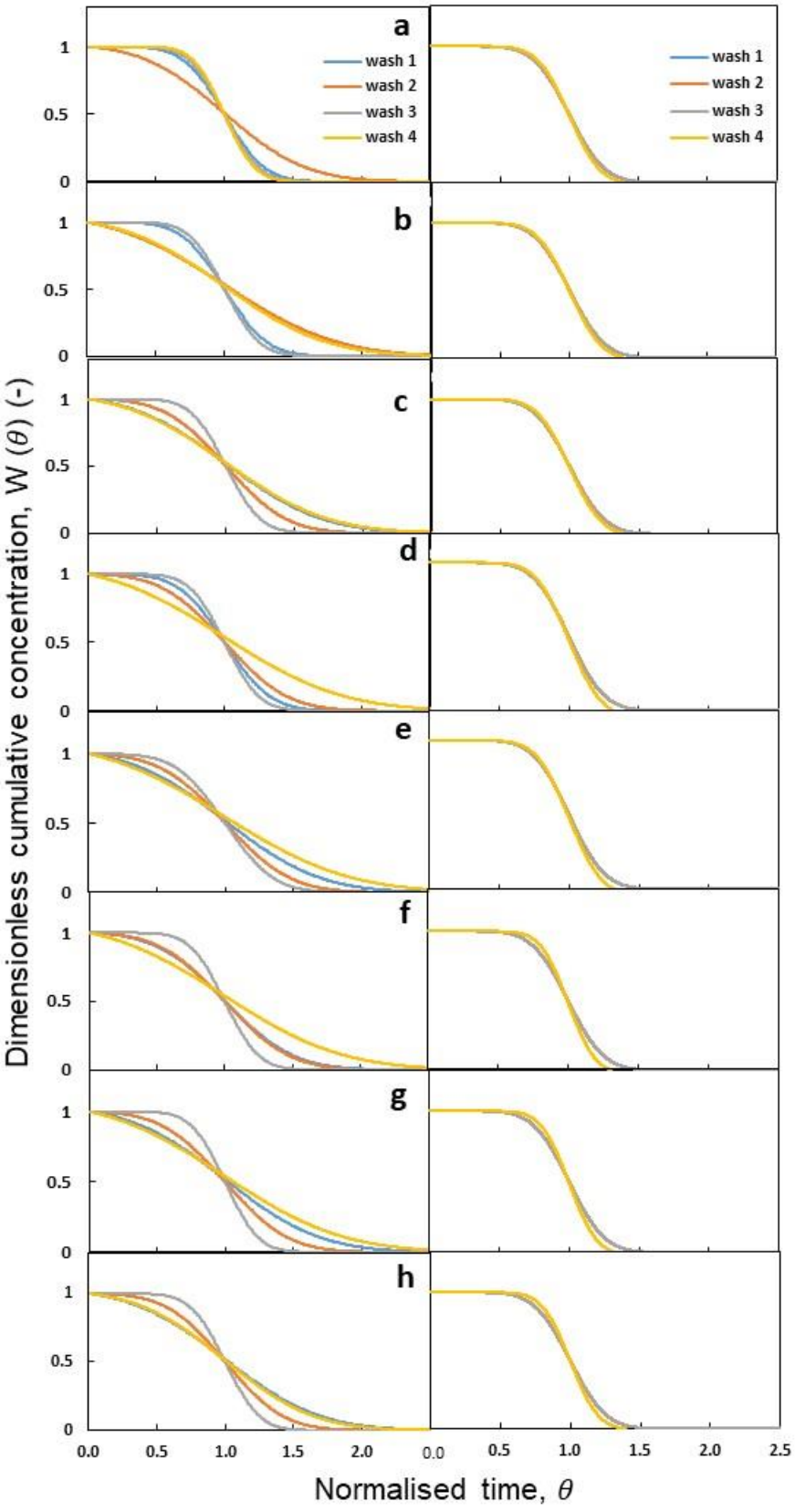

Figure 5.7 Dimensionless cumulative concentration *W (θ)* curves in funnel (left side) and siphon (right side), for each individual strip represented from **A-H**.

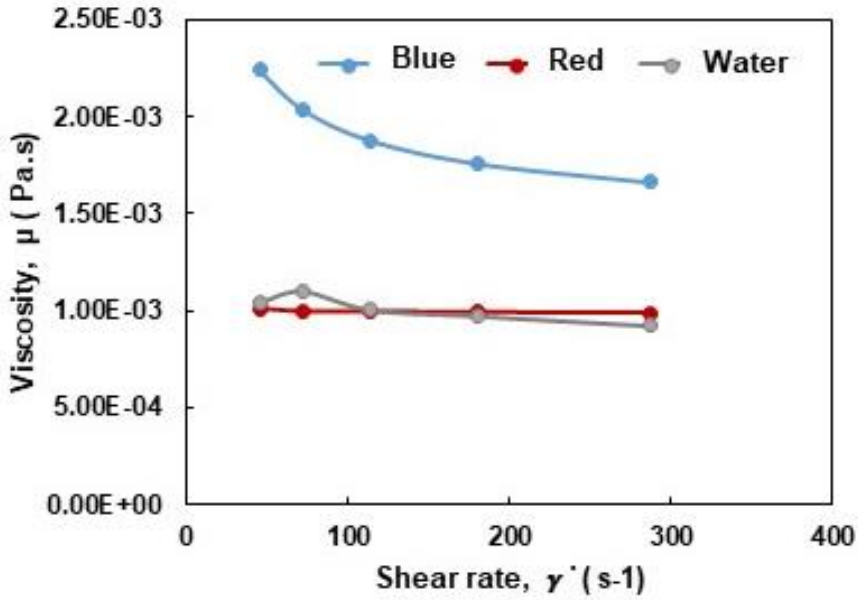

Figure 5.8 Viscosity measurements (average of triplicates) of wash (water), blue and red trace used in RTD response curves at room temperature.

5.3.2. Determination of axial dispersion parameter as level of backmixing and reproducibitity

The residence time distribution was successfully modelled to the dispersed plug flow model (from Equation 5.12). The ideal pulse enters the capillary via a diffusion-like process[190] which is superimposed on plug flow spreads axially. This process is called axial dispersion and is quantified by the dispersion coefficient, *D* which describes the level of backmixing [99], according Equation 5.12. An RTD that strongly deviates from plug flow (only considered for ranges smaller than 0.01-0.02), can lead to a reduced equilibrium binding between capture antibody-antigen and therefore reduced sensitivity during immunoassay development.

In MCF-funnel, the value of H was 22 mm (with total MCF length L = 60 mm) and in MCF-siphon, the H value was 31 mm (with total MCF length L = 54 mm). Therefore, the volume V inside each MCF strip was calculated (assuming i.d each capillary 206 µm), being V_{Funnel}=7.33 µl and V_{Siphon}=10.33 µl, respectively. Values of D/uL and $\bar{t}$ were determined by the best fit of axial dispersion model given by Equation 5.12 and experimental RTD $F(\theta)$ curves by least square minimisation method. Those values are shown per MCF strip per step for both devices from Table 5.1 to Table 5.4. Comparing Table 5.1 and 5.2, the dimensionless axial dispersion values observed are more close to perfect flow in siphon than funnel, despite some deviations above range 0.01- 0.02. It is

also observed that higher D/uL values are achieved in all steps of funnel and siphon noticing it solely for dye step 2 and dye step 4 (both steps with blue Tracer). This is correlated to the higher viscosity observed in blue dye as discussed previously in Figure 5.8, which affects the dimensionless axial dispersion values according Equation 5.11. Axial dispersion deviations denoted mostly in funnel can result in a uneven spread of the immunoassay reagents flow through the microcapillaries, which is linked to repeateability of results and reproducibility of any immunoassay.

The flow inside microcapillaries is laminar (Re < 2100), described by a parabolic profile where flow is faster in the centre than at the edges resulting in radial mixing or also called radial dispersion caused by molecular diffusion. This process is fundamental to ensure a uniform distribution of fluid flow across the entire capillary. In an immunoassay, capture antibodies are immobilized on the surface wall of the MCF, where any antigens or bacterial cells have to reach the wall prior to establish the bound or equilibrium binding, thus more accurate assays. Backmixing is undesirable leading to cross contamination and inaccuracies of any experiment. High throughput ELISA requires minimal backmixing level, where flow is repeatable and each fluid into the microcapillary flows at same rate with a consistent change of concentration.

On the other hand, it is very common for microfluidic systems to present small deviations or irregularities in signal inlets (only noted in Funnel RTD curves) due to the small dimensions of microcapillaries. As explained from Equation 2.8, MCF capillary size is not uniform along it cross-section, affecting the flow velocities of each capillary. A smaller capillary has a bigger flow resistance than a larger one, and will therefore allow less fluid to pass through it, resulting in lower net flow velocities.

In contrast to conventional pressure-driven microfluidic approaches, MCF-siphon requires no seals, no pipette and no power, with zero dead volumes, no detectible cross-contamination and near to the ideal plug flow with negligible levels of backmixing which are aimed for high performance immunoassays. For instance, Juncker[185] and colleagues have reported an autonomous microfluidic capillary system using manual pipette and valves. Lee and team[196] have demonstrated a study using pressure-driven devices for water flow enhancement in hydrophilic channels demanding membrane holder in silicon rubber for sealing and membrane fracture prevention.

Table 5.1 Dimensionless axial dispersion group determined per strip per step in Funnel.

	D/uL (-)							
# MCF	Dye 1	Wash 1	Dye 2	Wash 2	Dye 3	Wash 3	Dye 4	Wash 4
1	0.13	0.03	0.14	0.11	0.15	0.02	0.12	0.02
2	0.13	0.03	0.09	0.21	0.08	0.02	0.18	0.17
3	0.16	0.15	0.11	0.06	0.12	0.02	0.12	0.17
4	0.17	0.04	0.11	0.07	0.18	0.02	0.17	0.23
5	0.14	0.15	0.12	0.07	0.08	0.04	0.13	0.26
6	0.17	0.08	0.12	0.07	0.08	0.02	0.12	0.23
7	0.14	0.15	0.12	0.07	0.08	0.02	0.12	0.23
8	0.15	0.15	0.13	0.06	0.08	0.02	0.12	0.13

Table 5.2 Dimensionless axial dispersion group determined per strip per step in siphon.

	D/uL (-)						
# MCF	Wash 1	Dye 2	Wash 2	Dye 3	Wash 3	Dye 4	Wash 4
1	0.02	0.07	0.02	0.03	0.02	0.05	0.02
2	0.02	0.08	0.02	0.03	0.02	0.07	0.01
3	0.02	0.02	0.02	0.03	0.02	0.04	0.02
4	0.02	0.07	0.02	0.03	0.02	0.07	0.02
5	0.02	0.07	0.02	0.03	0.02	0.07	0.02
6	0.02	0.06	0.02	0.03	0.02	0.07	0.01
7	0.02	0.07	0.02	0.03	0.02	0.09	0.01
8	0.02	0.07	0.02	0.03	0.02	0.09	0.01

Mean residence time ($\bar{t}$) of both devices per MCF strip per step were summarized in Table 5.3 and 5.4 respectively. This parameter describes the amount of time a particle/molecule spend inside the microcapillaries. It is remarkable the different range of D/uL of comparing both devices, where siphon present at least the double values in comparison to funnel. The higher values shown by siphon are due longer MCF height *H* used which can be easily decreased by changing the geometry of device for smaller MCF lengths. In turn, it is evident the effect of viscosity of blue trace when observing values of $\bar{t}$. Siphon present consequent effects in values for blue dye (dye 2 and dye 4) with values around 34 - 43 sec and consecutively in washout steps afterwards with values from 56 to 61 sec.

Table 5.3 Mean residence time per strip per step accessed from funnel device.

	Mean residence time, $\bar{t}$							
# MCF	Dye 1	Wash 1	Dye 2	Wash 2	Dye 3	Wash 3	Dye 4	Wash 4
1	6.75	8.79	9.59	7.17	4.92	7.64	8.99	14.09
2	6.39	6.63	4.73	14.16	5.41	10.23	7.68	15.95
3	7.66	6.86	7.86	17.30	3.79	10.11	8.77	15.95
4	8.53	9.49	7.69	16.15	4.25	9.23	11.04	14.77
5	7.74	9.80	8.68	16.40	3.85	9.79	10.07	13.25
6	9.29	10.15	9.54	18.79	3.85	10.06	9.72	16.22
7	7.93	8.74	8.66	17.41	3.73	9.05	9.13	13.73
8	6.82	6.82	8.82	15.92	3.80	10.28	10.18	14.65
Average	7.64 $\pm$ 0.97	8.41 $\pm$ 1.44	8.20 $\pm$ 1.56	15.41 $\pm$ 3.59	4.20 $\pm$ 0.63	9.55 $\pm$ 0.90	9.45 $\pm$ 1.03	14.83 $\pm$ 1.12

Table 5.4 Mean residence time per strip per step accessed from siphon device.

	Mean residence time, $\bar{t}$						
MCF	Wash 1	Dye 2	Wash 2	Dye 3	Wash 3	Dye 4	Wash 4
1	24.83	39.88	56.76	15.58	28.29	38.34	53.87
2	25.41	40.92	57.48	15.68	28.55	34.75	56.29
3	25.56	42.77	57.51	15.51	30.05	33.52	54.15
4	24.79	37.37	60.77	15.41	29.52	34.63	57.14
5	24.79	37.37	60.77	15.41	29.52	34.63	57.14
6	24.05	34.20	56.32	16.57	28.56	34.75	57.78
7	25.18	37.37	61.03	16.42	30.50	43.12	56.74
8	25.18	37.37	61.03	16.42	30.50	43.12	56.74
Average	24.99 $\pm$ 0.51	38.41 $\pm$ 2.66	58.96 $\pm$ 2.11	15.88 $\pm$ 0.50	29.44 $\pm$ 0.89	37.11 $\pm$ 3.97	56.23 $\pm$ 1.44

In theory, this might increase the assay time however more time incubations might benefit equilibrium capAb-antigen, minimizing shear stress and in turn make bioassays more effective. In turn, it is an established practice in immunoassays to use surfactants in the washing buffer to help removal of unbound molecules from the surface with minimum fluid shearing.

Due to deviations of values are influenced by viscosity of each dye, the average values for each strip for dimensionless axial dispersion (D/uL), axial dispersion (D) and residence time $(\bar{t})$ are shown individually per wash, blue and red dye in both devices. On the other hand MCF-siphon presents a low system standard variation (≈3-5% of residence time while MCF-funnel was ≈ 20-30% of residence time), which shows more reproducible flow and the effect of automation in siphon format.

Figure 5.9 informs in more detail this parameters for a reliable appreciation. Axial dispersion is determined from multiplication of the following parameters: dimensionless axial dispersion, MCF length (L) and mean flow velocity u calculated from ratio of L and $\bar{t}$. Plots in Figure 5.9A show higher values of D in funnel flow performance with blue dye while wash steps present the lowest values in both devices. On the other hand siphon present the lowest values of D. For each step it is lower than 5 x10^{-6} m^2/s and values are highly similar, demonstrating a more consistent flow in agreement with RTD results. Hornung and Mackley[190] have reported D values between 1–5 x10^{-10} m^2/s for 19-microcapillaries MCF with similar d_h, however these lower values are expected as the MCF lengths used were 10 m, promoting a greater time for fluid to disperse in the radial and axial directions.

Residence time demonstrated in plots from Figure 5.9B emphasized conclusions from Table 5.3 and 5.4, showing clearly siphon with at least double of residence time than funnel with less consistent behaviour. The higher H (31 mm) in comparison with H (22 mm) funnel is one of the big factors promoting the higher $\bar{t}$. This is related to pressure balance in Equation 5.9 where flow rate described in equation 5.10 is linked to specific geometry of designs. For this reason the volume of the fluid in MCF strip V, is different, being respectively 7.1 and 10 µl for MCF-funnel and MCF-siphon. Another issue influencing these values, is dead volume noticed in funnel, meaning not all fluid had passed through the capillaries, explaining this sharper discrepancy between both devices. Note, no visible air bubbles were introduced in the devices.

The experimental flow rate Q is calculated from ratio of V and mean residence time $\bar{t}$ (according Equation 5.7) with data shown by Figure 5.9C. This parameter is directly affected by mean residence time values, showing clearly Siphon with half values of flow rate, highlighting red dye with higher values in both devices consecutively. Siphon obtained lower mean superficial velocities (see Figure 5.9D), promoting lower shear stress which is beneficial in interaction between the capture antibody and bacteria for sensitive immunoassays, as seen in chapter 3.

Despite red dye present fast flow velocity due lower viscosity, funnel present three times higher velocity than siphon, which is intrinsiclly related to the total MCF length and flow rate according Equation 5.7.

Overall both devices have demonstrated an automated and power free performance. In terms of mitigation of human error, siphon can be considerate the most suitable since operates without any external support along repeatable multi step loading. In future, a refinement in design of both devices should be considerate to enhance both

performances, which include the adding of an hydrophobic cone on surface of funnel and reduction of MCF length in siphon.

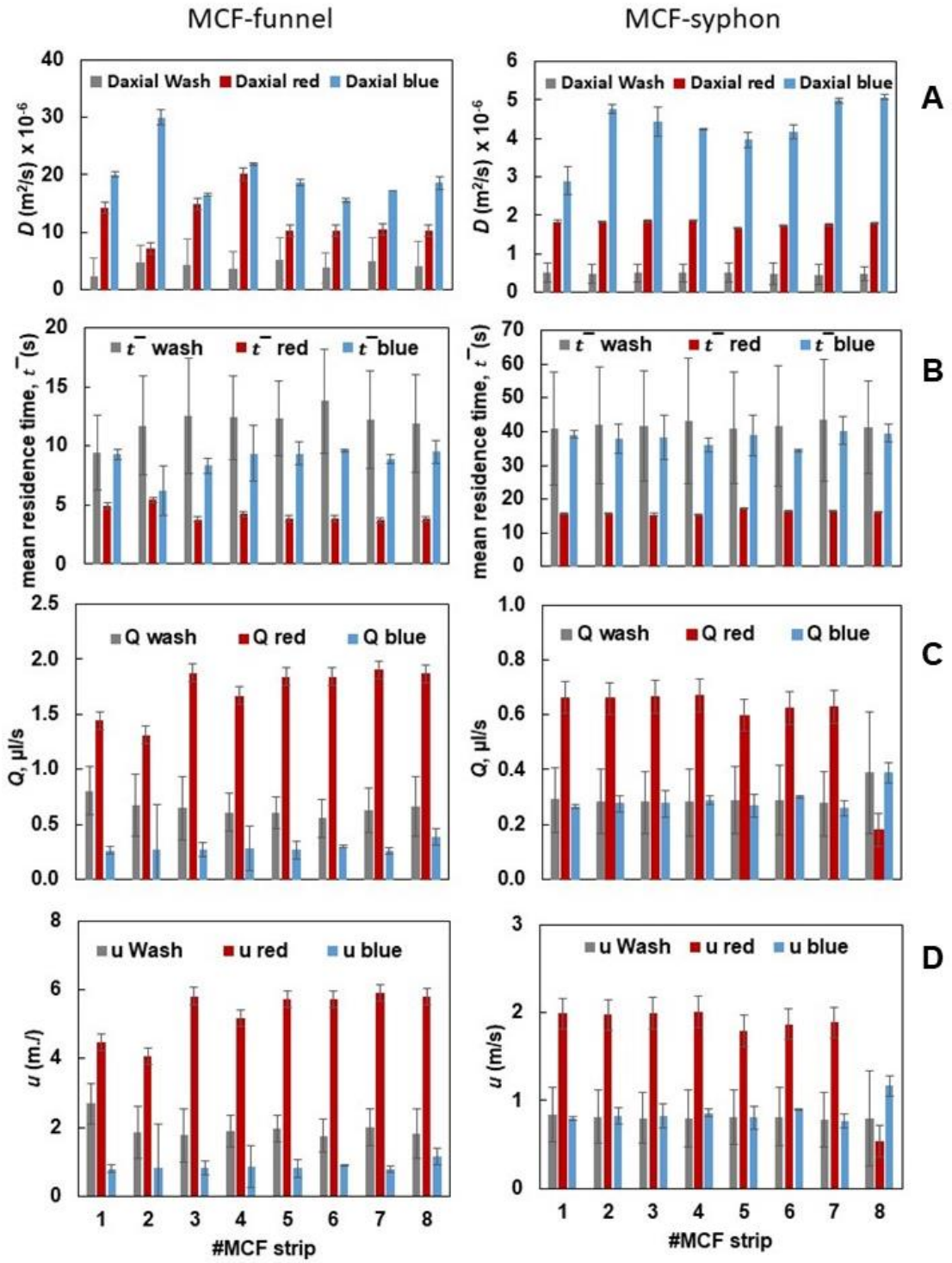

Figure 5.9 Hydrodynamic flow parameters from fitting axial dispersion model to RTD curves in MCF-funnel and MCF-siphon, specific for blue trace, red trace and wash. **A** Average of axial dispersion. **B** Mean residence time. **C** Flow rate. **D** Superficial flow velocity.

5.4 Conclusions

It was demonstrated two new microfluidic platforms powered exclusively by gravity which offers high-performance and flexibility not possible with conventional 'dip stick' diagnostic tests. Pulse input experiments using colorimetric dye traces were performed to study the fluid flow pattern and sucessfully modelled to a open-open boundaries axial dispersion model.

Gravity driven microfluidc devices show a residence time behavior within microcapillaries reasonably close to plug flow, however siphon showed a consistent and more reproducible flow. Dimensionless axial dispersion and mean residence time were parameters determined using solver's interaction and least square minimization method. MCF-siphon showed perfect steps in RTD with $F(\theta)$ sharper and similar than funnel. Some cross contamination was optically observed in paralel with some dead volume being the major disadvantages of MCF-funnel. Both devices showed an ideal plug flow with siphon presented a lower effective dispersion axial coefficient overall below 1×10^{-6} m^2/s, and more consistent D values per step per strip, in contrast to siphon around 6×10^{-6} m^2/s. Siphon demonstrated a more simplistic design and showed a superior performance due to low system standard variation $\approx$ 3-5% of residence time, not creating visible dead volumes or backmixing and producing a more reliable flow pattern. A microfluidic device under siphon action is unreported to date and has the potential to produce advanced and affordable adressing miniaturization challenges as shear stress and simplify fluid handling systems.

It is believed that gravity driven performance of miniaturized devices can implement a beneficial step-change for development of inexpensive, sensitive and power-free point-of-care diagnostics for low income settings. A proof of concept exploiting the potential MCF-siphon to quantify *E. coli* in synthetic urine will be presented in chapter 6.

CHAPTER 6 | Power-free multi-step fluorescent immunoassay for *E. coli* detection in the MCF-siphon

Abstract

In this chapter a power-free multi-step fluorescent *E. coli* immunoassay was performed in a novel and first ever MCF-siphon. This simple-to-use automated platform consists of 8 FEP-Teflon® strips coated with a hydrophilic layer of polyvinyl alcohol to drive the gravity action. Despite a high background level promoted by the crosslinker, the analytical performance obtained was improved by adding 2% w/w of rabbit serum in blocking agent. This enabled detection of $9x10^4$ CFU/ml *E. coli* in less than 20 minutes from a range of 0 to 10^8 CFU/ml of *E. coli* spiked in synthetic urine. It is still not sufficient for clinical use but shows proof of concept and it is expected that sensitivity can be improved substantially by further assay development. The proof-of-concept provides a reliable fluid system minimizing cross-contamination and offering more reproducible and homogenous assays.

Overall, MCF-siphon microfluidic device is an autonomous generation of gravity driven devices for point-of-care, enabling in future the integration with affordable readout systems as camera for portable and off-the-shelf technology in low resource settings.

6.1 Introduction

Microfluidics based diagnostics have contributed in last years for development of user-friendly and high throughout devices to adress the diverse health care point-of-needs.[8,197] Analytical performance, reliability and sensitivity are a few funtionalities exploited by surface modification of microfluidic devices, through automation of reagents loading and integrating multiple processes in a single step.[70,198,199]

To our knowledge, there are no previous reports of any gravity driven microfluidic device reling on siphon action for any point-of-care application. This gravity driven platform, described previously in chapter 5 as MCF-siphon, presents a sophisticated yet simplistic off-the-shelf design. Made from a 3D-printing technique its structure integrates 8 inexpensive MCF strips with inner surface wall coated hydrophilicly with crosslinked polyvinyl alcohol (PVOH). Siphon action is fully automated, battery and power free. The reagent loading relies solely on gravity action without any pipetting or pump support.[94] Therefore, here it was attempted the integration of the rapid and sensitive immunoassay developed in chapter 4 into this new autonomous MCF-siphon with the aim of increasing repeatability, eradicating human error from manual incubations and enabling increased throughput.

Advanced point-of-care diagnostics aim to reduce the complexity of microfluidic designs and external use of support equipment without loss of performance. A full hydrodynamic characterisation in chapter 5 revealed MCF-siphon has a consistent and reproducible performance. Perfect step impulse demonstrating a near plug flow with negligible levels of backmixing and effective dispersion axial coefficient lower than 5×10^{6} m^2/s between eight strips per step. Therefore, all these key factors are crucial to standardize fluid shear of reagents loading and maximize interactions between probe and antigen. Due to MCF neck design, liquid is loaded solely by surface tension liquid-air and then liquid-liquid without any cross-contamination or dead volumes. Hence, MCF-siphon ensures a reliable and homogeneous flow for achieving sensitive immunoassays. On the other hand, its design exploits lower volume of reagents to deal with (≈80 µl per step) and small low cost MCF lengths (54 mm) which reduces immunoassay costs.

Controversially, the further performance of this fluorescent *E. coli* immunoassay in MCF-siphon relies on the key step of antibody immobilization. This is critical for synergistically achieving the ideal antibody orientation, adjacent enhanced antibody-antigen binding and reduce background.[11,50,200] Despite capture antibodies being sucessfuly imobilized by passive adsorption into FEP-Teflon® platform for several purposes, some researchers[201,200,102] suggested covalent immobilization can favour

beneficial antibody structure avoiding blockage or inactivated sites into microfluidic surface, over passive adsorption. Studentsov et al.[202] have indicated PVOH as a possible blocking agent into immunoassays. Pivetal and coleagues have tested PVOH after passive adorption immobilized capture antibody into MCF, which revealed a reduction of ELISA backgroung at low concentrations of IL-1β however with some signal inhibition of high concentrations of cardiac biomarker.[94]

Siphoning is one of the hydrodynamic operating principles under artificial gravity in centrifugal microfluidic devices. The development of this novel MCF-siphon microfluidic platform for *E. coli* detection is pioneering, without any reports in the POC field with similar design and operation. So far, siphon principle is very often exploited in extraction of plasma from a blood sample (separation) after sedimentation in artificial gravity. For example, Steigert and team[203] have reported novel and fully integrated centrifugal microfluidic "lab-on-a-disk" for rapid colorimetric assays in human whole blood, integrating an hydrophilic siphon-based metering and sedimentation for plasma extraction. Du and colleagues[204] developed an automated microfluidic chip-based on gravity-driven flow injection analysis. Yao and team[205] reported a microfluidic device based on gravity and electric force driving for flow cytometry and fluorescence activated cell sorting. Laschi and colleagues[206] have developed a new gravity-driven microfluidic-based electrochemical assay coupled to magnetic beads for nucleic acid detection of Legionella pneumophila.
In fact, gravity-driven flow enable to conduct immunoassays with a more robust, standard and reliable fluid flow with advantage that no external power source is required and manufacturing process is simplified.

The aim of the present study is to verify feasibility of running fluorescence immunoassay for *E. coli* detection in power-free mode using hydrophilic MCF strips covalently modified by PVOH. The proof-of-concept of this power-free multi-step MCF-siphon was validated with synthetic urine and integrating a camera as optical readout system, achieving a LoD of 9 x10^4 CFU/ml in 20 min, from a range of 10^0-10^7 CFU/ml.

6.2 Material and Methods

6.2.1 Reagents and materials

Goat anti-rabbit IgG (H+L) secondary antibody, Biotin conjugated (# 11543350) to quantify the capture antibody immobilized purchased from Fisher Scientific UK Ltd. Rabbit serum (#R9133) from Sigma Aldrich (Dorset, UK) was purchased as blocking buffer components. Fluorescent intensity was imaged using a black box suite with a Blue LED excitation transilluminator (IO rodeo, Pasadena, USA) assembled with a matched amber

acrylic emission filter, using a Canon S120 digital camera (Canon, London, UK). All image analysis was processed by ImageJ bundled with 64-bit Java 1.8.0_112(NIH, USA).[163]

Remaining reagents used in this experimental chapter were described in previous sections
3.2.1 and 5.2.1.

6.2.2 Measurement of liquid rise by coating Teflon-FEP microcapillaries with PVOH

Modification of inner surface of Microcapillaries for measurement of liquid rise was according protocol described in section 5.2.3. Liquid rise is given by the height (H) which liquid rises in a vertically positioned tube by the ‘’force’’ resulting from surface tension between the liquid and capillary wall and represented by the mass balance given by equation 6.1:

$$\Delta P_L = \Delta P_H + \Delta P_F \tag{6.1}$$

Being ΔP_L the interfacial pressure of liquid, ΔP_H the hydrostatic pressure difference and ΔP_F the frictional pressure loss. For an empty capillary, where surface tension of liquid is null ($\Delta P_L = 0$), the mass balance is given by:

$$\Delta P_H = \Delta P_F \tag{6.2}$$

Laplace pressure drop between air-water-wall interfaces is shown by:

$$\Delta P_L = \frac{4\gamma}{d_h} cos\theta \tag{6.3}$$

where γ is the surface tension of water (72.8 mN m^{-1}), θ the contact angle (in radians), d_h the hydraulic diameter. The pressure head in the liquid height H is given by Equation 5.9. The pressure drop imposed by frictional losses in the capillary is given by the Darcy-Weisbach equation:

$$\Delta P_F = f_D \frac{\rho u^2}{2 d_h} H \tag{6.4}$$

where u is the superficial flow liquid velocity (m s^{-1}) and considering laminar flow regime inside of capillaries, Darcy friction factor f_D is demonstrated by:

$$f_D = \frac{64}{Re} \tag{6.5}$$

with Reynolds number (Re) represented by equation 2.9, and liquid rise given by Equation 5.2.

In order to measure the liquid rise after covalent coating, a 15 cm long dried MCF strip was immersed in a cuvette with ultra-pure water until the liquid level inside each capillary reached equilibrium. Once capillary rise had taken place and the meniscus reached equilibrium, the maximum height of liquid in each capillary was recorded. This precedure was repeated for the 3 concentrations of 0.1, 0.15 and 0.2 mg/ml PVOH solution in triplicate and results recorded and measured with a ruler. Also the same procedure was repeated adding 1 and 2 washing step with deionised water, consecutively.

6.2.3 Siphon driven microfluidic device as automated fluid handling system

Siphon was designed in house and manufactured according protocol described in section 5.2.4

6.2.4 Hydrophilic surface modification of 10–bore FEP microcapillaries

To produce a suitable inner surface of FEP microcapillaries to perform immunoassays for *E. coli* detection, (Figure 6.1B (i)), MCF connectors were adapted to ensure uniform filling of 10 paralel microarrays assembled to a terumo syringe 2.5 ml luer lock.

In 100 cm of MCF Strip, 1 ml of 40 μg/ml solution of polyclonal capture antibody in PBS was passively immobilized for 2 hours and aftewards, 1 ml of 0.1 mg/ml PVOH in PBS was loaded for another 2 hours. According to each experiment, MCF strip was incubated for 2 hours with one of the described blocking buffers (Protein free (TBS), 2% w/w rabbit serum in Protein free (TBS), 5% w/w rabbit serum in Protein free (TBS), 8% w/w rabbit serum in Protein free (TBS) or 10% w/w rabbit serum in Protein free (TBS)). After that, normal procedure with PBST washing, trimming and drying was repeated. Finally ready to use, MCF strips were coupled into silicon rubbers connected to syringes or assembling into MCF-siphon according to Figure 6.1B (ii).

6.2.5 Quantitation of immobilized capture antibody

A fluorescent immunoassay with polyclonal anti-rabbit detAb was used to quantify the capture antibody density immobilized into inner surface of microcapillaries. MCF strips (4 cm length) were prepared using the first procedure described in section 6.2.4 and assembled to individual 1 ml syringes connected by a 2 mm silicon rubber.

A range of different concentrations of polyclonal anti-rabbit detAb (0 to 10 µg/ml in 3%w/w BSA) were tested whereby 150 µl was placed into a multi-well plate and aspirated for 3 minutes incubation following washing step with PBST. Afterwards 150 µl of 4 µg/ml Alkaline phosphatase was incubated for another 4 minutes following 3 washings steps with APwash.

At the end AttoPhos® AP fluorescent was added and fluorescence signal measured by camera in a black box suite, with snapshots collected over time and quantified by ImageJ (NIH)[163]. This procedure was equally repeated with a hydrophobic MCF strip without any covalent coating.

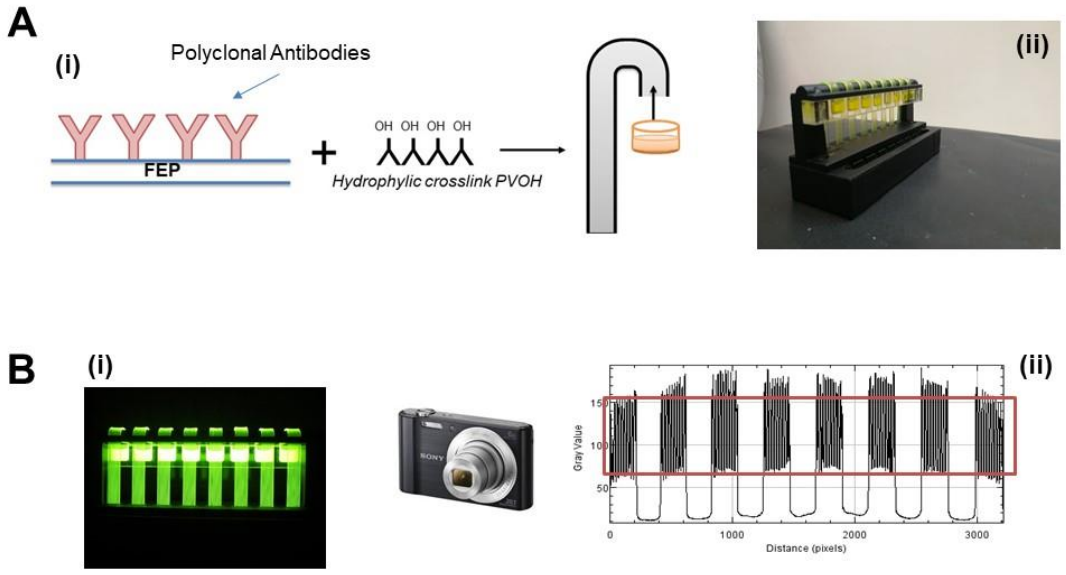

Figure 6.1 A Schematic design of FEP- Teflon® MCF where polyclonal capAb is passively immobilized with consecutive crosslink coating of PVOH to enable siphon action load reagent by gravity in (i) and siphon microfluidic device showing fluorescent intensity in (ii). **B** Fluorescent signal measured by camera in a black box (i) and quantified by ImageJ in (ii).

6.2.6 *E. coli* sample preparation

E. coli K12 ‘’wild type’’ (NCIMB 11290) samples were prepared according section 3.2.3.

6.2.7 Fluorescent *E. coli* immunoassay

Fluorescent immunoassay adopted in siphon microfluidic device is similar to the procedure adopted in chapter 4, changing the volume of sample and reagents per well for 80 µl and MCF length strips for 54 mm. Serial dilutions of *E. coli* K12 range from 10^8 to 10^0 CFU/ml in synthetic urine were loaded into the reservoir and synthetic urine used as negative control.

After pre-preparation MCF strips, 40 µg/ml detection antibody solution (detAb) in 3% w/w BSA was incubated for 3 minutes. Consecutively MCF strips were washed using washing buffer comprisingPBS 0.01M with 0.05% v/v Tween 20 (PBST) and loaded 4 µg/ml streptavidine alkaline phosphatase in Tris-Buffered saline (TBS), pH 7 over 4 minutes. This was followed by 3 consecutive washings comprised by APwashing buffer and finally AttoPhos® was added for enzymatic substrate conversion into fluorescence product as described in Figure 6.1C (i).

Siphon microfluidic device was placed into a black box with a blue LED excitation transiluminator and fluorescent signal quantitation captured through a matched amber acrylic emission filter, imaging by a Canon S120 digital camera. Fluorescence intensity for each individual capillary from the grey scale peak intensity was then converted and quantified by ImageJ[163] software as seen by Figure 6.1 C (ii). Each data point represents the mean fluorescence intensity of 10 individual capillaries within each MCF test strip, and error bars indicate standard deviation of these 10 replicate assays. Note, after experiments, MCF strips were disposed of and MCF-siphon device washed with distillated water and afterwards sterilized with 1 % v/v Virkon or 70 % v/v Industrial Methylated Spirits (IMS). Negative control strips were incubated with synthetic urine without *E. coli*. All *E. coli* samples tested in each experiment, negative control composed by synthetic urine without bacteria and positive control composed by LB agar were plated in LB agar, overnight to assess viability and contamination at any stage.

6.3 Results and discussion

6.3.1. Covalent surface modification of FEP microcapillaries via crosslink PVOH

The influence of surface modification via PVOH onto FEP capillaries was studied, testing different concentrations of hydrophilic coating and fluorescence signal quantified after performing fluorescent immunoassay. The understanding of equilibrium concentration of inert crosslinker into inner surface of microcapillaries is fundamental for lowering non specific and cross talk signal within the assay.[45,58] Besides concentration of PVOH enabling the gravity loading of multistep immunoreagents including washings, it might also affect the positive liquid rise to fill the capillaries. In the first studies with crosslink PVOH coated into FEP- Teflon® reported by Pivetal and team[94], they sugested the use in lower concentrations (0.1 – 0.2 mg/ml) for lower background signal. Indeed the same study showed passive adsorption of capAb resulted in lower background in comparison to covalently immobilized capAb.

Based on that, passive immobilization of 40 µg/ml polyclonal capture antibody, was performed here, following hydrophilic surface modification with different concentrations of crosslink (0.10, 0.15 and 0.20 mg/ml PVOH), blocking buffer incubation with protein free and final washing with PBST. In order to understand the background effect caused by PVOH different immunoassays were performed, following the simple procedure used to detect and quantify *E. coli* in chapter 4.

Briefly, 2 min of 250 µl of PBS 0.1M, 3 min incubation of 250 µl of 40 µg/ml detAb, 250 µl wash with PBST, 4 min incubation with 250 µl of 4 µg/ml alkaline phosphatase, three steps with 250 µl of alkaline phosphatase washing and finally incubation with 250 µl Athophos and fluorescence intensity observed via gel scanner. Figure 6.2A revealed no influence of fluorescence intensity (FI) signal in presence or absence of capAb testing 0.10 or 0.15 mg/ml of PVOH. In contrast the use of 0.20 mg/ml of PVOH contributed to a tripling of the non specific signal in comparison with lower concentrations of PVOH. Despite 0.10 and 0.15 mg/ml of PVOH showed similar FI there was an increment of background in almost 20000 (a.u) in comparison with hydrophobic FEP- Teflon® strips as seen in Figure 6.2B.

Assuming 0.10 mg/ml of PVOH as concentration less susceptible to cause backgroung, liquid rise of MCF strips was measured and shown by Figure 6.2C. A positive *H* is not influenced by presence of capAb or blocking even as well not noticeable any effect of second or third washing.

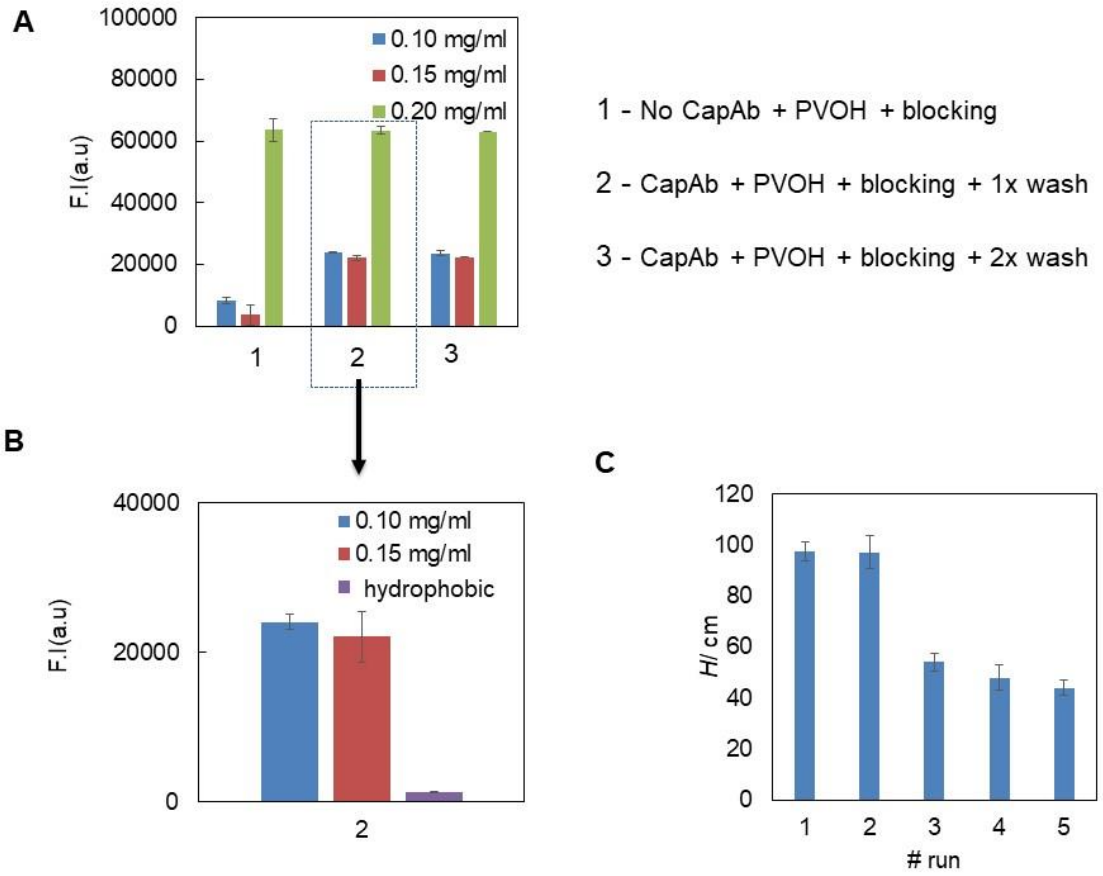

Figure 6.2 Background analysis based on concentration of PVOH. **A** No specific signal measured by fluorescence intensity of immunoassay varying different concentrations of PVOH. **B** Background comparison of MCF strips coated with PVOH or no covalent modification. **C** Capillary rise of MCF strips coated with 0.1 mg/ml PVOH in different conditions: 1- No CapAb - PVOH – blocking, 2 - CapAb - PVOH – Blocking, 3- CapAb-PVOH-Blocking – 1x wash, 4 - CapAb-PVOH - blocking – 2x wash, 5- CapAb - PVOH - blocking - 3 wash.

At this stage, only once washing with PBST can reduce *H* by about 40 cm, which does not affect hydrodynamic flow performance of siphon which operates with only 5.4 cm MCF length. The use of very low concentrations of PVOH is therefore validated to be used in MCF-siphon device to perform power free immunoassays.

6.3.1. Quantitation of immobilized capture antibody

In order to validate the influence of surface chemistry modification and presence of capAb after surface modification with PVOH, an ELISA was carried out using on anti-

rabbit polyclonal detection antibody at a range of concentrations (0; 0.04; 0.4; 4 & 10 µg/ml). The capAb was successfully immobilized and captured after hydrophilic modification onto FEP capillaries surface as indicated by Figure 6.3A (i) and (ii). Nevertheless the capture of polyclonal capture antibody is not influenced by concentration of PVOH, being in agreement with results reported by Pivetal et al.[94]. Without capAb background signal is null validating specific detection of polyclonal detAb anti-rabbit.

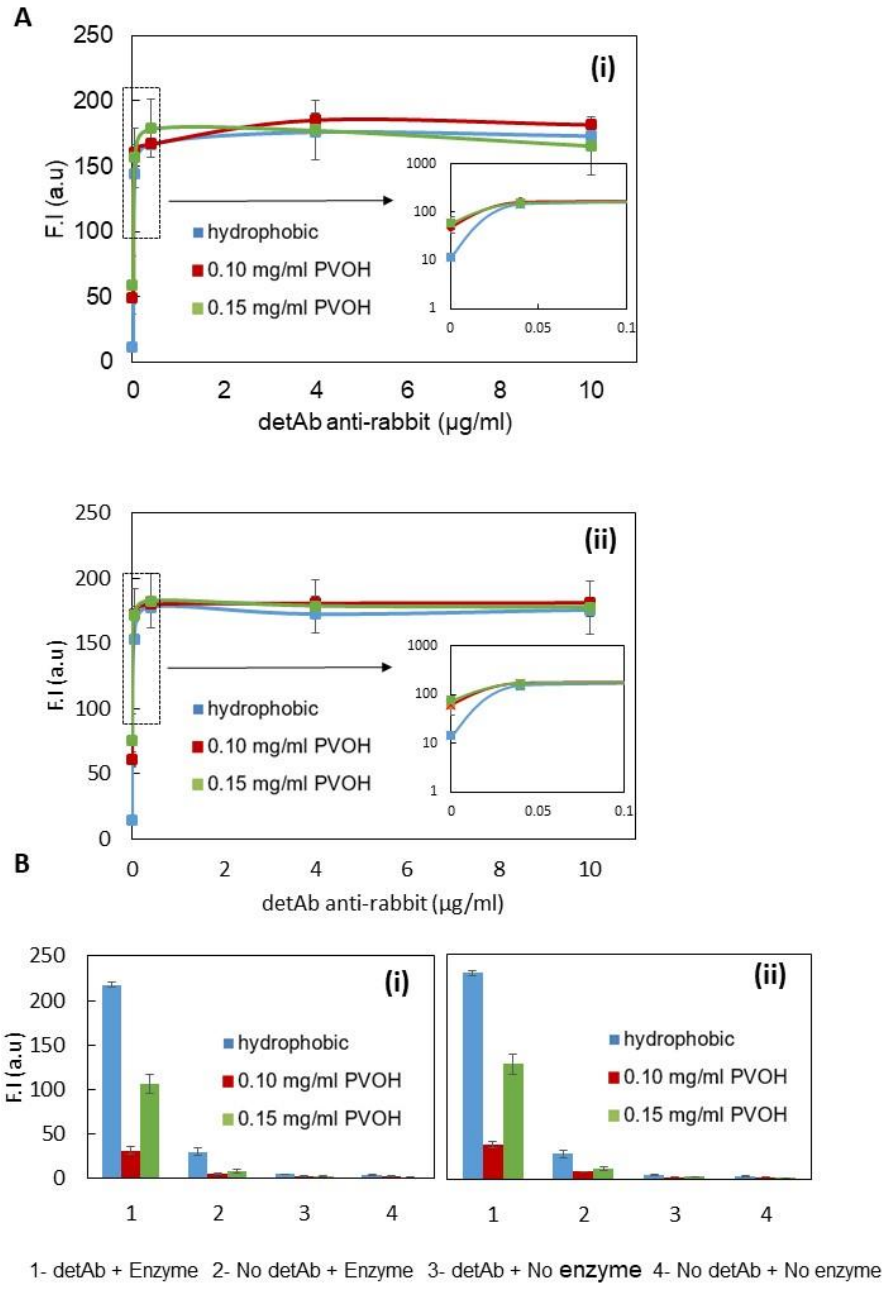

Figure 6.3 Quantitation of immobilized capture antibody. **A** Comparison between covalent and no covalent surface modification after Attophos conversion at 2 min represented by (i) and 5 minutes by (ii). **B** Effect of detAb and enzyme on background assay at 2 minutes (i) 3 min (ii).

It is known various steps of immunoassays (capAb, blocking agent, diluent buffers and time incubations) can promote an increase of nonspecific signal detection.[45] As mentioned in section 2.7 of chapter 2, surface chemistry, capture antibody and blocking agent are paramount steps, which influence equilibrium antibody-antigen and might prevent nonspecific signal.[58]

In order to understand some of this key features to maximize sensitivity while minimizing nonspecific binding, further immunoassay tests were carried out in presence and absence of 40 µg/ml detAb anti-*E. coli* and enzyme alkaline phosphatase. Figure 6.3B revealed a clear detection of capAb in presence of detAb and enzyme being fluorescence signal dramatically reduced in absence of one of immunoassays components or vanished in absence of both. Observed fluorescence signal along time does not change.

6.3.2. Fluorescence quantitation of *E. coli* in siphon microfluidic device

After first tests to understand ideal concentration of PVOH, effective presence of immobilized capAb and background signal, an *E. coli* fluorescence immunoassay experiments in siphon microfluidic device was performed. A replicate assay according to conditions used in chapter 4 was attempted to quantify *E. coli* in synthetic urine , After optimized camera settings and optical environment conditions in black box
E. coli samplse in synthetic urine were displaced into reservoirs and incubated from range 0 to 10^8 CFU/ml. All data shown by Figure 6.4 was performed with siphon microfluidic device, with each point indicative of an assembled strip.

Contrary to manual incubation of syringes carried on in chapter 4, reagents loading in siphon device was fast (less than 40 sec) after 1st sample incubation that generally takes longer (60-90 sec). However, the full response curve showed no sensitive response as seen by Figure 6.4A (i) and high background (Figure 6.4A (ii)). The lower analytical assay performance drove us to study some key parameters to improve sensitivity and minimize background.

Following the previous assay conditions, a range of capAb concentration [10-40 µg/ml] was studied, using 10^5 CFU/ml as bacterial sample diluted in synthetic urine and as control synthetic urine without bacteria. Results showed the best signal obtained was with 10 µg/ml capAb, although the lack of consistency over the decreasing range is noted. Note, the antibody-antigen equilibrium have been achieved for a range of 40 µg/ml in chapter 4. Due to that, and avoiding a total modification of the *E. coli* immunoassay previously developed, the concentration of 40 µg/ml of capAb was kept and the influence of other factors in the assay were studied.

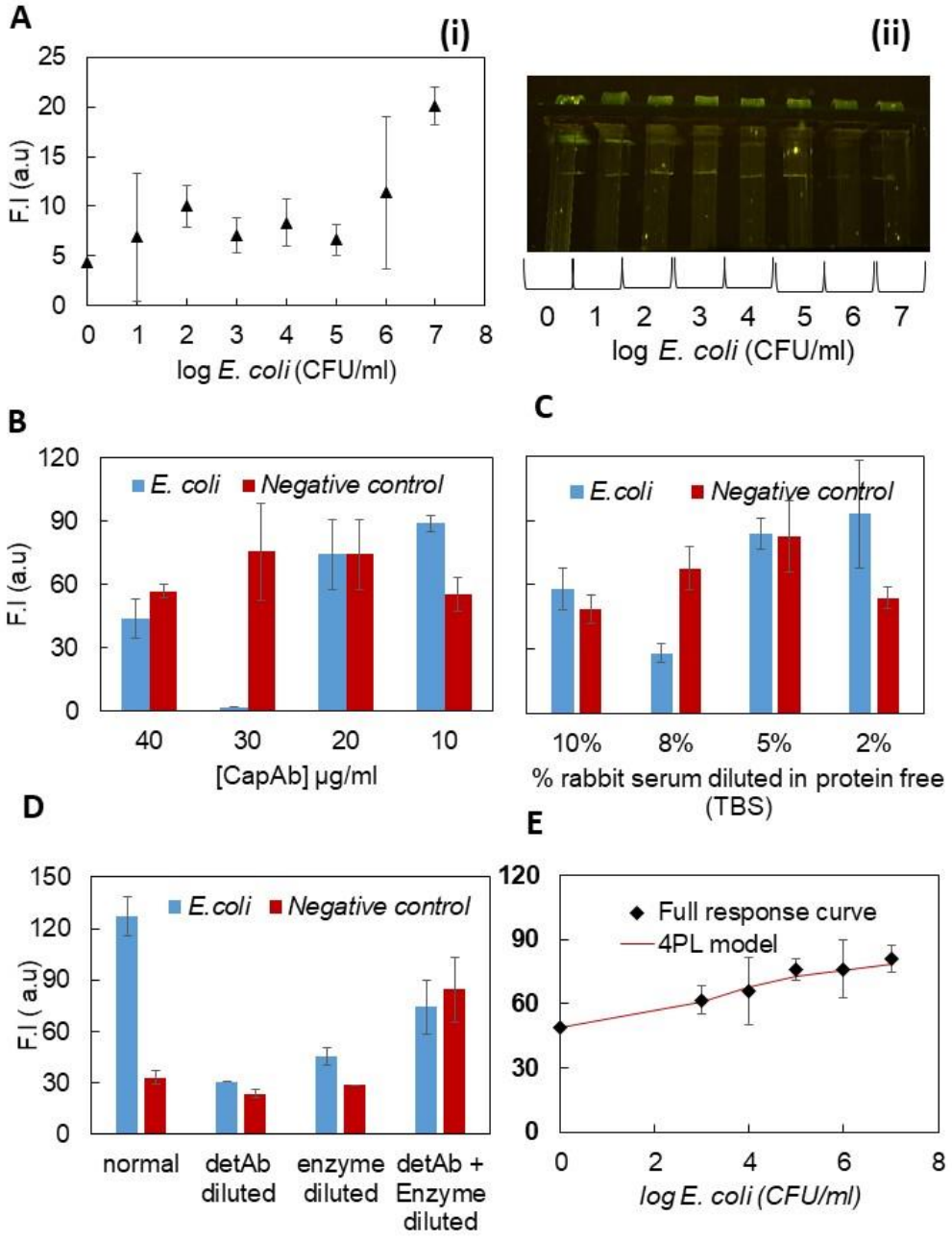

Figure 6.4 Development and enhancement of fluorescent *E. coli* immunoassay into MCF-siphon. **A** Initial full response curve for *E. coli* quantitation (using protein free (TBS) as blocking and 19 min of incubation time plus Atthophos) in (i) and (ii) showing respective MCF strips captured by camera after 2 min of Atthophos conversion. **B** Study of influence of capture antibody concentration in *E. coli* immunoassay performance where negative control consisted in synthetic urine without bacteria. **C** Reduction of background assay by testing different % w/w of rabbit serum diluted in protein free (TBS). **D** Influence of 2% w/w of rabbit serum in diluent buffer of detection antibody and alkaline phosphatase. **E** Fluorescent *E. coli* quantitative immunoassay in siphon microfluidic device after 2 min of Atthophos conversion.

Following same strategy of assay optimization described in chapter 4 and immunoassay optimization methods sugested by Cox and team[45], the influence of a different blocking agent was studied. Rabbit serum in lower percentages, between 2% to 10% w/w, (as suggested by supplier of polyclonal rabbit antibodies (capAb & detAb)) was diluted in protein free (TBS) agent, keeping 40 µg/ml of capAb. The use of 2% w/w rabbit serum diluted in blocking buffer obtained the best signal response as seen by Figure 6.4C. Further experiments have carried on with MCF strips coated with 40 µg/ml of capAb and this 2% w/w rabbit serum in protein free (TBS), testing the influence of adding 2% w/w of rabbit serum in diluent buffers of detAb and enzyme (3% w/w BSA and Tris buffer). Background and specific signal were not improved demontrating best signal-to-noise ratio by a normal assay (Figure 6.4D).

Final response curve was obtained keeping concentrations of capAb and detAb with a limit of detection (LoD) of $9x10^4$ CFU/ml in 20 min total assay. Despite not ideal LoD for a UTI at point-of-need of clinical settings (10^3 CFU/ml)[34] a positive improvement was conducted by adding 2% (w/w) of rabbit serum in assay blocking. It is important highlight that commercial kits for urinalysis identify *E. coli* infection based on presence of leukocytes, nitrites, albumin,creatinine, pH change and so on, being unable to quantify bacteria levels.[13,34,175]

Comparing performance of this new *E. coli* assay in MCF-siphon to some of microfluidic systems reported in table 2.2 from literature review of chapter 2. For example Laczka and team[83] achieved an limit of detecion of 10^4-10^5 cells/ml in PBS by an electrochemical microelectrode capacitive Immunosensor in 1h. Shih and colleagues[40] reported a paper-based ELISA detecting 10^4-10^5 cells/ml in culture medium in 5h.
It is clear *E. coli* immunoassay in MCF-siphon provides autonomy eliminating error-prone from handling steps, where the user only needs to deliver the required amount of solution in the wells, avoiding cross contamination by bench contact, dead volumes and providing homogeneous flow in each strip (see constant velocity per strip per step demonstrated by MCF-siphon in Figure 5.10D of chapter 5). Nevertheless *E. coli* assay in MCF-siphon is performed without sample prepraration in synthetic urine, presents low assay time even in comparison to hydrophobic assay presented in chapter 4, is a low cost and simple device conducting immunoassays without external power and present a lower limit detection in comparison to other microfluidics approaches reported in literature. Thus, it will be critical to adress lower performance and overcome surface chemistry drawbacks of this new approach to achieve the clinical thershold for an UTI's.

Sensitivity and assay performance can be improved with some assay development work. The continuous study of different concentrations (capAb in parallel with detAb), time incubations of different steps, variation of enzyme concentration and lately diluent buffer

can in future drive to an impressive analytical performance of this *E. coli* immunoassay into siphon microfluidic.

It is relevant to emphasize the simplistic assay handling enabled by simple design of siphon device favouring a non cross reactive and fast (<40 sec per step) multi reagent steps. The new gravity driven device promoted a more efficient and consistent loading, due low system standard variation ≈ 3-5% of residence time (see table 5.4 in chapter 5) ensuring reproducibility of the assay in comparison to fluid handling system operated by manual syringes incubation or multi syringe device described in chapter 4.

6.4 Conclusions

Siphon device surpass manual incubation used in chapter 4 promoting a more reliable and reproducible assay in a uniform hydrodynamic flow as accessed in chapter 5. In a short time of assay develoment, the quantitation of *E. coli* with LoD of $9x10^4$ CFU/ml in less than 20 min was achieved, despite far the UTI goal < 10^3 CFU/ml or LoD obtained by smartphone *E. coli* quantitation. This is due a high background level promoted by hydrophilic surface modification of inner FEP capillaries by PVOH. Future assay development can improve sensitivity and limit of detection for clinical purpouse.

This new immunoassay adresses a simple fluid handling in a new gravity driven microfluidic device which promotes autonomy, power-free and multi-step incubation eliminating error-prone from handling steps. Moreover it minimize the risk of cross-contamination between strips observed by absence of dead volumes in hydrodynamic characterization of chapter 5 or by bench contact. Yet, this microfluidic approach offers reproducibility by efficient and homogenous MCF strip loading observed by lower system standard variation ≈ 3-5% of residence time and constant velocity overall.

Future developments can launch a new generation of siphon microfluidic devices operating in many multi point-of-need purposes and be integrated with off the shelf technologies as smartphones, operating as effectives diagnostics in low resource settings.

CHAPTER 7 | Conclusions and Future perspectives

7.1 Conclusions

Biosensors capable of detecting and identifying bacteria are now critically needed to monitor the global spread of antimicrobial resistance. Advanced point-of-care diagnostics aim to exploit microfluidic platforms with performance of healthcare laboratory equipment in a format compatible with ASSURED (affordable, sensitive, specific, user-friendly, rapid & robust, equipment-free and delivered) requirements for affordable and effective diagnostics worldwide. However, in spite of this, portable diagnostic tests developed to date lack the specificity, limit of detection and speed for effective implementation in bacteria detection at point-of-care.

Thus, miniaturization, sensitivity, specificity, affordability and automation are some of technological challenges to achieve a commercial high throughput device for rapid bacterial detection that remain.

This PhD project presented novel experimental insights for sensitive and rapid detection of *E. coli* using polyclonal antibodies immobilized on the inner surface of the ultra-low cost melt-extruded, fluoropolymer microcapillary film (MCF). This miniaturized platform consists in 10 parallel microarray with approximately 200 µm of internal diameter and produced by an inexpensive and easily manufacturing process.

Understanding equilibrium interaction between bacteria and capture antibody (capAb) probe within microcapillaries is paramount to achieve lower limit of detection (LoD) and speed up the immunoassays. Therefore, studying the miniaturization of such bioassays was the first milestone of this research, resulting in the identification of three major challenges for miniaturisation of bacteria detection: the interrogation volume, gravity and shear stress. None of these could be solved with the most sophisticated imaging equipment available and entirely relied on novel engineering and design options. MCF platform showed immunospecificity of the capAb for *E. coli K-12* detection and high affinity binding between surface-capAb-antigen. Capture and settling of bacterial cells happened during the time scale of sample incubation (5 min), with cells' settling helping to promote antibody-bacteria binding. Small interrogation volume, gravity and the shear rates produced by flow of reagents through microcapillaries reduce by around 10-fold the efficiency of *E. coli* cells capture. Moreover, it was noticed a negligible effect of washing in high density of cells which is paramount for decrease background in multi-step immunoassays. The ability of passing a large volume of sample through the capAb coated

microcapillaries enabled a >100 fold reduction in the limit of detection of a fluorescent sandwich immunoassay for *E. coli* quantitation.

This proof-of-concept was successfully achieved with the commercial immunoreagents, the inexpensive FEP-Teflon platform and off-the-shelf smartphone technology. Unrivalled LoD of up to 240 CFU/ml in synthetic urine in less than 25 minutes was achieved without sample preparation nor concentration, fundamental to reduce complexity and assay time for point-of-care diagnostics. Replicas of full response curves performed with 10^0-10^7 CFUs/ml of *E. coli* K12 in synthetic urine yielded recovery values in the range 80-120% with and assay precision below 20%, therefore comparable to other high-performance automated immunoassays.

In order to provide simplistic systems to deliver fluid for power-free, high throughput multi-steps immunoassays, reducing manual error prone and increase repeatability, two new pressure driven microfluidic devices were designed and manufactured. MCF-funnel and MCF-siphon uniquely combine the reagents and sample loading in sequence solely driven by gravity to perform power free immunoassays integrating the MCF hydrophilicly coated by the PVOH hydrogel. Particularly, these would benefit low income countries where patients have limited access to centralised labs and the costs of testing must be low.

Hydrodynamic characterization revealed gravity driven microfluidic devices presenting a residence time behaviour within microcapillaries reasonably close to ideal plug flow, however siphon showed a consistent and more reproducible flow. That was demonstrated by achieving an overall dimensionless axial dispersion between 0.01-0.02 showing perfect trace impulse without visible contamination or dead volume in comparison to MCF-funnel. Siphon presented a lower axial dispersion overall below $5x10^{-6}$ m^2/s, and more consistent *D* values per step per strip, inversely to funnel around $20x10^{-6}$ m^2/s.

A microfluidic device under siphon action is unreported to date and due its superior performance it was attempted to validate a proof of concept of *E. coli* detection in the novel MCF-siphon. *E. coli* fluorescent immunoassay in siphon achieved a LoD of 9 $x10^4$ CFU/ml in synthetic urine, using camera as the inexpensive readout system. Performance below that required clinically to detect *E. coli* in a UTI is intrinsically related to the high background signal due surface modification of inner capillaries by PVOH, although it was possible to speed up the assay for 20 minutes with this new design exploiting low volume reagents and sample.

Ongoing work towards the desired sensitivity is therefore needed, exploiting different blocking agents, immunoreagents concentration, incubation times, diluent buffers in order to reduce interference of PVOH layer in background signal. Further integration with fluorescence signal detection by smartphone would approach this novel diagnostic

test for bacterial screening and quantitation in remote areas outside of centralized healthcare systems.

7.2 Further Work

Many other suggestions can be considered and discussed for further proof of concept validation and future commercialisation of *E. coli* detection POC test in FEP-Teflon®.

Particularly for clinical applications, the sensitivity of the biosensors would need to be tested with real biological samples. In urine, many constituents can vary over a broad range such as pH from 4.5 and 9, healthy urine has very few cells whereas an infected samples can have high concentrations of bacteria cells and white blood cells higher than 10^8 cells/ml.[176] Specifically for UTI, any successful biosensor must have the ability to rule out infection, be rapid (less 1h) for effective treatment prescription, automated with minimal intervention of patient, robust assay protocol compatible with biological samples, incorporation of pathogen identification with antimicrobial susceptibility testing and versatile to be adaptable for the different pathogen profiles in different clinical scenarios.

Pre-clinical tests for POC diagnostic validation would demand safe laboratory conditions, for analysis of at least 100 urine samples from patients. Urine is composed by around 95% water and 5% of solids that are generally urea, uric acid, chloride, sodium potassium, creatinine and other dissolved ions, inorganic and organic compounds (proteins, hormones and metabolites). This would give an overview of matrix interference in assay performance by pH, viscosity sample, and presence of urine constituents, validating specificity of polyclonal antibodies in terms of presence of other bacterial strains common in UTI as *Pseudomonas sp, Klebsiella sp*. and *Enterobacteriaceae sp*. On the other hand, 10-bore MCF would allow to develop a multiplexing bacterial assay by individual capillary incubation of sample spiked with different bacterial strains responsible for UTI, which would be a clear advantage regarding urinalysis dipsticks in addition to the rapid quantitative response achieved in this work.

Basis on the diversity of bacterial strains originating a urinary tract infection, biosensor diagnosis for UTI has moved beyond proof-on-concept stage into validation phase with clinical samples. Development of assays for rapid pathogen identification and antibiotic susceptibility test would lead to a potential paradigm-shift for UTI diagnosis and correct prescription of antibiotics according patient, helping to fight against antimicrobial resistance worldwide. The new gravity driven devices would enable to exploit this potential

in a power-free and automated performance, bringing more informed and accurate healthcare decisions in antibiotic prescriptions.

CHAPTER 8 | List of References

1. European Comission. One Health Action Plan against Antimicrobial Resistance. (2017).
2. O'Neill, J. Review on Antimicrobial Resistance. Tackling a Global Health Crisis: Rapid Diagnostics : Stopping Unnecessary Use of Antibiotics. *Indep. Rev. AMR* 1–36 (2015).
3. Ayukekbong, J. A., Ntemgwa, M. & Atabe, A. N. The threat of antimicrobial resistance in developing countries: Causes and control strategies. *Antimicrob. Resist. Infect. Control* 6, 1–8 (2017).
4. Kokkinis, G., Plochberger, B., Cardoso, S., Keplinger, F. & Giouroudi, I. A microfluidic, dual-purpose sensor for in vitro detection of Enterobacteriaceae and biotinylated antibodies. *Lab Chip* 16, 1261–1271 (2016).
5. Foudeh, A. M., Fatanat Didar, T., Veres, T. & Tabrizian, M. Microfluidic designs and techniques using lab-on-a-chip devices for pathogen detection for point-of-care diagnostics. *Lab Chip* 12, 3249–3266 (2012).
6. O'Neill, J. Tackling Drug-Resistant Infections Globally: final report and Recommendations. (2016).
7. Center for disease Dynamics, E. & P. the State of the World 's Antibiotics. *State World 's Antibiot.* (2015).
8. Nayak, S., Blumenfeld, N. R., Laksanasopin, T. & Sia, S. K. Point-of-Care Diagnostics: Recent Developments in a Connected Age. *Anal. Chem.* 89, 102–123 (2017).
9. Price, C. P. Regular review: Point of care testing. *BMJ* 322, 1285–1288 (2001).
10. Mabey, D., Peeling, R. W., Ustianowski, A. & Perkins, M. D. Diagnostics for the developing world. *Nat. Rev. Microbiol.* 2, 231–240 (2004).
11. Gubala, V., Harris, L. F., Ricco, A. J., Tan, M. X. & Williams, D. E. Point of Care Diagnostics: Status and Future. *Anal. Chem.* 84, 487–515 (2012).
12. Olanrewaju, A. O., Ng, A., Decorwin-Martin, P., Robillard, A. & Juncker, D. Microfluidic Capillaric Circuit for Rapid and Facile Bacteria Detection. *Anal. Chem.* 89, 6846–6853 (2017).
13. Cho, S., Park, T. S., Nahapetian, T. G. & Yoon, J. Y. Smartphone-based, sensitive µPAD detection of urinary tract infection and gonorrhea. *Biosens. Bioelectron.* 74, 601–611 (2015).
14. Zourob, M., Elwary, S. & Turner, A. *Principles of Bacterial Detection*. *Principles of Bacterial Detection: Biosensors, Regognition Receptors and Microsystems* (2008).

doi:10.1093/pcp/pcw027

15. J.W.A. Findlay, W. C. S., , J.W. Lee, G.D. Nordblom, I. Das, B.S. DeSilva, M. N. K. & Bowsher, R. R. Validation of immunoassays for bioanalysis: a pharmaceutical industry perspective. *J. Pharm. Biomed. Anal.* 21, 1249–1273 (2000).
16. Yoo, J. H., Woo, D. H., Chun, M. S. & Chang, M. S. Microfluidic based biosensing for Escherichia coli detection by embedding antimicrobial peptide-labeled beads. *Sensors Actuators, B Chem.* 191, 211–218 (2014).
17. Safavieh, M., Ahmed, M. U., Tolba, M. & Zourob, M. Microfluidic electrochemical assay for rapid detection and quantification of Escherichia coli. *Biosens. Bioelectron.* 31, 523–528 (2012).
18. Law, J. W. F., Mutalib, N. S. A., Chan, K. G. & Lee, L. H. Rapid metho ds for the detection of foodborne bacterial pathogens: Principles, applications, advantages and limitations. *Front. Microbiol.* 5, 1–19 (2014).
19. Su, W., Gao, X., Jiang, L. & Qin, J. Microfluidic platform towards point-of-care diagnostics in infectious diseases. *J. Chromatogr. A* 1377, 13–26 (2015).
20. Stamm, W. E. & Norrby, S. R. Urinary Tract Infections: Disease Panorama and Challenges. *J. Infect. Dis.* 183, S1–S4 (2001).
21. Grabe, M. *et al.* Guidelines on Urological Infections. (2015).
22. Guido Schmiemann, Eberhardt Kniehl, Klaus Gebhardt, Martha M. Matejczyk, E. H.-P. Diagnosis of urinary tract infections. *Dtsch Arztebl Int* 34, 361–7 (2010).
23. Barbosa, A. I., Castanheira, A. P., Edwards, A. D. & Reis, N. M. A lab-in-a-briefcase for rapid prostate specific antigen (PSA) screening from whole blood. *Lab Chip* 14, 2918–2928 (2014).
24. Barbosa, A. I., Gehlot, P., Sidapra, K., Edwards, A. D. & Reis, N. M. Portable smartphone quantitation of prostate specific antigen (PSA) in a fluoropolymer microfluidic device. *Biosens. Bioelectron.* 70, 5–14 (2015).
25. Castanheira, A. P., Barbosa, A. I., Edwards, A. D. & Reis, N. M. Multiplexed femtomolar quantitation of human cytokines in a fluoropolymer microcapillary film. *Analyst* 149, 5609–5618 (2000).
26. Poolman, J. T. Escherichia coli. *Int. Encycl. Public Heal.* 585–593 (2017). doi:10.1016/B978-0-12-803678-5.00504-X
27. Ewing, W. H. *Isolation and Identification of Escherichia coli serotypes associated with diarrheal diseases*. *CDC Information center, centers for disease control Atlanta* (1963).
28. Stenutz, R., Weintraub, A. & Widmalm, G. The structures of Escherichia coli O-polysaccharide antigens. *FEMS Microbiol. Rev.* 30, 382–403 (2006).
29. Alexander, C. & Rietschel, E. T. Bacterial lipopolysaccharides and innate immunity.

J. Endotoxin Res. 7, 167–202 (2001).

30. E. coli bacterium morphology. Available at: http://www.ecl-lab.com/en/ecoli/index.asp, November 2018.
31. Espy, M. J. *et al.* Real-Time PCR in Clinical Microbiology : Applications for Routine Laboratory Testing. 19, 165–256 (2006).
32. Fu, Z., Rogelj, S. & Kieft, T. L. Rapid detection of Escherichia coli O157:H7 by immunomagnetic separation and real-time PCR. *Int. J. Food Microbiol.* 99, 47–57 (2005).
33. Ana L. Flores-Mireles, Jennifer N. Walker, Michael Caparon, and S. J. H. Urinary tract infections: epidemiology, mechanisms of infection and treatment options. *Nat Rev Microbiol.* 13, 269–284 (2015).
34. Aspevall, O., Hallander, H., Gant, V. & Kouri, T. European guidelines for urinalysis: A collaborative document produced by European clinical microbiologists and clinical chemists under ECLM in collaboration with ESCMID. *Clin. Microbiol. Infect.* 7, 173–178 (2001).
35. Hammett-stabler, C. A. & Webster, L. R. *A Clinical Guide to urine drug testing*. (2008).
36. David, S. *et al.* Assessment of pathogenic bacteria using periodic actuation. *Lab Chip* 13, 3192–3198 (2013).
37. Kong, W., Xiong, J., Yue, H. & Fu, Z. Sandwich Fluorimetric Method for Specific Detection of Staphylococcus aureus Based on Antibiotic-Affinity Strategy. *Anal. Chem.* 87, 9864–9868 (2015).
38. Chang, M. S., Yoo, J. H., Woo, D. H. & Chun, M. S. Efficient detection of Escherichia coli O157:H7 using a reusable microfluidic chip embedded with antimicrobial peptide-labeled beads. *Analyst* 140, 7997–8006 (2015).
39. Zhu, H., Sikora, U. & Ozcan, A. Quantum dot enabled detection of Escherichia coli using a cell-phone. *Analyst* 137, 2541–2544 (2012).
40. Shih, C. M. *et al.* Paper-based ELISA to rapidly detect Escherichia coli. *Talanta* 145, 2–5 (2015).
41. Chang, W. H. *et al.* Rapid detection and typing of live bacteria from human joint fluid samples by utilizing an integrated microfluidic system. *Biosens. Bioelectron.* 66, 148–154 (2015).
42. Mairhofer, J., Roppert, K. & Ertl, P. Microfluidic systems for pathogen sensing: A review. *Sensors (Switzerland)* 9, 4804–4823 (2009).
43. Wild, D. in (ed. Wild, D. B. T.-T. I. H. (Fourth E.) (Elsevier, 2013). doi:https://doi.org/10.1016/B978-0-08-097037-0.00001-4
44. Chin, C. D., Linder, V. & Sia, S. K. Commercialization of microfluidic point-of-care

diagnostic devices. *Lab Chip* 12, 2118–2134 (2012).

45. Cox, K. L. *et al.* Immunoassay Methods. *Assay Guid. Man.* 43 (2012). doi:NBK92434 [bookaccession]
46. David R. Davies, E. A. P. & Sheriff, S. Antibody -antigen complexes. *Annu. Rev. Biochem.* 59, 439–73 (1990).
47. Edited by Norman H. L. Chiu and Theodore K. Christopoulos. *Advances in Immunoassay technology*. (2012). doi:10.2307/488965
48. Deshpande, S. S. Enzyme ImmunoassaysmFrom Concept to Product Development Exquisite Specificity--The Monoclonal Antibody Revolution Introductory Immunobiology Stress-inducible Cellular Responses. 25, 1997 (1997).
49. Lipman, N. S., Jackson, L. R., Trudel, L. J. & Weis-Garcia, F. Monoclonal Versus Polyclonal Antibodies: Distinguishing Characteristics, Applications, and Information Resources. *ILAR J.* 46, 258–268 (2005).
50. Klonisch, T. *et al.* Enhancement in antigen binding by a combination of synergy and antibody capture. *Immunology* 89, 165–171 (1996).
51. Barbosa, A. I. & Reis, N. M. A critical insight into the development pipeline of microfluidic immunoassay devices for the sensitive quantitation of protein biomarkers at the point of care. *Analyst* 142, 858–882 (2017).
52. Brian law (ed.). *Immunoassay: A practical guide*. (CRC PRESS, 1996).
53. Hosseini, S., Vazquez, P., Rito-Palomares, M. & Martinez-Chapa, S. O. in *SpringerBriefs in Applied Sciences and Technology* 67–115 (2018). doi:10.1007/978-981-10-6766-2_5
54. Crowther, J. R. *The ELISA guidebook*. *Springer* 516, (2009).
55. Tate, J. & Ward, G. Interferences in immunoassay - Google Scholar. *Clin. Biochem. Rev.* 25, 105–120 (2004).
56. Bio-Rad Laboratories. *ELISA Basics Guide*. (2017).
57. Hage, D. S. Immunoassays. *Anal. Chem.* 67, 455–462 (1995).
58. Crowther, J. R. *The ELISA Guidebook*. (Humana Press, 2000).
59. 4PL model. Available at: https://www.myassays.com/four-parameter-logistic-regression.html.
60. Shrivastava A. and Gupta V. Methods for the determination of limit of detection and limit of quantitation of the analytical methods. *Chronicles Young Sci.* 2, 21–25 (2011).
61. Berthold Technology. Available at: https://kem-en-tec-nordic.com/berthold-technologies/. (Accessed: 20th August 2011)
62. Joaquim M.S Cabral, Maria Raquel Aires-Barros, M. G. *Engenharia Enzimática*. (Lidel, 2003).

63. Rajendran, V. K. *et al.* Gravity-driven microfluidic particle sorting device with hydrodynamic separation amplification. *Lab Chip* 79, 1369–1376 (2017).
64. Safavieh, M., Ahmed, M. U., Sokullu, E., Ng, A. & Zourob, M. A simple cassette as point-of-care diagnostic device for naked-eye colorimetric bacteria detection. *Analyst* 139, 482–487 (2014).
65. Vaitukaitis, J. L. Development of the Home Pregnancy Test. *Annu. New York Acad. Sci.* 1038, 220–222 (2004).
66. Chin, C. D., Linder, V. & Sia, S. K. Lab-on-a-chip devices for global health: Past studies and future opportunities. *Lab Chip* 7, 41–57 (2007).
67. Golberg, A. *et al.* Cloud-enabled microscopy and droplet microfluidic platform for specific detection of Escherichia coli in water. *PLoS One* 9, (2014).
68. Stratz, S., Eyer, K., Kurth, F. & Dittrich, P. S. On-chip enzyme quantification of single Escherichia coli bacteria by immunoassay-based analysis. *Anal. Chem.* 86, 12375–12381 (2014).
69. Ikami, M. *et al.* Immuno-pillar chip: A new platform for rapid and easy-to-use immunoassay. *Lab Chip* 10, 3335–3340 (2010).
70. Goluch, E. D. *et al.* A bio-barcode assay for on-chip attomolar-sensitivity protein detection. *Lab Chip* 6, 1293–1299 (2006).
71. Yetisen, A. K., Akram, M. S. & Lowe, C. R. Lab on a Chip. 2210–2251 (2013). doi:10.1039/c3lc50169h
72. Beom Seok Lee, Jung-Nam Lee, Jong-Myeon Park,Jeong-Gun Lee, Suhyeon Kim, Y.-K. C. and C. K. A fully automated immunoassay from whole blood on a disc. *Lab Chip* 9, 1548–1555 (2009).
73. Lai, S. *et al.* Design of a Compact Disk-like Microfluidic Platform for Enzyme-Linked Immunosorbent Assay. *Anal. Chem.* 76, 1832–1837 (2004).
74. Lafleur, L. *et al.* Progress toward multiplexed sample-to-result detection in low resource settings using microfluidic immunoassay cards. *Lab Chip* 12, 1119–1127 (2012).
75. longitude price. Available at: http://longitudeprize.org.
76. Whitesides, G. M. The origins and the future of microfluidics. *Nature* 442, 368–373 (2006).
77. Gorkin, R. *et al.* Centrifugal microfluidics for biomedical applications. *Lab Chip* 10, 1758–1773 (2010).
78. Peeling, R. W. Diagnostics in a digital age: An opportunity to strengthen health systems and improve health outcomes. *Int. Health* 7, 384–389 (2015).
79. Ogbu, U. C. & Arah, O. A. World Health Organization. *International Encyclopedia of Public Health* 461–467 (2016). doi:10.1016/B978-0-12-803678-5.00499-9

80. Wang, S. *et al.* Portable microfluidic chip for detection of Escherichia coli in produce and blood. *Int. J. Nanomedicine* 7, 2591–2600 (2012).
81. Liao, J. C. *et al.* Use of Electrochemical DNA Biosensors for Rapid Molecular Identification of Uropathogens in Clinical Urine Specimens Use of Electrochemical DNA Biosensors for Rapid Molecular Identification of Uropathogens in Clinical Urine Specimens. *J. Clin. Microbiol.* 44, 561–570 (2006).
82. Boehm, D. A., Gottlieb, P. A. & Hua, S. Z. On-chip microfluidic biosensor for bacterial detection and identification. *Sensors Actuators, B Chem.* 126, 508–514 (2007).
83. Laczka, O. *et al.* Improved bacteria detection by coupling magneto-immunocapture and amperometry at flow-channel microband electrodes. *Biosens. Bioelectron.* 26, 3633–3640 (2011).
84. Bercovici, M. *et al.* Rapid detection of urinary tract infections using isotachophoresis and molecular beacons. *Anal. Chem.* 83, 4110–4117 (2011).
85. Sanvicens, N. *et al.* Quantum dot-based array for sensitive detection of Escherichia coli. *Anal. Bioanal. Chem.* 399, 2755–2762 (2011).
86. Rajendran, V. K., Bakthavathsalam, P. & Jaffar Ali, B. M. Smartphone based bacterial detection using biofunctionalized fluorescent nanoparticles. *Microchim. Acta* 181, 1815–1821 (2014).
87. Angus, S. V., Cho, S., Harshman, D. K., Song, J. Y. & Yoon, J. Y. A portable, shock-proof, surface-heated droplet PCR system for Escherichia coli detection. *Biosens. Bioelectron.* 74, 360–368 (2015).
88. Mark, D., Haeberle, S., Roth, G., Von Stetten, F. & Zengerle, R. Microfluidic lab-on-a-chip platforms: requirements, characteristics and applications. *Chem. Soc. Rev.* 1153–1182 (2010). doi:10.1039/b820557b
89. Stefan haeberle and Roland Zengerle. Microfluidic platforms for lab-on-a-chip applications. *Lab chip* 7, 1094–110 (2007).
90. Mark, D., Haeberle, S., Roth, G., Von Stetten, F. & Zengerle, R. Microfluidic lab-on-a-chip platforms: Requirements, characteristics and applications. *NATO Sci. Peace Secur. Ser. A Chem. Biol.* 305–376 (2010). doi:10.1007/978-90-481-9029-4-17
91. Liu, M., Sun, J. & Chen, Q. Influences of heating temperature on mechanical properties of polydimethylsiloxane. *Sensors Actuators, A Phys.* 151, 42–45 (2009).
92. Alvaro Mata, A. J. F. & Roy, and S. Characterization of Polydimethylsiloxane (PDMS) Properties for Biomedical Micro/Nanosystems. *Biomed. Microdevices* 7, 281–293 (2005).
93. Ebnesajjad, S. in (ed. Ebnesajjad, S. B. T.-F. (Second E.) 1–6 (William Andrew Publishing, 2015). doi:https://doi.org/10.1016/B978-1-4557-3197-8.00001-8

94. Pivetal, J. *et al.* Covalent immobilisation of antibodies in Teflon-FEP microfluidic devices for the sensitive quantification of clinically relevant protein biomarkers. *Analyst* 142, 959–968 (2017).
95. Grover, W. H., Von Muhlen, M. G. & Manalis, S. R. Teflon films for chemically-inert microfluidic valves and pumps. *Lab Chip* 8, 913–918 (2008).
96. Gooch, J. W. Teflon FEP. *Encycl. Dict. Polym.* 731–731 (2011). doi:10.1007/978-1-4419-6247-8_11595
97. Edwards, A. D., Reis, N. M., Slater, N. K. H. & MacKley, M. R. A simple device for multiplex ELISA made from melt-extruded plastic microcapillary film. *Lab Chip* 11, 4267–4273 (2011).
98. Castanheira, A. P., Barbosa, A. I., Edwards, A. D. & Reis, N. M. Multiplexed femtomolar quantitation of human cytokines in a fluoropolymer microcapillary film. *Analyst* 140, 5609–5618 (2015).
99. Danckverts, P. V. in *Chemical Engineering Science* 50, 3857–3866 (1952).
100. Geankoplis C.J. *Transport Process and Unit Operations*. (Prentice-Hall International, Inc., 1983).
101. Reynolds, O. On the Dynamical Theory of Incompressible Viscous Fluids and the Determination of the Criterion. *Philos. Trans. R. Soc. A Math. Phys. Eng. Sci.* 186, 123–164 (1895).
102. Buijs, J., Norde, W. & Lichtenbelt, J. W. T. Changes in the Secondary Structure of Adsorbed IgG and F(ab') $_2$ Studied by FTIR Spectroscopy. *Langmuir* 12, 1605–1613 (1996).
103. Barbosa, A. I. The development and optimisation of a novel microfluidic immunoassay platform for point of care diagnostics. (2015).
104. E.coli size. http://book.bionumbers.org/how-big-is-an-e-coli-cell-and-what-is-its-mass/. [Online] [Cited: June 22, 2016.]. 2016 (2016).
105. Kai, J. *et al.* A novel microfluidic microplate as the next generation assay platform for enzyme linked immunoassays (ELISA). *Lab Chip* 12, 4257–4262 (2012).
106. Kim, D. & Herr, A. E. Protein immobilization techniques for microfluidic assays. *Biomicrofluidics* 7, (2013).
107. Rusmini, F., Zhong, Z. & Feijen, J. Protein immobilization strategies for protein biochips. *Biomacromolecules* 8, 1775–1789 (2007).
108. Barbosa, A. I., Wichers, J. H., Amerongen, A. Van & Reis, N. M. Towards One-Step Quantitation of Prostate-Specific Antigen (PSA) in Microfluidic Devices : Feasibility of Optical Detection with Nanoparticle Labels. 718–726 (2017). doi:10.1007/s12668-016-0390-y
109. Sista, R. S. *et al.* Heterogeneous immunoassays using magnetic beads on a digital

microfluidic platform. *Lab Chip* 8, 2188–2196 (2008).

110. Reis, N. M., Pivetal, J., Loo-Zazueta, A. L., Barros, J. M. S. & Edwards, A. D. Lab on a stick: Multi-analyte cellular assays in a microfluidic dipstick. *Lab Chip* 16, 2891–2899 (2016).
111. Gopinath, S. C. B., Tang, T. H., Chen, Y., Citartan, M. & Lakshmipriya, T. Bacterial detection: From microscope to smartphone. *Biosens. Bioelectron.* 60, 332–342 (2014).
112. Park, T. S., Li, W., McCracken, K. E. & Yoon, J. Y. Smartphone quantifies Salmonella from paper microfluidics. *Lab Chip* 13, 4832–4840 (2013).
113. Kuswandi, B., Nuriman, Huskens, J. & Verboom, W. Optical sensing systems for microfluidic devices: A review. *Anal. Chim. Acta* 601, 141–155 (2007).
114. Mark C. Pierce, Shannon E. Weigum, Jacob M. Jaslove, Rebecca Richards-Kortumb, c, and T. S. T. Optical systems for point-of-care diagnostic instrumentation: analysis of imaging performance and cost. *Lab Chip* 42, 1–27 (2014).
115. Myers, F. B. & Lee, L. P. Innovations in optical microfluidic technologies for point-of-care diagnostics. *Lab Chip* 8, 2015–2031 (2008).
116. Erickson, D. *et al.* Smartphone technology can be transformative to the deployment of lab-on-chip diagnostics. *Lab Chip* 14, 3159–3164 (2014).
117. Shen, L., Hagen, J. A. & Papautsky, I. Point-of-care colorimetric detection with a smartphone. *Lab Chip* 12, 4240–4243 (2012).
118. Oncescu, V., O'Dell, D. & Erickson, D. Smartphone based health accessory for colorimetric detection of biomarkers in sweat and saliva. *Lab Chip* 13, 3232–3238 (2013).
119. Hongying Zhu, Serhan O. Isikman, Onur Mudanyali, Alon Greenbaum, and A. O. Optical Imaging Techniques for Point-of-care Diagnostics Hongying. *Lab Chip* 13, 51–67 (2013).
120. Roda, A. *et al.* Smartphone-based biosensors: A critical review and perspectives. *TrAC - Trends Anal. Chem.* 79, 317–325 (2016).
121. Bates, M. & Zumla, A. Rapid infectious diseases diagnostics using Smartphones. *Ann Transl Med* 3, 1–5 (2015).
122. Hong, J. Il & Chang, B. Y. Development of the smartphone-based colorimetry for multi-analyte sensing arrays. *Lab Chip* 14, 1725–1732 (2014).
123. Ahmet F. Coskun, Richie Nagi, Kayvon Sadeghi, Stephen Phillipsa,b,§, and A. O. Albumin testing in urine using a smart-phone. *Lab Chip* 13, 4231–4238 (2013).
124. Sasso, L. A., Road, T., Johnston, I. H. & Zahn, J. D. Automated microfluidic processing platform for multiplexed magnetic bead immunoassays Lawrence.

Microfluid Nanofluidics 13, 603–612 (2012).

125. Waldbaur, A., Rapp, H., Länge, K. & Rapp, B. E. Let there be chip - Towards rapid prototyping of microfluidic devices: One-step manufacturing processes. *Anal. Methods* 3, 2681–2716 (2011).
126. Zimmermann, M., Schmid, H., Hunziker, P. & Delamarche, E. Capillary pumps for autonomous capillary systems. *Lab Chip* 7, 119–125 (2007).
127. Gilmore, J., Islam, M. & Martinez-Duarte, R. Challenges in the use of compact disc-based centrifugal microfluidics for healthcare diagnostics at the extreme point of care. *Micromachines* 7, (2016).
128. Yang, Y., Kim, S. & Chae, J. Separating and detecting escherichia coli in a microfluidic channel for urinary tract infection applications. *J. Microelectromechanical Syst.* 20, 819–827 (2011).
129. Berleman, J. E. *et al.* Exopolysaccharide microchannels direct bacterial motility and organize multicellular behavior. *ISME J.* 10, 2620–2632 (2016).
130. Licata, N. A., Mohari, B., Fuqua, C. & Setayeshgar, S. Diffusion of Bacterial Cells in Porous Media. *Biophys. J.* 110, 247–257 (2016).
131. Ping, L., Wasnik, V. & Emberly, E. Bacterial motion in narrow capillaries. *FEMS Microbiol. Ecol.* 91, 1–7 (2015).
132. Hill, J., Kalkanci, O., McMurry, J. L. & Koser, H. Hydrodynamic surface interactions enable escherichia coli to seek efficient routes to swim upstream. *Phys. Rev. Lett.* 98, 1–4 (2007).
133. Adler, J. & Dahl, M. M. A Method for Measuring the Motility of Bacteria and for Comparing Random and Non-random Motility. *J. Gen. Microbiol.* 46, 161–173 (1967).
134. Berg, H. C. Motile Behavior of Bacteria. *Phys. Today* 53, 24–29 (2000).
135. Berke, A. P., Turner, L., Berg, H. C. & Lauga, E. Hydrodynamic attraction of swimming microorganisms by surfaces. *Phys. Rev. Lett.* 101, 1–4 (2008).
136. DiLuzio, W. R. *et al.* Escherichia coli swim on the right-hand side. *Nature* 435, 1271–1274 (2005).
137. Berg, H. C. How to track bacteria. *Rev. Sci. Instrum.* 42, 868–871 (1971).
138. Lauga, E., DiLuzio, W. R., Whitesides, G. M. & Stone, H. A. Swimming in circles: Motion of bacteria near solid boundaries. *Biophys. J.* 90, 400–412 (2006).
139. Kaya, T. & Koser, H. Direct upstream motility in Escherichia coli. *Biophys. J.* 102, 1514–1523 (2012).
140. Frymier, P. D., Ford, R. M., Berg, H. C. & Cummings, P. T. Three-dimensional tracking of motile bacteria near a solid planar surface. *Proc. Natl. Acad. Sci.* 92, 6195–6199 (1995).

141. Duffy, K. J., Cummings, P. T. & Ford, R. M. Random walk calculations for bacterial migration in porous media. *Biophys. J.* 68, 800–806 (1995).
142. Edition, 2nd. *Cell Movements: from molecules to motility*. (2001).
143. Howard, B. *E. coli in Motion*. 49, (2004).
144. Berg, H. C. & Brown, D. A. Chemotaxis in Escherichia coli analysed by three-dimensional tracking. *Nature* 239, 500–4 (1972).
145. Wolfe, A. J. & Berg, H. C. Migration of bacteria in semisolid agar. *Proc. Natl. Acad. Sci.* 86, 6973–6977 (1989).
146. Nash, R. W., Adhikari, R., Tailleur, J. & Cates, M. E. Run-and-tumble particles with hydrodynamics: Sedimentation, trapping, and upstream swimming. *Phys. Rev. Lett.* 104, 1–4 (2010).
147. Zonia, L. & Bray, D. Swimming patterns and dynamics of simulated Escherichia coli bacteria. *J. R. Soc. Interface* 6, 1035–1046 (2009).
148. Li, G., Tam, L.-K. & Tang, J. X. Amplified effect of Brownian motion in bacterial near-surface swimming. *Proc. Natl. Acad. Sci.* 105, 18355–18359 (2008).
149. Shum, H., Gaffney, E. A. & Smith, D. J. Modelling bacterial behaviour close to a no-slip plane boundary: The influence of bacterial geometry. *Proc. R. Soc. A Math. Phys. Eng. Sci.* 466, 1725–1748 (2010).
150. Chattopadhyay, S., Moldovan, R., Yeung, C. & Wu, X. L. Swimming efficiency of bacterium Escherichia coli. *Proc. Natl. Acad. Sci.* 103, 13712–13717 (2006).
151. Tailleur, J. & Cates, M. E. Statistical mechanics of interacting run-and-tumble bacteria. *Phys. Rev. Lett.* 100, 3–6 (2008).
152. Van Teeffelen, S. & Löwen, H. Dynamics of a Brownian circle swimmer. *Phys. Rev. E - Stat. Nonlinear, Soft Matter Phys.* 78, 2–5 (2008).
153. Jing, W. *et al.* Microfluidic device for efficient airborne bacteria capture and enrichment. *Anal. Chem.* 85, 5255–5262 (2013).
154. Tu, S. I., Uknalis, J., Gore, M., Irwin, P. & Feder, I. Factors affecting the bacterial capture efficiency of immuno beads: A comparison between beads with different size and density. *J. Rapid Methods Autom. Microbiol.* 11, 35–46 (2003).
155. Dupont, A. & Lamb, D. C. Nanoscale three-dimensional single particle tracking. *Nanoscale* 3, 4532–4541 (2011).
156. Mandy LY Sin, Kathleen E Mach, P. K. W. and J. C. L. Advances and challenges in biosensor-based diagnosis of infectious diseases. 14, 225–244 (2014).
157. Eltzov, E. & Marks, R. S. Miniaturized Flow Stacked Immunoassay for Detecting Escherichia coli in a Single Step. *Anal. Chem.* 88, 6441–6449 (2016).
158. Clotilde, Laurie M.; Bernard, Clay IV; Salvador, Alexandra; Lin, Andrew; Lauzon, Carol R.; Muldoon, Mark; Xu, Yichun; Lindpaintner, Klaus; and Carter, J. M. A 7-

plex microbead-based immunoassay for serotyping Shiga toxin-producing Escherichia coli. *J. Microbiol. Methods* 92, 226–230 (2013).

159. Wang, N., He, M. & Shi, H. C. Novel indirect enzyme-linked immunosorbent assay (ELISA) method to detect Total E. coli in water environment. *Anal. Chim. Acta* 590, 224–231 (2007).
160. Gervais, L. & Delamarche, E. Toward one-step point-of-care immunodiagnostics using capillary-driven microfluidics and PDMS substrates. *Lab Chip* 9, 3330–3337 (2009).
161. Peter E. Andreotti, George V. Ludwig, Anne Harwood Peruski, James J. Tuite, Stephen S. Morse, and Leonard F. Peruski, J. Immunoassay of infectious agents Peter. *Biotechniques.* 35, 850–859 (2003).
162. Kunst, B. H., Schots, A. & Visser, A. J. W. G. Detection of flowing fluorescent particles in a microcapillary using fluorescence correlation spectroscopy. *Anal. Chem.* 74, 5350–5357 (2002).
163. Schneider, C. A., Rasband, W. S. & Eliceiri, K. W. NHI Image to ImageJ: 25 years of image analysis. *Nat. Methods* 9, 671–675 (2012).
164. Park, S., Kim, H., Paek, S. H., Hong, J. W. & Kim, Y. K. Enzyme-linked immuno-strip biosensor to detect Escherichia coli O157:H7. *Ultramicroscopy* 108, 1348–1351 (2008).
165. Jayamohan, H. *et al.* Highly sensitive bacteria quantification using immunomagnetic separation and electrochemical detection of guanine-labeled secondary beads. *Sensors (Switzerland)* 15, 12034–12052 (2015).
166. Ghinwa Naja, Pierre Bouvrette, Sabahudin Hrapovich, Y. L. and J. H. T. L. Detection of bacteria aided by immuno-nanoparticles. *J. RAMAN Spectrosc.* 38, 1383–1389 (2007).
167. Wang, H., Li, Y., Wang, A. & Slavik, M. Rapid, Sensitive, and Simultaneous Detection of Three Foodborne Pathogens Using Magnetic Nanobead–Based Immunoseparation and Quantum Dot–Based Multiplex Immunoassay. *J. Food Prot.* 74, 2039–2047 (2011).
168. Reis, N. M. & Li Puma, G. A novel microfluidic approach for extremely fast and efficient photochemical transformations in fluoropolymer microcapillary films. *Chem. Commun.* 51, 8414–8417 (2015).
169. Wioland, H., Lushi, E. & Goldstein, R. E. Directed collective motion of bacteria under channel confinement. *New J. Phys.* 18, (2016).
170. Buijs, J., Lichtenbelt, J. W. T., Norde, W. & Lyklema, J. Adsorption of monoclonal IgGs and their F(ab′)2fragments onto polymeric surfaces. *Colloids Surfaces B Biointerfaces* 5, 11–23 (1995).

171. Wu, X. *et al.* Development of sandwich ELISA and immunochromatographic strip methods for the detection of Xanthomonas oryzae pv. oryzae. *Anal. Methods* 7, 6190–6197 (2015).
172. Ahmed, A., Rushworth, J. V., Hirst, N. A. & Millner, P. A. Biosensors for whole-cell bacterial detection. *Clin. Microbiol. Rev.* 27, 631–646 (2014).
173. Alves, I. P. & Reis, N. M. Immunocapture of Escherichia coli in a fluoropolymer microcapillary array. *Journal of Chromatography A* (2018). doi:10.1016/j.chroma.2018.11.067
174. Zeinhom, M. M. A. *et al.* A portable smart-phone device for rapid and sensitive detection of E. coli O157:H7 in Yoghurt and Egg. *Biosens. Bioelectron.* 99, 479–485 (2018).
175. Lin, C. C., Tseng, C. C., Chuang, T. K., Lee, D. S. & Lee, G. Bin. Urine analysis in microfluidic devices. *Analyst* 136, 2669–2688 (2011).
176. Kathleen E. Mach, Pak Kin Wong, and J. C. L. Biosensor diagnosis of urinary tract infections: a path to better treatment. *Trends Pharmacol Sci.* 32, 330–336 (2012).
177. Ederveen, J. in (2010).
178. Lee, W. G., Kim, Y. G., Chung, B. G., Demirci, U. & Khademhosseini, A. Nano/Microfluidics for diagnosis of infectious diseases in developing countries. *Adv. Drug Deliv. Rev.* 62, 449–457 (2010).
179. Meng, X. *et al.* Conditional siphon priming for multi-step assays on centrifugal microfluidic platforms. *Sensors Actuators, B Chem.* 242, 710–717 (2017).
180. Sharma, S., Zapatero-Rodríguez, J., Estrela, P. & O'Kennedy, R. Point-of-Care diagnostics in low resource settings: Present status and future role of microfluidics. *Biosensors* 5, 577–601 (2015).
181. Samantha Byrnes , Gregory Thiessen, and E. F. Progress in the development of paper-based diagnostics for low-resource point-of-care settings. *Bioanalysis.* 5, 2821–2836 (2013).
182. Tay, A., Pavesi, A., Yazdi, S. R., Lim, C. T. & Warkiani, M. E. Advances in microfluidics in combating infectious diseases. *Biotechnol. Adv.* 34, 404–421 (2016).
183. Lade, R. K., Hippchen, E. J., Macosko, C. W. & Francis, L. F. Dynamics of Capillary-Driven Flow in 3D Printed Open Microchannels. *Langmuir* 33, 2949–2964 (2017).
184. Hosokawa, K., Omata, M., Sato, K. & Maeda, M. Power-free sequential injection for microchip immunoassay toward point-of-care testing. *Lab Chip* 6, 236–241 (2006).
185. Juncker, D. *et al.* Autonomous microfluidic capillary system. *Anal. Chem.* 74, 6139–6144 (2002).
186. Laksanasopin, T. *et al.* A smartphone dongle for diagnosis of infectious diseases at

the point of care. *Sci. Transl. Med.* 7, 273 (2015).

187. Martinez, A. W. *et al.* Simple Telemedicine for Developing Regions: Camera Phones and Paper-Based Microfluidic Devices for Real-Time, Off-Site Diagnosis. *Anal. Chem.* 80, 3699–3707 (2008).
188. Shaffer, A. *et al.* Regional blood flow measurement with pulsed Doppler flowmeter in conscious rat. (2019).
189. Mao, X., Waldeisen, R. & Jun Huang, T. Miniaturisation for chemistry , biology & bioengineering ‘“ Microfluidic drifting ”’— implementing three-dimensional hydrodynamic focusing with a single-layer planar microfluidic device {. *Lab Chip* 7, 1260–1262 (2007).
190. Hornung, C. H. & Mackley, M. R. The measurement and characterisation of residence time distributions for laminar liquid flow in plastic microcapillary arrays. *Chem. Eng. Sci.* 64, 3889–3902 (2009).
191. Levenspiel, O. *Chemical Reaction Engineering 3rd.* (1999). doi:10.1016/0009-2509(80)80132-1
192. Ejim, L. N. *et al.* A factorial approach to understanding the effect of inner geometry of baffled meso-scale tubes on solids suspension and axial dispersion in continuous, oscillatory liquid–solid plug flows. *Chem. Eng. J.* 308, 669–682 (2017).
193. Fogler, H. S. *Elements of chemical reaction engineering*. *Elements of Chemical Reaction Engineering* (Boston: Prentice Hall, 2016). doi:10.1016/j.memsci.2013.03.029
194. Cussler, E. L. in 1–14 (Cambridge University Press, 2009). doi:10.1017/CBO9780511805134.010
195. Inman, B. A. *et al.* The impact of temperature and urinary constituents on urine viscosity and its relevance to bladder hyperthermia treatment. *Int. J. Hyperth.* 29, 206–210 (2013).
196. Lee, K. P., Leese, H. & Mattia, D. Water flow enhancement in hydrophilic nanochannels. *Nanoscale* 4, 2621–2627 (2012).
197. Weigl, B., Domingo, G., LaBarre, P. & Gerlach, J. Towards non- and minimally instrumented, microfluidics-based diagnostic devices. *Lab Chip* 8, 1999–2014 (2008).
198. Laschi, S. *et al.* A new gravity-driven microfluidic-based electrochemical assay coupled to magnetic beads for nucleic acid detection. *Electrophoresis* 31, 3727–3736 (2010).
199. Shen, B., Xiong, B. & Wu, H. Convenient surface functionalization of whole-Teflon chips with polydopamine coating. *Biomicrofluidics* 9, 1–11 (2015).
200. Wiseman, M. E. & Frank, C. W. Antibody adsorption and orientation on hydrophobic

surfaces. *Langmuir* 28, 1765–1774 (2012).

201. Trilling, A. K., Beekwilder, J. & Zuilhof, H. Antibody orientation on biosensor surfaces: A minireview. *Analyst* 138, 1619–1627 (2013).
202. Studentsov, Y. Y. *et al.* Enhanced Enzyme-Linked Immunosorbent Assay for Detection of Antibodies to Virus-Like Particles of Human Papillomavirus. *J. Clin. Microbiol.* 40, 1755–1760 (2002).
203. Steigert, J., Brenner, T., Grumann, M. & Riegger, L. Integrated siphon-based metering and sedimentation of whole blood on a hydrophilic lab-on-a-disk. 675–679 (2007). doi:10.1007/s10544-007-9076-0
204. Du, W., Fang, Q., He, Q. & Fang, Z. High-Throughput Nanoliter Sample Introduction Microfluidic Chip-Based Flow Injection Analysis System with Gravity-Driven Flows. 77, 1330–1337 (2005).
205. Yao, B. *et al.* A microfluidic device based on gravity and electric force driving for flow cytometry and fluorescence activated cell sorting. 603–607 (2004).
206. Laschi, S., Miranda-castro, R., Gonza, E. & Marrazza, G. A new gravity-driven microfluidic-based electrochemical assay coupled to magnetic beads for nucleic acid detection. 3727–3736 (2010). doi:10.1002/elps.201000288